



# Selecting Analytic Tools for Concrete Dams Address Key Events Along Potential Failure Mode Paths

*FEMA P-1016 / July 2014*



**FEMA**



# **Selecting Analytic Tools for Concrete Dams to Address Key Events along Potential Failure Mode Paths**

**Federal Emergency Management Agency**

July 2014



# ACRONYMS AND ABBREVIATIONS

2D	two-dimensional
3D	three-dimensional
ACI	American Concrete Institute
DVD	digital versatile disc
FEM	finite element method
FEMA	Federal Emergency Management Agency
FERC	Federal Energy Regulatory Commission
ft	feet
g	acceleration in relation to gravity (1 g = 32.2 ft/s <sup>2</sup> )
GT-STRUDL	structural design and analysis software
ICODS	Interagency Committee on Dam Safety
kip	1,000 pounds
kip/ft <sup>3</sup>	1,000 pounds per cubic foot
kip-ft	1,000 pound-feet
lb/ft <sup>2</sup>	pounds per square foot
lb/ft <sup>3</sup>	pounds per cubic foot
lb/in <sup>2</sup>	pounds per square inch
NDSRB	National Dam Safety Review Board
PDF	portable document format
TVA	Tennessee Valley Authority
USACE	United States Army Corps of Engineers



# CONVERSION FACTORS

## To the International System of Units (SI) (Metric)

Pound-foot measurements in this document can be converted to SI measurements by multiplying by the following factors:

Multiply	By	To obtain
acre-feet	1233.489	cubic meters
cubic feet	0.028317	cubic meters
cubic feet per second	0.028317	cubic meters per second
cubic inches	16.38706	cubic centimeters
degrees Fahrenheit	$(^{\circ}\text{F}-32)/1.8$	degrees Celsius
feet	0.304800	meters
feet per second	0.304800	meters per second
gallons	0.003785	cubic meters
gallons	3.785412	liters
gallons per minute	0.000063	cubic meters per second
gallons per minute	0.063090	liters per second
inches	2.540000	centimeters
miles	1.609344	kilometers
pounds	0.453592	kilograms
pounds per cubic foot	16.01846	kilograms per cubic meter
pounds per square foot	4.882428	kilograms per square meter
pounds per square inch	6.894757	kilopascals
pounds per square inch	6894.757	pascals
square feet	0.092903	square meters
square inches	6.451600	square centimeters





# STANDARDS

## **Bureau of Reclamation**

*State-of-Practice for the Non-Linear Structural Analysis of Concrete Dams at the Bureau of Reclamation*, January 2006

*Design of Small Dams*, Denver, Colorado, Third Edition, 1987

*Design of Gravity Dams*, Denver, Colorado, 1976

*Design of Arch Dams*, Denver, Colorado, 1977

Publications are for sale at the National Technical Information Service:

<http://www.ntis.gov/>

## **Federal Energy Regulatory Commission**

*FERC Engineering Guidelines for the Evaluation of Hydropower Projects*

For further information on publications:

<http://www.ferc.gov/industries/hydropower/safety/guidelines.asp>

## **U.S. Army Corps of Engineers (USACE)**

- EM 1110-2-1612     *Ice Engineering*, October 2002
- EM 1110-2-2100     *Stability Analysis of Concrete Structures*, December 2005.
- EM 1110-2-2104     *Strength Design for Reinforced—Concrete Hydraulic Structures*, August 2003
- EM 1110-2-2200     *Gravity Dam Design*, June 1995
- EM 1110-2-2201     *Arch Dam Design*, May 1994
- EM 1110-2-6050     *Response Spectra and Seismic Analysis for Concrete Hydraulic Structures*, June 1999
- EM 1110-2-6051     *Engineering and Design—Time-History Dynamic Analysis of Concrete Hydraulic Structures*, December 2003
- EM 1110-2-6053     *Engineering and Design—Earthquake Design and Evaluation of Concrete Hydraulic Structures*, May 2007

For further information on publications:

<http://140.194.76.129/publications/>

# WEB SITES

The following Web sites can provide additional information related to organizations associated with concrete dams:

American Society of Civil Engineers:

<http://www.asce.org>

Association of State Dam Safety Officials:

<http://www.damsafety.org>

Bureau of Reclamation:

<http://www.usbr.gov>

Federal Emergency Management Agency:

<http://www.fema.gov/plan/prevent/damfailure>

<http://www.fema.gov/plan/prevent/damfailure/fema148.shtm>

Federal Energy Regulatory Commission:

<http://www.ferc.gov/industries/hydropower.asp>

International Boundary and Water Commission:

<http://www.ibwc.gov>

International Commission on Large Dams:

<http://icold-cigb.net>

National Performance of Dams Program:

<http://npdp.stanford.edu>

Natural Resources Conservation Service:

<http://www.nrcs.usda.gov/wps/portal/nrcs/main/national/home>

Tennessee Valley Authority:

<http://www.tva.gov>

United States Society on Dams:

<http://www.ussdams.org>

U.S. Army Corps of Engineers:

<http://www.usace.army.mil>



# PREFACE

The primary authors of this document in alphabetical order are Bruce Brand, P.E. (Federal Energy Regulatory Commission); David A. Dollar, P.E. (U.S. Army Corps of Engineers); Husein Hasan (Tennessee Valley Authority); Luis Hernandez (International Boundary and Water Commission, U.S. Section); Larry K. Nuss, P.E. (Bureau of Reclamation); Rex Rowell, P.E. (Tennessee Valley Authority); and William A. Wallace, P.E., SECB (U.S. Department of Agriculture, Natural Resources Conservation Service).

The technical editor for this manual was Lelon A. Lewis (Bureau of Reclamation). Additional technical assistance was provided by Cynthia Fields (Bureau of Reclamation) and Cindy Gray (Bureau of Reclamation).

Peer review of this manual was provided by Glenn Koester (Federal Energy Regulatory Commission); Robert Hall, David Schaff, Travis Adams, Greg Werncke, and Rick Poeppelman (U.S. Army Corps of Engineers); Jennifer Dickerson (Tennessee Valley Authority); Carlos Pena, Jr. (International Boundary and Water Commission, U.S. Section); Gregg Scott and Barbara Mills-Bria (Bureau of Reclamation); Stephen Reinsch (U.S. Department of Agriculture, Natural Resources Conservation Service); and Dan Hoang and Juan Uribe (Nuclear Regulatory Commission).

The National Dam Safety Review Board (NDSRB) reviewed this manual prior to issuance. The NDSRB plays an important role in guiding the National Dam Safety Program. The NDSRB has responsibility for monitoring the safety and security of dams in the United States, advising the Director of the Federal Emergency Management Agency (FEMA) on national dam safety policy, consulting with the Director of FEMA for the purpose of establishing and maintaining a coordinated National Dam Safety Program, and monitoring State implementation of the assistance program. The NDSRB consists of five representatives appointed from Federal agencies, five State dam safety officials, and one representative from the U.S. Society on Dams.

The authors also extend their appreciation to the following individuals for graciously providing information and permission to use their materials in this publication: Gregg A. Scott, Barbara Mills-Bria, and Chris Powell (Bureau of Reclamation) for their work upon which appendix A3 is based.

The authors caution the users of this manual that sound engineering judgment should always be applied when using references. Users should be aware that certain portions of references cited in this manual may have become outdated in regard to design and construction aspects and/or philosophies. While these references may still contain valuable information, users should not automatically assume that the entire reference is suitable for design and construction purposes. The authors utilized many sources of information in the development of this manual, including:

- Published design standards and technical publications of the various Federal agencies and organizations involved with the preparation of this manual.
- Published professional papers and articles from selected authors, technical journals and publications, and organizations.

- Experience of the individuals, Federal agencies, and organizations involved in the preparation of this manual.

Suggestions for changes, corrections, or updates to this manual should be directed to:

Bureau of Reclamation  
Denver Federal Center, Bldg. 67  
ATTN: Director of Dam Safety, 86-45000  
6th Avenue and Kipling Street  
Denver, CO 80225-0007

Please reference specific pages, paragraphs, or figures within the manual, together with proposed new material in any convenient format. Sources of proposed new material should be completely cited. Submission of material signifies permission for use in a future revised edition of this manual, but credit for such new material will be given where appropriate.

The material presented in this manual has been prepared in accordance with recognized engineering practices. The guidance in this manual should not be used without first securing competent advice with respect to its suitability for any given application. The publication of the material contained herein is not intended as representation or warranty on the part of individuals or agencies involved, or any other person named herein, that this information is suitable for any general or particular use, or promises freedom from infringement of any patent or patents.

Anyone making use of this information assumes all liability from such use. Any use of trade names and trademarks in this manual is for descriptive purposes only and does not constitute endorsement. The information contained herein regarding commercial products or firms may not be used for advertising or promotional purposes and is not to be construed as an endorsement of any product or firm.

Various computer codes were used in developing the example problems. The uses of these codes are not an endorsement or recommendation for their use.

# CONTENTS

	Page
1.1	Introduction ..... 1
2.1	Theory and Types of Concrete Dams ..... 1
2.1.1	Gravity Dams ..... 2
2.1.2	Arch Dams ..... 2
2.1.3	Buttress Dams ..... 3
3.1	Potential Failure Modes ..... 6
3.1.1	Defining Failure Criteria ..... 6
3.1.2	Developing Potential Failure Modes ..... 6
3.1.3	Sequence of Events ..... 10
3.1.4	Event Trees ..... 12
3.1.4.1	Advantages ..... 13
3.1.4.2	General Principles ..... 13
4.1	Relating Analyses to Failure Modes ..... 15
4.1.1	Limit Equilibrium Analysis ..... 15
4.1.2	Linear Finite Element Analyses ..... 17
4.1.3	Nonlinear Finite Element Analyses ..... 19
4.1.4	Static and Dynamic Analyses ..... 23
4.1.5	The Role of Standards-Based Criteria and Codes ..... 25
5.1	Focusing on Parameters Affecting Analysis ..... 25
5.1.1	Common Errors ..... 28
5.1.1.1	Unrealistic Boundary Conditions ..... 29
5.1.1.2	Finite Element Mesh Density ..... 30
5.1.1.3	Damping ..... 32
5.1.1.4	Failure Plane Tension/Cohesion ..... 33
5.1.2	Summary ..... 33
6.1	Uncertainty and Confidence ..... 34
6.1.1	Uncertainty ..... 34
6.1.2	Confidence ..... 36
7.1	Conclusions ..... 38
	Bibliography ..... 41

## Tables

Table	Page
4-1	Limitations of structural analysis methods to compute the structural response for various sequences of events of a potential failure mode ..... 16
4-2	General differences in various structural analysis methods ..... 17
4-3	Results of limit equilibrium analysis ..... 18
4-4	Forces, centroids, and moment ..... 24

## Figures

Figure		Page
2-1	Gravity dam, Bureau of Reclamation. ....	2
2-2	Arch dam, Bureau of Reclamation.....	3
2-3	Slab and buttress dam, Bureau of Reclamation. ....	4
2-4	Massive-head buttress dam, Bureau of Reclamation.....	4
2-5	Multiple-arch buttress dam, Bureau of Reclamation. ....	5
2-6	Multiple dome buttress dam, Bureau of Indian Affairs. ....	5
3-1	Construction photograph of a curved gravity dam showing the many complex features: contraction joints, shear keys, lift lines, thermal expansions, grouting, foundation discontinuities, material strengths, penstocks through the dam, outlet works, spillway sections, and spillway gates, Bureau of Reclamation.....	7
3-2	Potential failure modes given an initiating event.....	8
3-3	Possible failure mechanisms of a concrete gravity dam. ....	10
3-4	Event tree. In this example, increased reservoir load could cause sliding instability.....	14
4-1	Limit equilibrium analysis. ....	18
4-2	Linear finite element model: principal stress vectors. ....	20
4-3	Base stress from linear finite element analysis. ....	20
4-4	Base stress from nonlinear finite element analyses and limit equilibrium analysis. ....	21
4-5	Irregular base with nonlinear finite element analyses.....	22
4-6	Results from irregular base with nonlinear finite element analyses. ....	23
4-7	Results from applying instantaneous peak dynamic loads. ....	24
5-1	Base cracking example. ....	27
5-2	Base pressure distribution through a section of a concrete dam. ....	27
5-3	Modular ratio effects (note that this curve is specific for the example cited).....	28
5-4	Buttress dam finite element idealization. ....	29
5-5	Fine finite element mesh at reentrant corner.....	31
5-6	Stresses from the fine finite element mesh. ....	31
5-7	Coarse finite element model and stress results. ....	32
6-1	Uncertainty bands around a seismic hazard curve (peak acceleration vs. exceedance probability).....	35

## Appendices

### Appendix

A1	Increased Reservoir Level Causes Sliding in a Gravity Dam
A2	Earthquake Causes Sliding in a Gravity Dam
A3	Earthquake Causes Sliding in Foundation Leading to Dam Failure
A4	Increased Silt Load Causes Failure of Reinforced Concrete Corbels of a Buttress Dam
A5	Freeze-Thaw Deterioration Removes Concrete Cover and Causes Upstream Slab to Fall
B	Loads and Loading Requirements



## **1.1 Introduction**

The purpose of this document is to stress the importance of understanding the sequences of events leading to failure of concrete dams and selecting analysis methods that address these specific events. The selected analysis method may range from straightforward to complex, depending on the potential failure mode being analyzed. It is stressed that a less complex analysis with less uncertainty is the preferred strategy. Included in this report and the appendices are examples of this process. These examples are not intended to be a complete listing of concrete dam potential failure modes. Each dam is unique and has its own issues; therefore, it is important for the engineer to understand the potential failure modes and sequences of events that enable them.

In this document, failure is considered the uncontrolled release of the reservoir. However, this may or may not always be the case given the purpose or hazard of a structure or given an agency's requirements for a structure. How do we determine if a concrete dam can fail? Failure results from sequences of events that must follow one upon another. Because a dam cannot fail without the full chain of events, conclusively ruling out any event justifies concluding that the dam will not fail. This document introduces event trees. Event trees are pictorial representations of the sequences of events (called nodes) leading to failure. The possibility of each node occurring is evaluated by analyses.

It is the experience of the authors that engineers often rush to analysis without consideration of the failure process. As a result, expensive analyses are done that are not needed, waste time, and often do not answer the question of whether a dam will fail.

This document represents the collective experience of the Bureau of Reclamation, Federal Energy Regulatory Commission (FERC), International Boundary and Water Commission, U.S. Section, Natural Resources Conservation Service, Tennessee Valley Authority, and U.S. Army Corps of Engineers (USACE).

Note that this document should not be substituted for design criteria such as those established by these agencies.

Examples presented are for instructional purposes only. Assumptions made, material properties used, and loadings were selected to illustrate structural analysis methods and failure modes, and are not generally applicable.

## **2.1 Theory and Types of Concrete Dams**

This document addresses structural analysis of concrete dams related to potential failure modes. Embankment dams are not addressed in this document. The three basic types of concrete dams are gravity dams, arch dams, and buttress dams.

## 2.1.1 Gravity Dams

Gravity dams (figure 2-1) derive their strength from their weight. Shear resistance, which is a function of weight, friction angle, and cohesion, controls sliding. A gravity dam's weight, as defined by its geometry and concrete density, and its uplift pressures control overturning stability. All failure modes must somehow either decrease the net effect of the weight of the structure or the resistance against sliding and overturning, or increase the driving forces. In most situations, all three of these occur.



Figure 2-1: Gravity dam, Bureau of Reclamation.

The majority of gravity dams fall into the category of straight gravity dams. The upstream face of these dams is typically straight in plan view and perpendicular to the stream channel. Curved gravity dams, a subset of gravity dams, do not rely on the curvature for static stability. However, the curvature may increase their ability to withstand changes in loads from reductions in drainage, flooding, or seismic events.

## 2.1.2 Arch Dams

Arch dams (figure 2-2) distribute loads vertically to the foundation by cantilever action and horizontally to the abutments by arching action. The load distribution depends on the curvature of the dam, structural features, and material strength. Because concrete is strong in compression and weak in tension, arch dam design is based on maximizing compressive stress distributions and minimizing tensile stress distributions. Since the load is distributed to the foundation and abutments, the geometry and shear strength of the abutment contact are important. An arch dam relies on the abutments for stability.



Figure 2-2: Arch dam, Bureau of Reclamation.

### 2.1.3 Buttress Dams

Buttress dams consist of buttresses transverse to the dam axis that support longitudinal elements, such as flat slabs, domes, massive heads, or arches that contain the reservoir. The upstream face of the dam is typically sloped up to about a 45-degree angle. Therefore, hydrostatic pressures that produce the driving forces also provide a downward vertical force that adds to structural stability. Overall stability of buttress dams is accomplished by the same means as for gravity dams.

A variety of dams fall into this category. A slab and buttress dam (figure 2-3) typically consists of buttresses, flat or tapered slabs, and struts between the buttresses. For a massive-head buttress dam (figure 2-4), the geometry of the individual buttresses consists of a downstream stem that is widened at the upstream face to form a “massive head.” The massive heads of adjacent buttresses are in contact typically with water-stops between them, providing a watertight upstream face. For a multiple-arch (figure 2-5) or dome (figure 2-6) buttress dam, the arches are integral parts of the upstream side of the buttresses, and reinforcement is continuous from the arches into the buttresses.

The main advantage of a buttress dam is reduced concrete volumes. Many of these dams were constructed when labor and steel costs were more than offset by the cost savings of reduced concrete volume. At or above the foundation, uplift affects buttress dams less than gravity dams because uplift pressures are reduced between the buttresses, and the remaining uplift pressures

**Selecting Analytic Tools for Concrete Dams to Address  
Key Events Along Potential Failure Mode Paths**

---



**Figure 2-3: Slab and buttress dam, Bureau of Reclamation.**



**Figure 2-4: Massive-head buttress dam, Bureau of Reclamation.**



Figure 2-5: Multiple-arch buttress dam, Bureau of Reclamation.

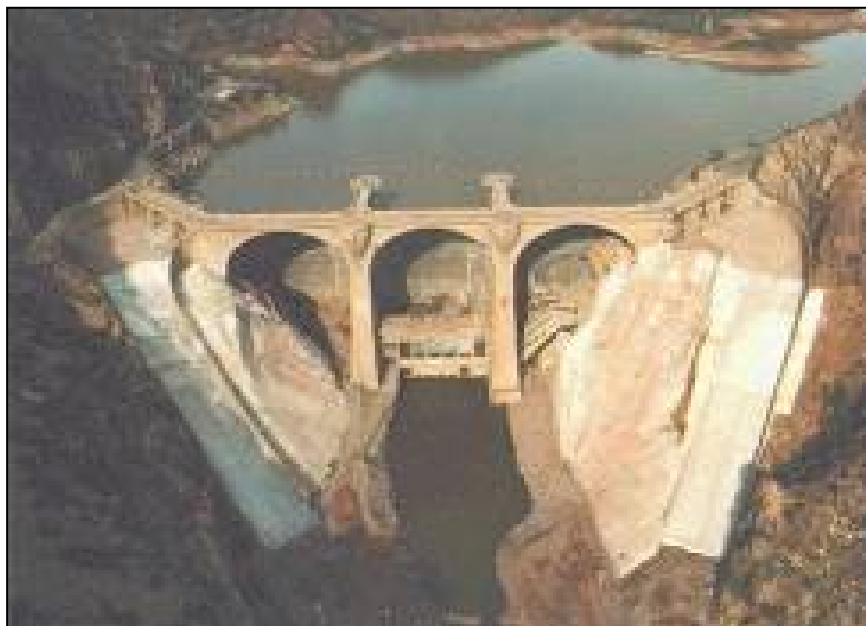


Figure 2-6: Multiple dome buttress dam, Bureau of Indian Affairs.

act on the relatively small surface area of the buttresses' footprint. Historically, this type of dam was considered to be more forgiving to variations in foundation conditions. However, it must be realized that each individual buttress must be stable on its own. Failure modes associated with buttress dams include the typical gravity dam failure modes, as well as modes associated with lateral movement of the buttresses and strength-related modes of the reinforced concrete elements.

## **3.1 Potential Failure Modes**

Identifying, fully describing, and evaluating site-specific potential failure modes and sequences leading to failure are arguably the most important initial steps in conducting a structural analysis for a concrete dam. The process this document suggests is to: (1) define failure criteria, (2) identify potential failure modes, (3) develop a sequence of events (nodes) for a failure to transpire, (4) select a node with the most likely chance to circumvent the failure process, (5) select a structural analyses method to compute the response of the dam at that node, (6) quantify the uncertainty, and (7) build the case that the failure process terminates or does not terminate at that node. This chapter explains steps 1 through 3. Appendix A provides five examples of the entire process.

### **3.1.1 Defining Failure Criteria**

Failure for dams is usually defined as uncontrolled release of the reservoir. This may or may not always be the case, and the purpose and hazard of the structure, as well as agency requirements, may change the definition of failure. In the examples in appendix A, failure is defined as uncontrolled release of the reservoir.

### **3.1.2 Developing Potential Failure Modes**

One person can develop potential failure modes, or a multidisciplined team can. It all depends on the intended use for the potential failure modes and how comprehensive they need to be. A facilitated multi-discipline team is best for developing potential failure modes for a concrete dam because concrete dams are complex structures—as shown in the curved gravity dam under construction in figure 3-1—and synergy develops in a group. A complete understanding of the structure involves team members with specialties in hydrology and hydraulics, seismology, concrete construction, concrete materials, structural stability, foundation materials, rock mechanics, foundation stability, and operations of the dam. The team would consist minimally of a structural engineer, geotechnical engineer, and geologist. The team is greatly enhanced when field personnel are included. Materials engineers are included when there are issues with the concrete or foundation. Specialists in hydrology or seismology are included when these are issues (FERC, 2005).

The team should review initial designs and assumptions, construction records, historic inspections, as-built drawings, material testing, field investigations, rehabilitations, instrumentation data, structural and stability analyses, and current operations. The team brainstorms potential failure modes after reviewing historic data and before visiting the site. The potential failure modes are then reviewed after a site visit. Site inspections would identify new misalignments, deterioration, seepage, plugged drains, and cracking that may not be in the historic records.

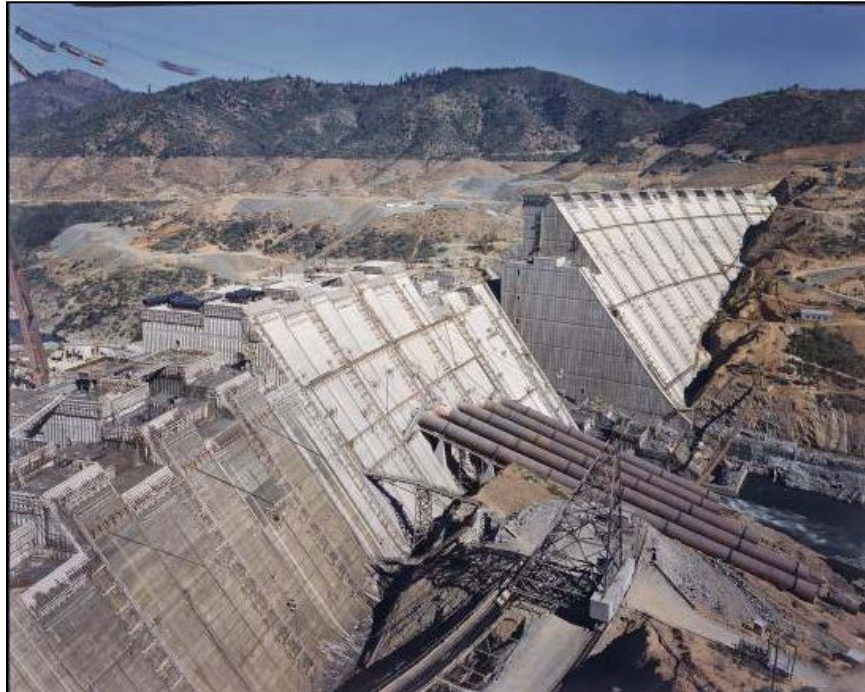


**Figure 3-1: Construction photograph of a curved gravity dam showing the many complex features: contraction joints, shear keys, lift lines, thermal expansions, grouting, foundation discontinuities, material strengths, penstocks through the dam, outlet works, spillway sections, and spillway gates, Bureau of Reclamation.**

Failures start with some initiating event that causes an adverse change in the structure. During normal operating conditions, these actions might be clogging of drains leading to increased uplift pressures, degradation of the grout curtain leading to increased seepage and increased uplift pressures, alkali-aggregate reaction in the concrete leading to reduced concrete strength, or corrosion of the reinforcing steel in a buttress dam leading to reduced capacity of the member. During a hydrologic event, these actions might be a rising reservoir that increases hydrostatic loads on the structure, a rising reservoir that overtops the dam and erodes the foundation, or increasing flow through the spillway that causes cavitation. During a seismic event, increased inertial forces on the structure might lead to overstressing, or displacement of the foundation under the dam could cause overstressing or misalignment. See appendix B for a discussion of loads.

## Selecting Analytic Tools for Concrete Dams to Address Key Events Along Potential Failure Mode Paths

---

There are two basic methods of developing potential failure modes. Both should be used to make sure all modes are captured.

The first method starts with initiating events (or loads) like the ones listed in appendix B, and then determines the impact of the initiating events on the structure (figure 3-2). For instance:

- Increasing reservoir level:
  - Increases stress levels, cracks the dam, and causes the dam to slide
  - Overtops the dam, erodes the abutment, and causes sliding
- Increasing uplift pressure:
  - Reduces the normal force on slide planes and increases the potential for sliding by reducing frictional resistance
- Seismic load:
  - Increases stress levels, cracks the dam, and causes the dam to slide

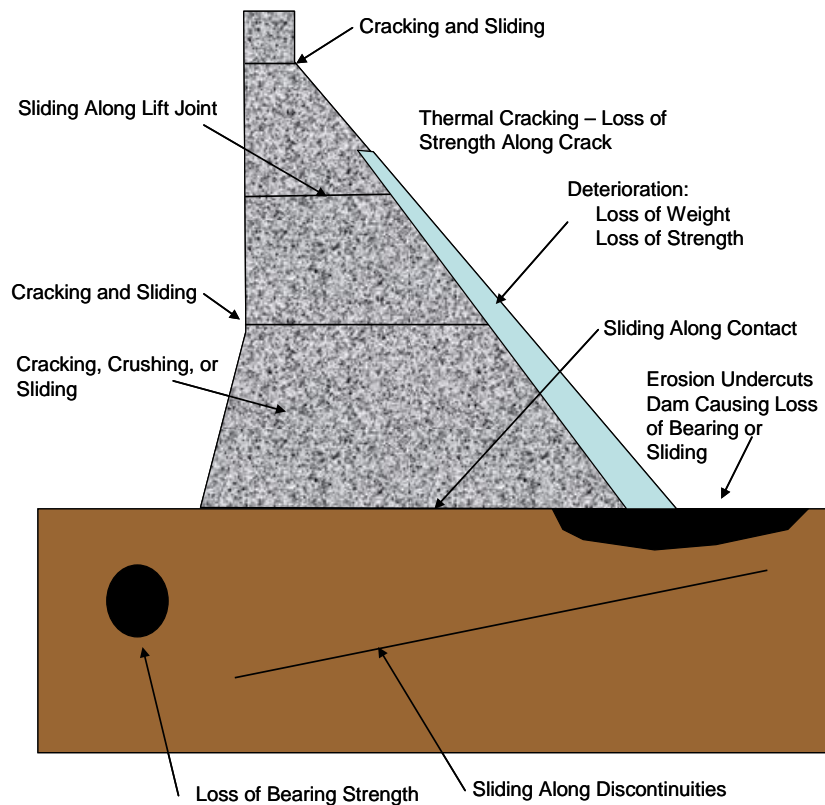


**Figure 3-2: Potential failure modes given an initiating event.**



- Alkali-aggregate reaction:
  - Reduces the strength of the concrete and reduces the load-carrying capacity
  - Expands the concrete mass and binds mechanical equipment
- Human interaction:
  - Causes a spillway gate failure, causing the reservoir to rise
  - Fails to open the spillway gates, causing the reservoir to rise
- Landslide:
  - Causes a large rock mass to move into the reservoir, causing the reservoir to rise
  - Causes a large wave in the reservoir that overtops the dam
- Leaching of foundation material:
  - Reduces the bearing capacity in the foundation, and the dam settles

The second method starts with possible failure modes and then determines what types of loads would cause the failure modes. For example, looking at the concrete gravity dam in figure 3-3, the possible modes of failure and the possible loads that might cause that failure are:

- Sliding along an unbonded lift joint
  - Causes: reservoir water, earthquake, ice, silt, or increase in uplift
- Concentration of stress at upstream change in geometry results in cracking, then sliding
  - Causes: increase in reservoir, ice, silt, or earthquake
- Loss of foundation bearing strength
  - Causes: leaching of material from the foundation mass
  - Causes: piping of soil material due to seepage
  - Causes: erosion of the foundation and undercutting during overtopping
- Sliding along a discontinuity in the foundation
  - Causes: increase in reservoir, earthquake, or increase in uplift
- Loss of material along the downstream face
  - Causes: freeze-thaw damage or overtopping flows

Once potential failure modes were identified, the team would rank the modes and identify the most critical.



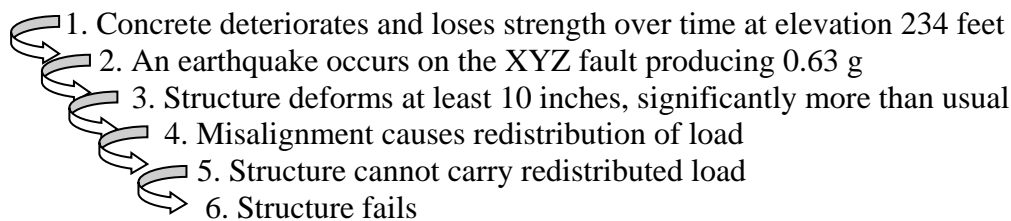
More importantly, developing the entire sequence of events provides a clearer understanding for the structural engineer of what is needed from a structural analysis. In the above example, a structural analysis targeted on node 1 would compute the tensile stress at the heel due to flood loading above elevation 960 feet, on node 2 would compute crack length and uplift pressures, on node 3 would compute sliding factors of safety, or on node 4 would identify mechanisms that might stop sliding if sliding starts.

When describing the sequences of events, it is desirable to have specific details. For example, the following shows an insufficient description and a sufficient description of the sequence of events for a particular potential failure mode:

- Without sufficient detail: Sliding along an unbonded lift joint in the dam.
- With sufficient detail: As a result of high reservoir levels, sliding commences on an unbonded lift joint in buttress number 26 at elevation 950 feet, identified from a coring program in 1995. As the portion of the buttress above elevation 950 feet slides, the minimal reinforcing steel along the lift joint yields, and sliding continues. Differential movement between the buttresses causes misalignment of the upstream face slab. The face slab becomes unseated along the simple support condition along the corbel and face slab. The shear key along the face slab and buttress provides minimal resistance to sliding. The lift joint between slabs opens and eliminates the 3-dimensional (3D) support along the face slab, and the slab fails because of lack of support or overstressing. Breach potentially occurs in two bays on either side of the buttress down to elevation 950 feet.

The following are more examples of initiating events and the sequences that need to occur for failure:

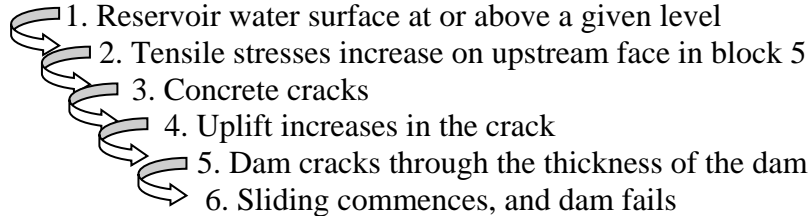
- Deterioration of concrete under all loads: This potential failure mode results from deteriorating and weakening of the concrete at specific locations. The deterioration of the concrete is allowed to progress to the point where the applied loads are greater than the strength of the concrete, and failure occurs. The loads might be during normal operating conditions, during a flood, or during a seismic event. The critical initiating event occurs when the strength of the concrete is less than the applied stress. The structure might fail in different ways, depending on whether the structure is loaded in tension or compression, or by misalignment.

- 
1. Concrete deteriorates and loses strength over time at elevation 234 feet
  2. An earthquake occurs on the XYZ fault producing 0.63 g
  3. Structure deforms at least 10 inches, significantly more than usual
  4. Misalignment causes redistribution of load
  5. Structure cannot carry redistributed load
  6. Structure fails

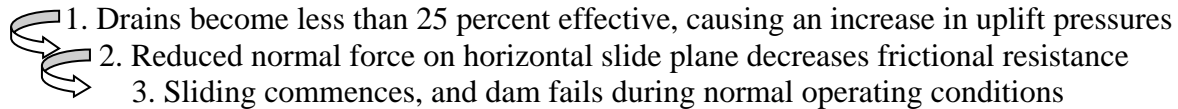
## Selecting Analytic Tools for Concrete Dams to Address Key Events Along Potential Failure Mode Paths

---

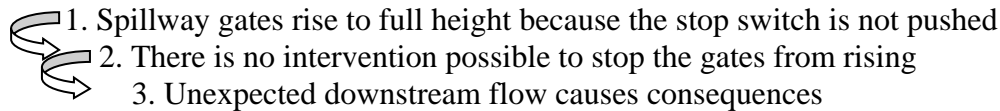
- Flood loading overloads concrete dam: This potential failure mode occurs during a flood when increased water and uplift overload the dam causing cracking of concrete to the point that the dam fails by sliding.



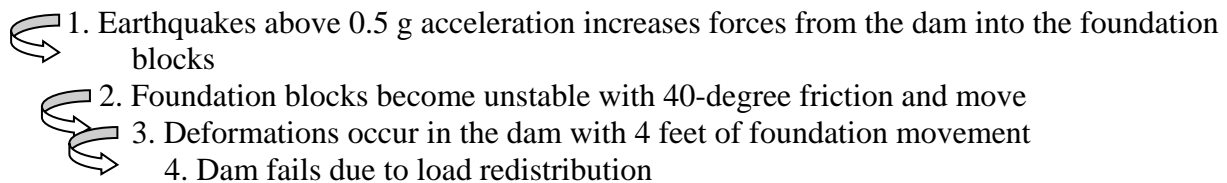
- Uplift increases under concrete dam: This potential failure mode occurs when the drains in the dam become ineffective due to plugging and uplift pressures increase under the dam. The normal force along a horizontal slide plane reduces the frictional resistance, and the dam fails due to sliding.



- Human error when operating spillway: This potential failure mode occurs when there is a human error when operating a spillway gate. In this case, a mechanism is initiated that raises the gates to their full height without the ability to stop the gate from rising. There is uncontrolled release through the spillway.



- Earthquake overloads foundation blocks and causes failure of dam: This potential failure mode is caused by an earthquake that increases loads from the dam into the foundation and also causes inertia forces of the foundation blocks. It has been established that there are removable foundation blocks in the abutment.



### 3.1.4 Event Trees

An event tree is a graphical representation of the potential progression of failure engineer. It provides an efficient way to organize the chronological sequence of events for a particular

potential failure mode from the initiating cause on the left, through a series of linked events (nodes or branches), to the failure or no failure condition on the right (see figure 3-4). Each node represents an event or condition with possible outcomes or states that need to exist for failure to ultimately occur or not occur.

Event trees can be developed in a qualitative sense without assigning probabilities and used in a failure-modes-and-effects analysis. The same qualitative event trees can be used and expanded in a quantitative risk analysis. Event trees are easily understood because they portray the chronological sequence of events that must occur for failure to happen. Event trees aid in understanding of the steps needed in a potential failure mode. This decomposition aids in the structural analyst's understanding the failure mode and also in briefings to management.

### **3.1.4.1 Advantages**

Event trees have the advantage of being:

- Well suited for displaying the chronological order of events
- Well suited for displaying dependencies between events and in which order they occur
- Able to facilitate communication about assumptions in developing the model
- Easily understood by managers
- Well suited to display details of the problem
- Drawn on standard computer spreadsheets or specialty software
- Intuitive because the events from left to right are the sequence of events that occur given the previous event or condition to the left

### **3.1.4.2 General Principles**

Event trees visually show the sequence of events leading to failure. Event trees also follow the basic principles of probability theory and can be used to quantify the probability of the failure mode if likelihoods are assigned at each node of the event tree. This document describes potential failure modes and associated structural analysis. This document does not discuss probability or risks, but the following list shows how an event tree can be used to quantify risks.

- Each branch from a node must be mutually exclusive from the other events so that there is no overlap in probability between branches. In other words, probabilities for events emanating from a single node of an event tree add to 1.

## Selecting Analytic Tools for Concrete Dams to Address Key Events Along Potential Failure Mode Paths

---

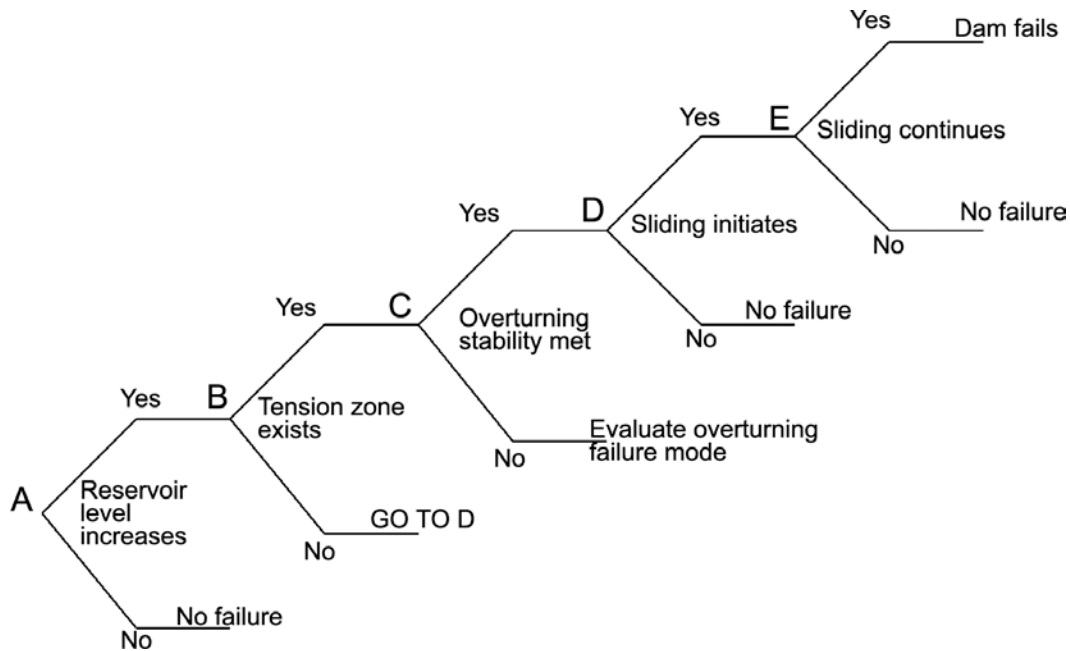


Figure 3-4: Event tree. In this example, increased reservoir load could cause sliding instability.

- Probabilities are positive. There is no such thing as a negative probability.
- If probabilities are assigned to a node, the probabilities are between 0 and 1. In percent, this is between 0 and 100 percent. There is no such thing as a 110-percent chance of an event occurring.
- If probabilities are assigned to nodes, the probabilities along each path can be multiplied together from left to right. The product of multiplying probabilities along a path is the probability of occurrence of that event.
- If probabilities are assigned to an event tree, adding the products of all the failure paths in the event tree for a given initiating condition or event gives the probability of having a failure due to the initiating event.
- The occurrence of every event in the tree is conditional on the event to the left having occurred.

An initiating event could produce multiple failure modes. For example, a flood may produce sliding or overturning in a gravity dam. Each potential failure mode requires its own tree.

## 4.1 Relating Analyses to Failure Modes

Analyzing potential failure modes allows the engineer to characterize how a structure might fail and identify the sequence of events leading to failure. Structural analysis is used to determine the structural response of a given node. For instance, the first event might be that an increased load causes the concrete to crack. There are various methods to determine if the concrete will crack, such as structural analysis, physical testing, or scale-model testing. Structural analysis uses either limit equilibrium analysis or various types of finite element methods (FEM), namely, 2-dimensional (2D) linear elastic, 2D nonlinear, 3D linear elastic, or 3D nonlinear.

It must be realized that each one of these analysis methods has a certain level of applicability and represents a certain level of reality. Table 4-1 summarizes the applicability of different analysis techniques. The technique chosen should be the one that answers the specific question being asked with minimum effort. These methods also vary greatly in cost, difficulty, and level of effort as generally indicated in table 4-2. Of course, these indicators depend on the availability of finite element mesh generators, post-processing capabilities, and the experience of the structural analyst. The acceptability of the results depends on the acceptability of the material properties being used, the acceptability of the loading condition, and the way the structure was modeled. An assumed, yet conservative, material property may be sufficient without testing to satisfy stability requirements. However, more importantly, applicability of the analysis method being used depends on the question being asked.

The following examples compare and contrast different analysis techniques as they are applied to the same dam.

### 4.1.1 Limit Equilibrium Analysis

Traditionally, analyses of the stability of dams were based on a set of assumed failure modes. The failure modes consisted of rigid body motions that were kinematically admissible. If force and moment equilibrium could be satisfied within the limits of the foundation and concrete strength, the dam was considered stable.

Figure 4-1 and table 4-3 show the results of a conventional 2D limit equilibrium analysis. In this case, stability means that the resultant vector lies within the footprint of the dam, so that rigid body overturning will not occur, and that the resultant intersects the foundation at an angle that is not more acute than the foundation friction angle, thus preventing sliding.

When applicable, limit equilibrium analyses provide unambiguous answers to the question of dam stability because they presuppose a failure mode and then evaluate its possibility. Their results are easily understood and can be presented concisely as shown in table 4-3. They are attractive for this reason.

## Selecting Analytic Tools for Concrete Dams to Address Key Events Along Potential Failure Mode Paths

**Table 4-1: Limitations of structural analysis methods to compute the structural response for various sequences of events of a potential failure mode**

<b>Initiating event:</b> Earthquake <b>Failure mode:</b> Sliding in a concrete gravity dam					
<b>Sequence of events initiated by seismic loading</b>					
	Upstream cracks appear	Cracks penetrate through dam	Sliding begins	Duration of shaking fails dam	Dam fails after earthquake
<b>Considerations for types of analyses / capability</b>					
<b>Method</b>	<b>Can upstream stresses be computed?</b>	<b>Can the analysis show if the dam cracks through?</b>	<b>Can analysis show if the dam slides given loads and shear strengths?</b>	<b>Can analysis show how far the dam can slide?</b>	<b>Can the analysis perform a post-seismic stability study?</b>
Limit equilibrium	Yes, assumes plane sections remain plane, so lacks accuracy	Yes, pre-supposes crack	Yes, it can determine if sliding commences	Yes, using a Newmark type approach	Yes, only sliding factor of safety computed
2D FEM linear	Yes, includes flexibility but no 3D effects	No, computed stresses can be higher than the strength	No, only sliding factor of safety computed by integrating stresses	No, unrealistic linear strength carries all imposed loads	No, only sliding factor of safety computed by integrating stresses
2D FEM nonlinear	Yes, includes 2D flexibility and nonlinear but no 3D effects	Yes, but 3D effects not included	Yes, but 3D effects not included	Yes, but 3D effects not included	Yes, but 3D effects not included
3D FEM linear	Yes, includes 3D flexibility but no nonlinearity	No, computed stresses can be higher than the strength	No, only sliding factor of safety computed by integrating stresses	No, unrealistic linear strength carries all imposed loads	No, only sliding factor of safety computed by integrating stresses
3D FEM nonlinear	Yes, best available, includes 3D flexibility and nonlinearity	Yes, best available	Yes, best available	Yes, best available	Yes, best available



**Table 4-2: General differences in various structural analysis methods**

Method	Cost	Difficulty: easy (x); difficult (xxxxxxxxx)	Time to complete
Limit equilibrium	\$	x	Hours
2D FEM linear	\$\$	xxx	Days
2D FEM nonlinear	\$\$\$	xxxxx	Weeks
3D FEM linear	\$\$\$\$	xxxxxxx	Month
3D FEM nonlinear	\$\$\$\$\$	xxxxxxxxx	Months

Note: Cost, difficulty, and timeframe symbols are general qualitative indicators and not directly relatable to each other. For instance, \$\$\$ does not indicate 3 times the cost of \$. The ratings depend on the level of expertise of the engineer, on the availability of the software and preprocessors, and on having the input ready to go.

The 2D gravity dam analysis shown below is accurate if the underlying assumptions apply to the case being studied. A few of these underlying assumptions need to be considered, in particular that:

- The base of the dam is approximately planar
- Normal stress distribution on the dam base is trapezoidal
- Tension between the base and foundation is not allowed
- 2D analysis is appropriate

### **4.1.2 Linear Finite Element Analyses**

Linear analyses have a critical role in structural analysis toolboxes. Results from linear finite element analyses provide an essential baseline to compare to nonlinear analyses, determine the natural frequency of the structure, and provide stresses and displacements in the dam for behavior in the linear range of behavior. If results stay in the linear range, it is not necessary to conduct nonlinear analyses. Nonlinear analyses run in “linear mode” should produce results comparable to linear analysis results. Computed stress levels that are unrealistic or well into the nonlinear range of the material justify performing nonlinear analyses.

Linear finite element analyses in the dynamic realm are useful in determining natural frequencies of vibration and mode shapes. This information is useful in selecting site-specific ground motions.

## Selecting Analytic Tools for Concrete Dams to Address Key Events Along Potential Failure Mode Paths

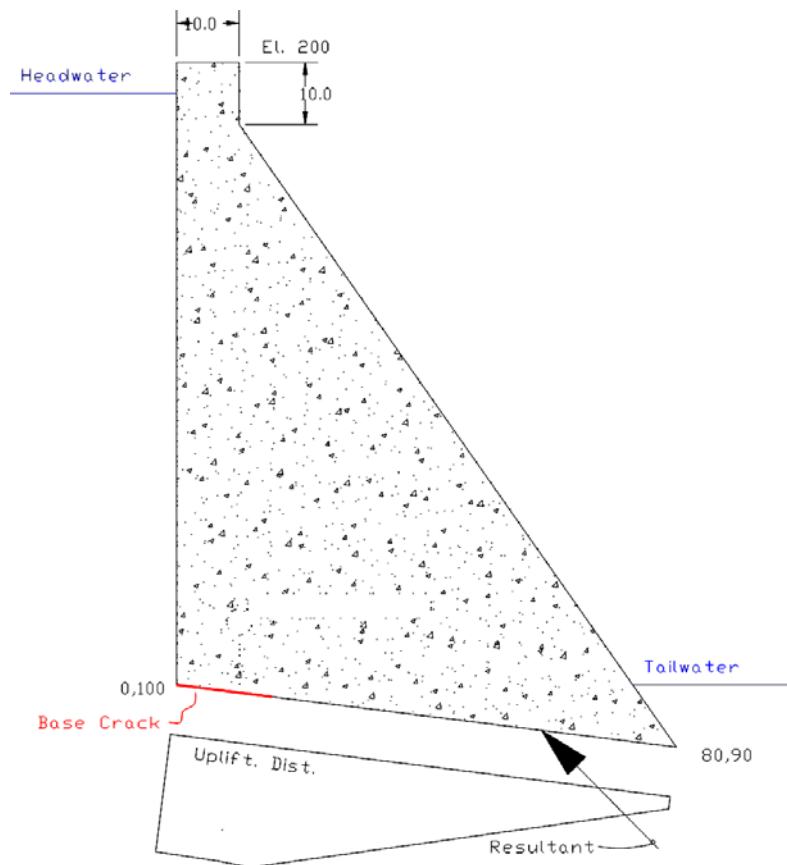


Figure 4-1: Limit equilibrium analysis.

Table 4-3: Results of limit equilibrium analysis

Force	Fx (kip)	Y= (ft)	Fy (kip)	X= (ft)	Moment (0,0) (kip-ft)
Dam weight	0.00	0.00	-630.00	26.55	16,725.00
Headwater	281.58	131.67	0.00	0.00	37,074.70
Tailwater	-3.12	93.33	-2.18	77.67	-121.58
Uplift	38.74	96.30	309.94	29.63	-5,451.91
Totals	317.20		-322.24		48,226.21

Notes:

1. Resultant location at X = 58.4 ft, Y = 92.7 ft, 19 percent of base cracked
2. Sliding safety factor = 0.79, 51.6 degrees required for factor of 1.0
3. Input parameters:
  - Concrete unit weight = 0.15 kip/ft<sup>3</sup>
  - Foundation friction angle = 45 degrees
  - Head/tailwater elevations = 195/100 ft

kip = 1,000 pounds, ft = feet, kip-ft = 1,000 pound-feet, kip/ft<sup>3</sup> = 1,000 pounds per cubic foot

However, linear finite element analysis does not address failure. It answers a different question, providing stresses and deflections subject to a different set of assumptions. The assumption underlying linear finite element analysis is that the dam and foundation form a continuous, linear, elastic solid. Cracking, crushing, or slipping cannot be directly modeled. Because it is not sufficient in itself to evaluate a dam at impending failure, it cannot be compared directly with limit equilibrium analysis. Tension (sometimes unrealistic tension) is allowed between the dam and foundation. However, even with these limitations, linear finite element analysis can provide some insight into dam behavior. For dynamic loading, the vibration mode shapes and natural frequencies generated by linear analysis are of some interest. For reinforced concrete structures such as slab and buttress dams, moment and force resultants from linear models are useful in evaluating the adequacy of members.

A linear finite element analysis of the dam depicted in figure 4-1 is shown in figure 4-2. Because there is an assumption of elastic continuity between the dam and the foundation, uplift is assumed to vary linearly from headwater to tailwater. Note that in figure 4-2, tensile stress develops at the heel of the dam. A stress singularity occurs at the reentrant corner. The question that suggests itself is, “Will cracking occur as a result of this tension?” This question was disallowed in the limit equilibrium analysis because one of the initial assumptions was a trapezoidal base pressure distribution with no tension.

Answering the question of whether cracking will occur does not specifically address any failure mode. All concrete dams have cracks in them, and the fact that an analysis indicates a crack is likely at the upstream heel is not in itself conclusive. What is of some interest is the distribution of shear and normal stresses that the finite element analysis reveals (see figure 4-3).

Note that the normal stress is not trapezoidal as was assumed in the limit equilibrium analysis. There is a large tensile peak near the heel, as was evident in the principal stress vector plot in figure 4-2. Also, there is a compressive spike near the toe. The shear stress variation, which is not typically dealt with in limit state analysis, has peaks near the heel and toe of the dam that are over twice the average shear stress. If cohesion were relied upon for stability, the cohesive shear strength would have to be in excess of the highest peak shear stress, not just the average. Note also that the high shear stress near the heel is in a tensile region.

Limit equilibrium analysis evaluates failure modes (sliding and overturning) subject to a base pressure distribution that may not be very accurate. Linear finite element analysis provides more detailed information about stress distributions, but does not allow for redistribution of stress due to cracking. It also computes where possibly unsustainable tension and shear stresses are likely to develop in areas of the dam base.

### **4.1.3 Nonlinear Finite Element Analyses**

There are several types of nonlinearity. For this discussion, we will focus on the effects of cracks. Cracks can open in the presence of tensile stresses, and sliding can occur along cracks. These are the nonlinear effects that will be considered.

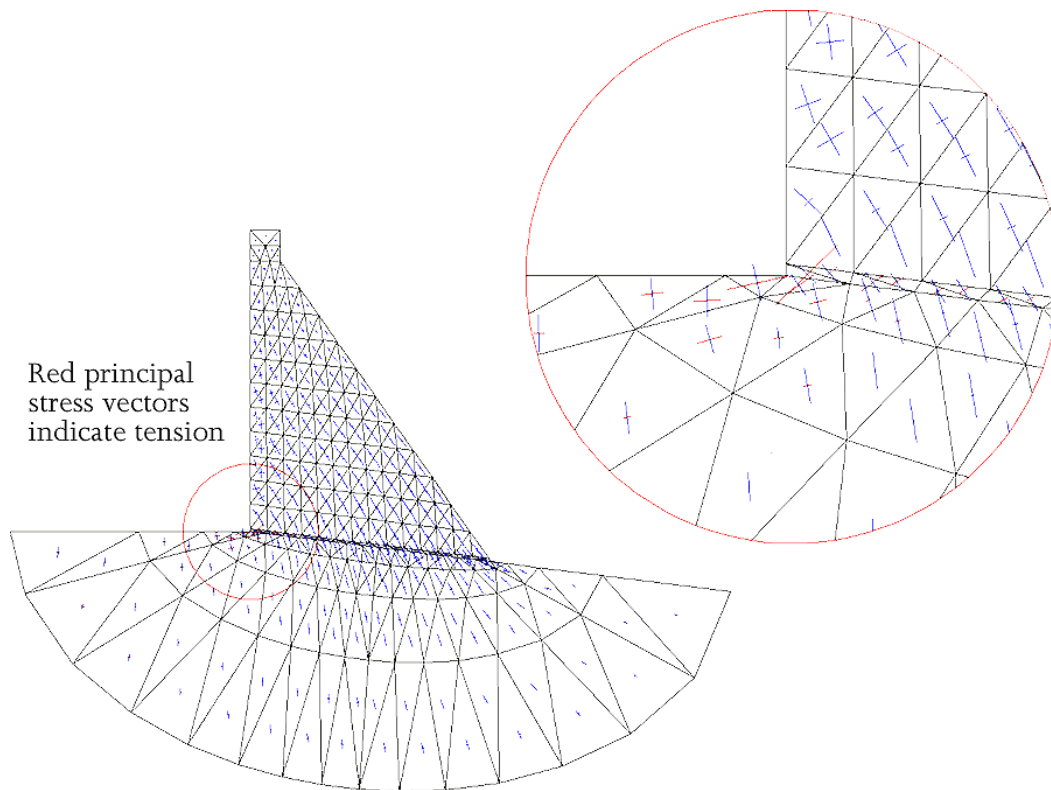


Figure 4-2: Linear finite element model: principal stress vectors.

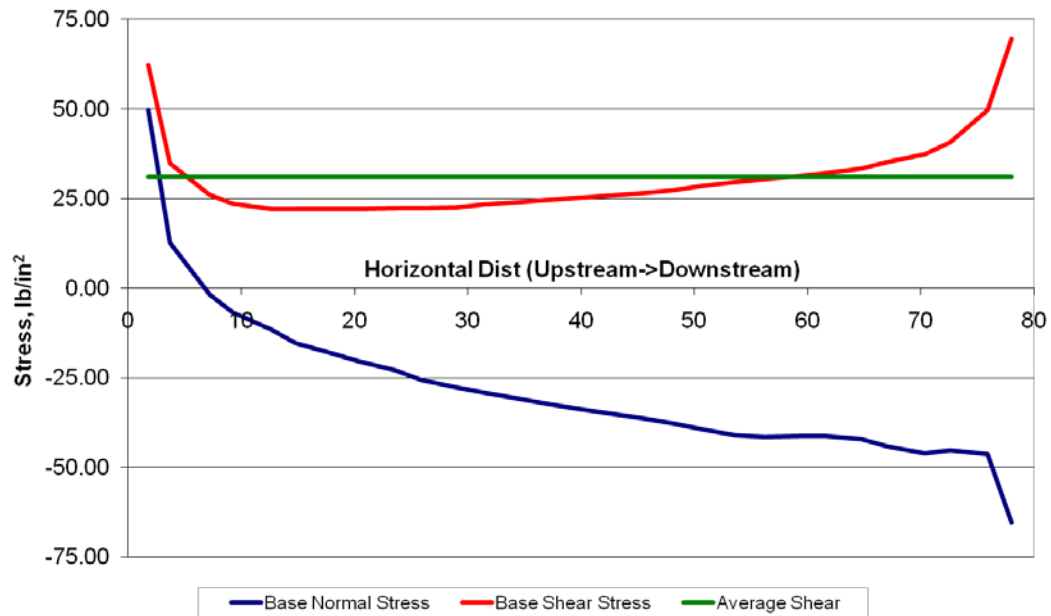
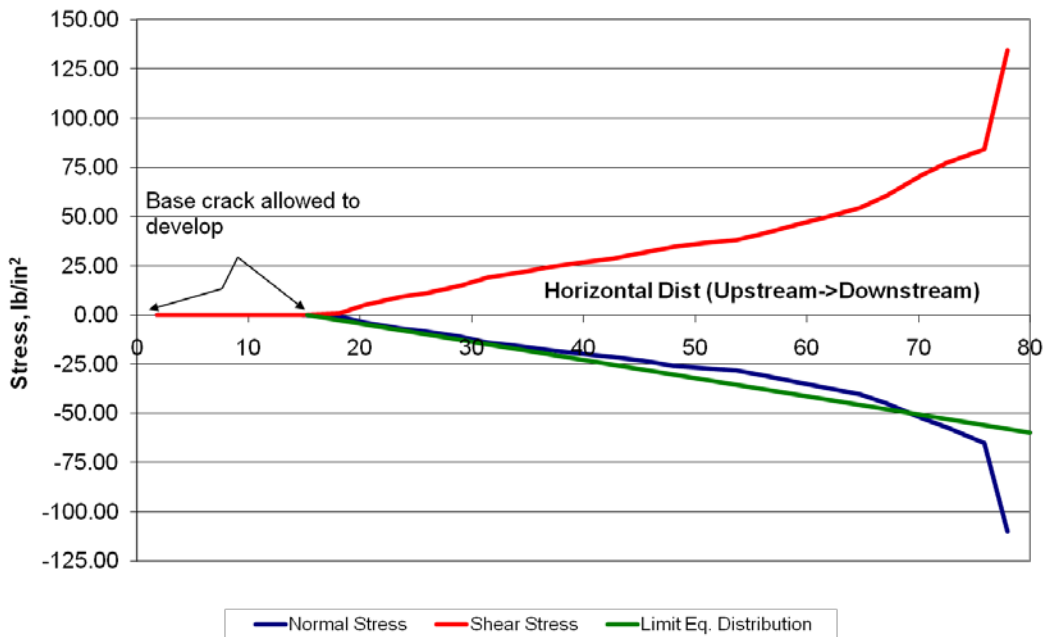


Figure 4-3: Base stress from linear finite element analysis.

If a finite element model that allows base cracking and sliding to develop is used to analyze the same dam under the same loading condition, the results will be more in line with the original limit equilibrium analysis described in section 4.1. Figure 4-4 shows base contact stress as determined by a nonlinear finite element model with interface elements. Note the assumed trapezoidal base pressure distribution from the limit equilibrium model (green line) plotted for comparison. The length of base cracking calculated by the nonlinear finite element solution (18 feet) is similar to that calculated by the limit equilibrium method (15 feet). The base normal stress distributions are similar with the exception of the area near the toe of the dam, where the finite element analysis indicates a local compressive stress peak.



**Figure 4-4: Base stress from nonlinear finite element analyses and limit equilibrium analysis.**

Since there is close agreement between the limit equilibrium and nonlinear finite element analysis, one might question the merits of nonlinear finite element analysis. It is more difficult to perform, and while it comes closer to modeling the failure state of a dam, as the actual limiting condition is approached, the nonlinear finite element solution fails to close. Therefore, a clear factor of safety cannot be given. All one can say is that the solution closed at a friction angle greater than the minimum friction angle required for a safety factor of 1.0. In this case, the analysis failed to close at base friction angles below 53.5 degrees. (Remember that the limit equilibrium analysis showed that 51.6 degrees was required for stability.) In this example, limit state analysis provided the best results and should be considered perfectly adequate for analysis of this dam.

The value of nonlinear finite element solutions becomes apparent when the failure mechanism cannot be reduced to a simple, statically determinate, rigid body movement. Consider the case depicted in figure 4-5. Here, an irregular base changes the failure mode.

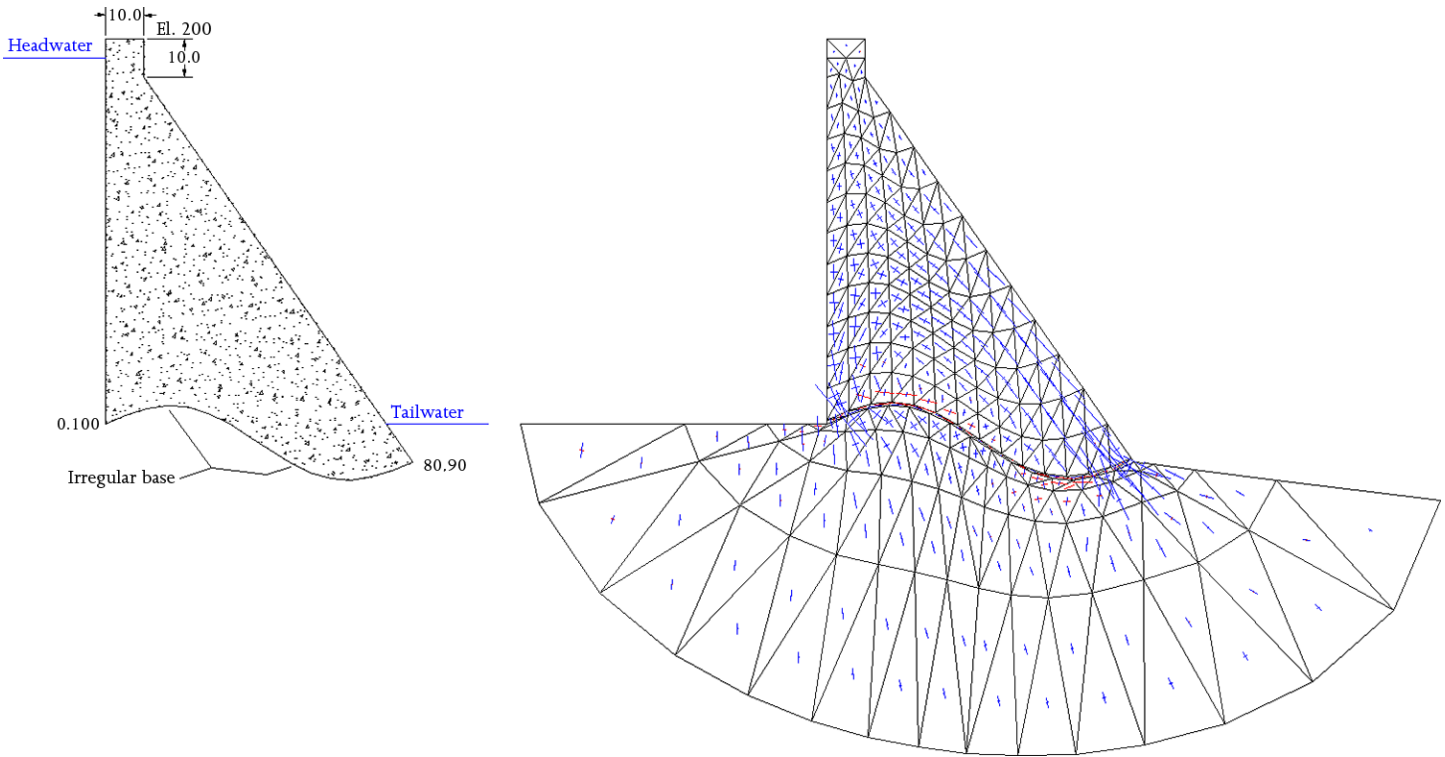


**Figure 4-5: Irregular base with nonlinear finite element analyses.**

For the structure to fail, it has to slide up and over foundation irregularities or shear through intact concrete or foundation rock. The distribution of shear and normal forces reflects this (figure 4-6). Note that between 10 and 65 feet, the dam separates from the foundation because of the shape of the contact and the downstream direction of sliding.

In this case, the friction angle required for solution closure is 18.3 degrees. If the irregularity of the dam-to-foundation contact is ignored and a planar failure surface is assumed, 51.6 degrees is what is required for stability (see figure 4-1). Clearly, this is a big difference. Note also that at incipient failure, the peak normal stress is 250 pounds per square inch ( $\text{lb}/\text{in}^2$ ) compression, which is small with respect to typical concrete compressive strengths, but is still over four times the value given by the limit equilibrium solution with a planar base.

In reality, failure surfaces are seldom easily analyzed planes or circular arcs. In addition, if 3D effects such as curvature in plan and narrow valley geometry are significant, finite element analysis with nonlinear contact elements is best for modeling these failure mechanisms.

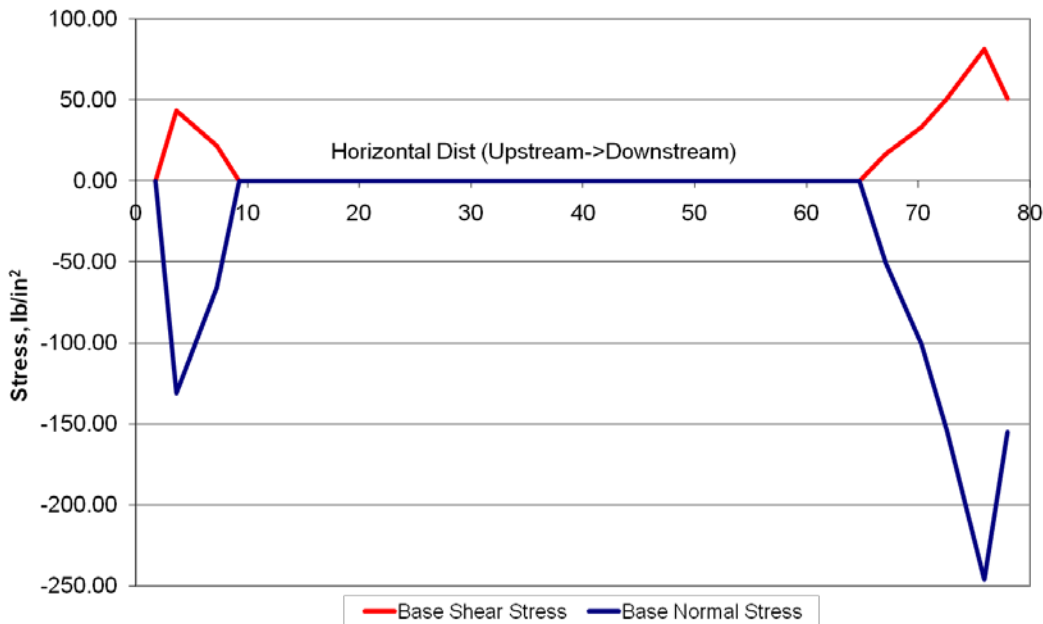


**Figure 4-6: Results from irregular base with nonlinear finite element analyses.**

#### 4.1.4 Static and Dynamic Analyses

Loads that are applied at a rate comparable to the natural frequency of the structure (several hertz) are considered dynamic. It is a misconception to refer to short-term static loading as dynamic. Sustained loads that last for longer than a minute are static. Therefore, flood loading, no matter how short the duration, is static and should be treated as any other static load.

Seismic loading and, in some cases, loading from impact, are the typical dynamic loads that can affect a dam. Because of the oscillatory nature of seismic loading, it is not appropriate to apply instantaneous peak dynamic loading to the structure as if these loads were static. The example in figure 4-7 shows the problem with this approach. The dam from figure 4-1 is loaded with a peak horizontal acceleration of 0.365 g. In addition to the normal static loads, the horizontal inertia of the dam and the hydrodynamic pressure according to Westergaard are applied, and the calculation results are listed in table 4-4. Note that the resultant moves about 98 feet outside the base of the dam, indicating that the dam will overturn.

But this is clearly a ridiculous result, because the dam cannot overturn in the fraction of a second that this set of loads implies. A few hundredths of a second later, the dynamic loading would be reversed, and the resultant would move well back inside the dam footprint.

## Selecting Analytic Tools for Concrete Dams to Address Key Events Along Potential Failure Mode Paths

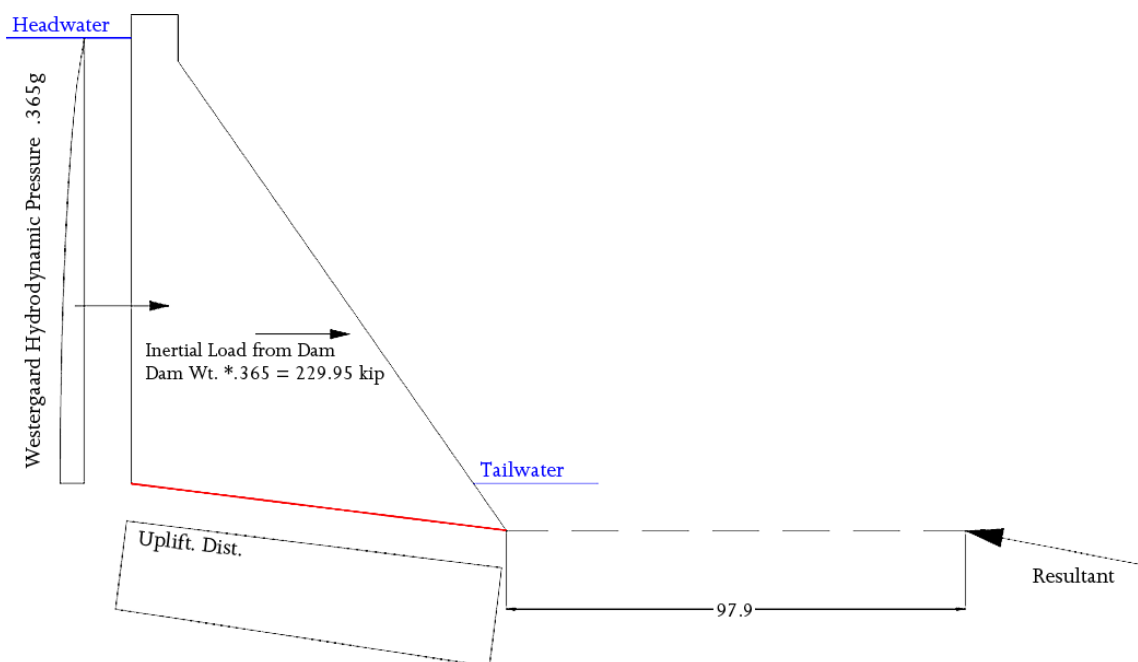


Figure 4-7: Results from applying instantaneous peak dynamic loads.

Table 4-4: Forces, centroids, and moment

Force	F <sub>x</sub> (kip)	Y= (ft)	F <sub>y</sub> (kip)	X= (ft)	Moment (0,0) (kip-ft)
Dam weight	0.00	0.00	-630.00	26.55	16,725.00
Headwater	281.58	131.67	0.00	0.00	37,074.70
Tailwater	-3.12	93.33	-2.18	77.67	-121.58
Uplift	62.74	94.91	501.93	40.75	-14,500.99
Dam inertia	229.95	131.87	0.00	0.00	30,322.36
Westergaard	105.00	137.90	0.00	0.00	14,480.00
Totals	676.2		-130.3		83,979.5

What the above analysis does indicate is that seismic loading would likely damage the contact between the dam and foundation, leaving a damaged dam to resist post-earthquake static loads. As a result of the instantaneous opening and closing of a foundation crack, post-earthquake uplift may be higher. Shear strength between the dam and foundation may be reduced.

Appendix A2 presents a detailed example of a seismically related failure including all appropriate analyses.



### **4.1.5 The Role of Standards-Based Criteria and Codes**

The discussion above focused on failure modes and how to analyze them. All these analyses are attempting to determine the load set and downgraded material strength assumptions that would bring the dam to a state of incipient failure. All other states are then compared to this limit state. Building codes such as the American Concrete Institute (ACI) 318, ACI 350, American Society of Civil Engineers 7, and codes from the American Institute of Steel Construction attempt to ensure that failure states are never approached, let alone exceeded. Allowable loading is often further limited by other considerations such as durability or stiffness. It must be understood that exceeding values from code calculations does not necessarily indicate failure. Also, design codes presuppose a class of structures. For example, ACI 318 presupposes concrete beams, columns, walls, and floor slab-type elements whose behavior is governed by beam theory and Kirchhoff-Love plate theory. Unreinforced massive concrete structures are not directly addressed.

Codes are generally used for the design of new structures; the designer uses strength reduction factors to attain levels of safety. By contrast, the response of existing structures to initiating events for given potential failure modes is assessed without strength reduction factors or load factors to compute the “true” strength or limit state of the structure.

These codes are valuable if the dam or dam appurtenances are of the form that the codes envisioned. For example, a slab and buttress dam is more similar to a reinforced concrete office building than to a massive gravity dam. In such a case, ACI 318 and ACI 350 are very valuable. It would be prudent to evaluate the acceptability of such a dam using the ACI code for the strength limit state.

In short, building codes are helpful when analyzing structures of the form for which they were intended. They should be a source of information when assessing the various structural elements of concrete dams.

## **5.1 Focusing on Parameters Affecting Analysis**

Evaluation of dam structures requires that the engineer make assumptions and use various parameters and analysis methods to develop a reasonably accurate representation of structural behavior. The impacts of particular parameters on analysis results vary based on the type of analysis being performed. Some typical structural parameters are:

- Joint friction angle and cohesion (concrete and rock)
- Modulus of elasticity (concrete and rock)
- Poisson’s ratio (concrete and rock)
- Coefficient of thermal expansion (concrete)

## Selecting Analytic Tools for Concrete Dams to Address Key Events Along Potential Failure Mode Paths

---

- Unit weight (concrete, rock, and water)
- Damping (system)
- Geometry (dam and foundation)
- Mesh coarseness (dam, foundation, and water)
- Boundary conditions (foundation and reservoir)

Accurate determination of parameters is often a daunting task. For example, to determine the shear strength to be used in a sliding analysis, a coring program through the joint must be undertaken. A sample must be recovered intact and relatively undisturbed. If asperities, roughness on a joint plane, are to be considered, the sample must be large enough to capture the asperities. One sample can be tested multiple times, but it will only yield peak shear strength on its initial shearing. Sufficient samples must be obtained to account for the normal variation.

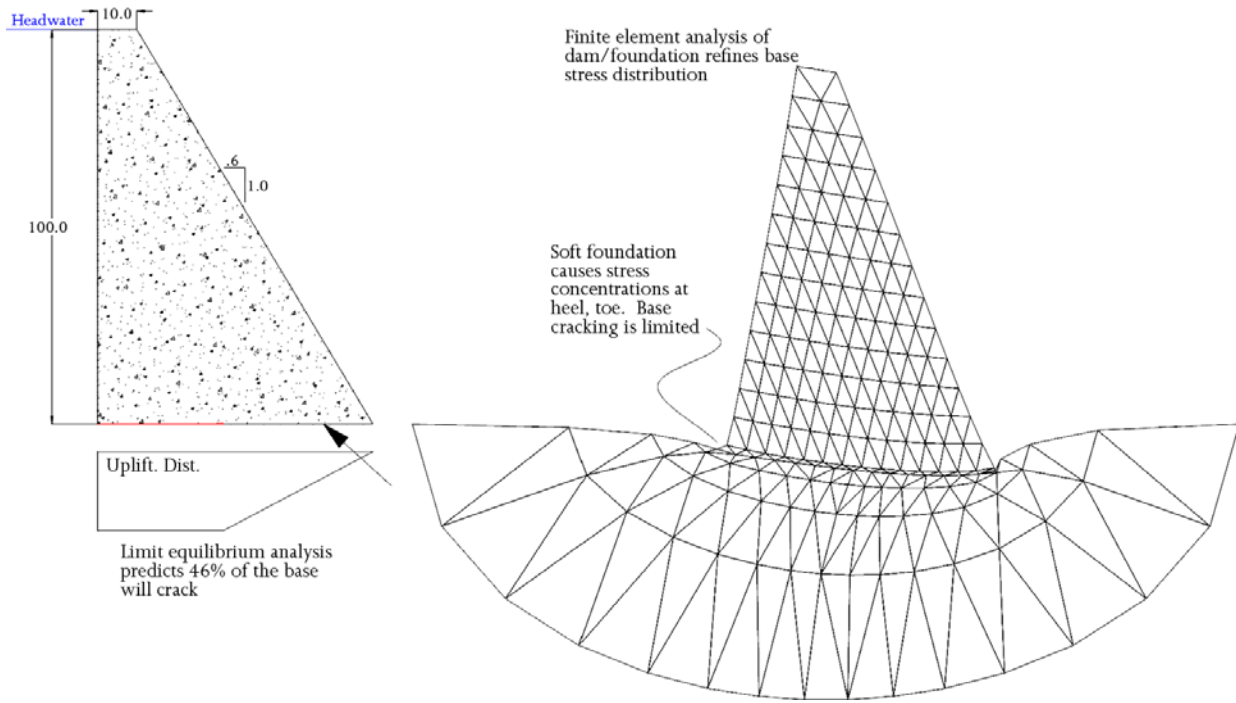
Because of the difficulty in recovering and testing statistically significant samples, it behooves the analyst to understand what effect parameter variation would have on analysis results. Some parameters have little effect on analysis outcome and therefore do not need to be determined with great accuracy. Some parameters are important while others will make very little difference on the analysis results or ultimately, the risk estimation.

Consider the effect of the modulus of elasticity on the predicted base cracking in a gravity dam. For this specific example, the limit equilibrium gravity analysis of the section in figure 5-1 indicates that 46 percent of the base would crack. However, an analyst may want to consider the effect of dam/foundation interaction. To do this, the moduli of elasticity of both the dam and foundation are required. Foundation elasticity is difficult to determine because rock masses are jointed and nonhomogeneous. An NX core sample (i.e., a 2.36-inch-diameter core) can be tested, but the value of the modulus obtained from such an exercise may not be indicative of foundation behavior. While there are several methods to determine the rock mass modulus, it may not be necessary, as discussed below.

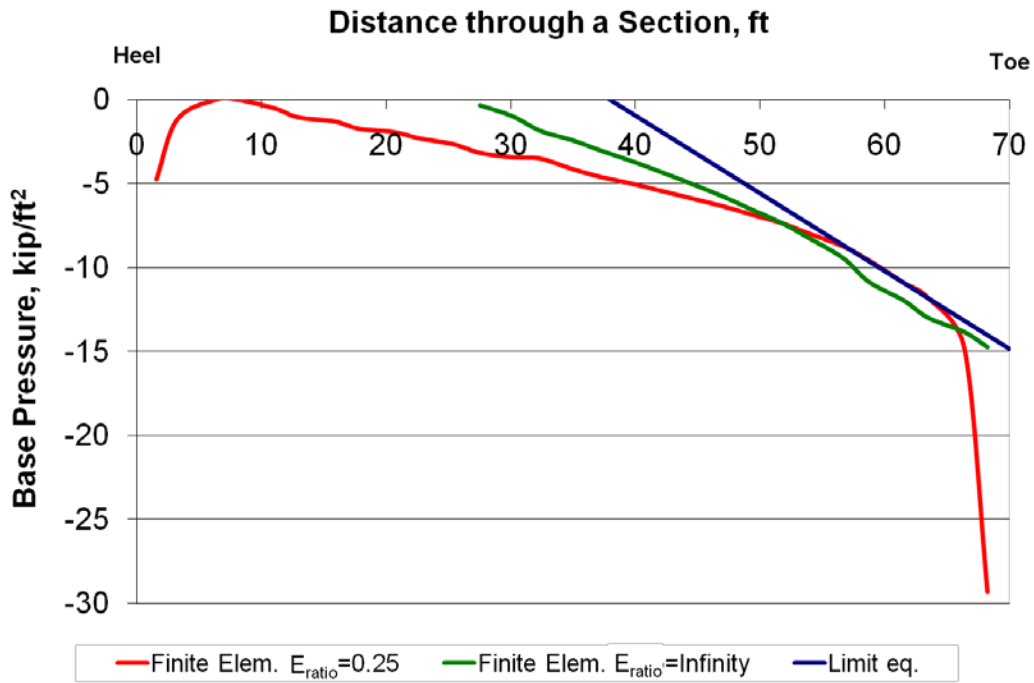
One point that should be understood is that the outcome of the analysis is contingent on the ratio of the rock modulus to the dam modulus,  $E_{\text{ratio}}$ . Absolute values do not matter. This means that, analytically, one can worry about varying just one parameter instead of two. Analyses can then be done varying the ratio with the results discussed below.

Figure 5-2 shows that when the foundation is soft with respect to the concrete dam ( $E_{\text{rock}}/E_{\text{conc}} = E_{\text{ratio}} = 0.25$ ), the entire foundation contact is in compression. When the foundation is infinitely stiff, the base pressure distribution starts to resemble that assumed in the limit equilibrium gravity analysis. Figure 5-3 shows the variation of calculated base cracking with respect to modular ratio.

**Selecting Analytic Tools for Concrete Dams to Address Key Events Along Potential Failure Mode Paths**



**Figure 5-1: Base cracking example.**



**Figure 5-2: Base pressure distribution through a section of a concrete dam.**

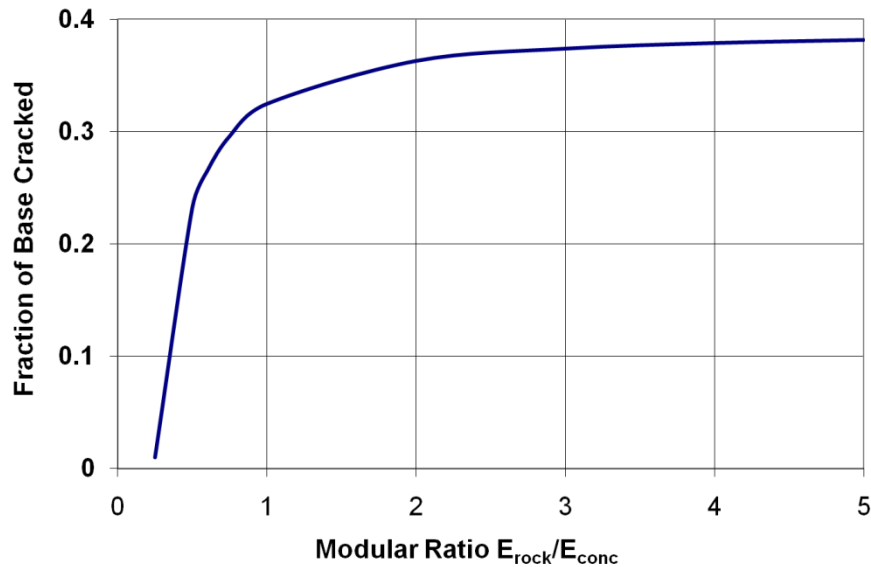


**Figure 5-3: Modular ratio effects (note that this curve is specific for the example cited).**

Note that if the foundation is as stiff as the dam or stiffer, predicted base cracking changes very little. Therefore, accurate determination of foundation stiffness is not important in this range. However, if the foundation is soft with respect to the modulus of the dam, the effect of the modular ratio is considerable. In such a situation, accurate determination of the modular ratio matters a great deal.

What has been presented here with respect to modular ratio pertains only to its effect on static analysis and base cracking. Absolute values of foundation and dam elastic moduli can be important in a dynamic analysis.

The modular ratio was the only parameter considered in depth here, but what can be noted about this parameter's effect is instructive in dealing with all parameters.

### 5.1.1 Common Errors

Below are presented a few common errors surrounding modeling assumptions. This is not an exhaustive list; rather, it is an attempt to pass on what has been learned through particular mistakes.

### 5.1.1.1 Unrealistic Boundary Conditions

Boundary conditions specified incorrectly in finite element models can lead to significant error. If the foundation is represented by solid finite elements, the extent of the foundation modeled should be validated to ensure that the boundary conditions do not affect the results. The example in figure 5-4 is an analysis of a buttress arch dam.

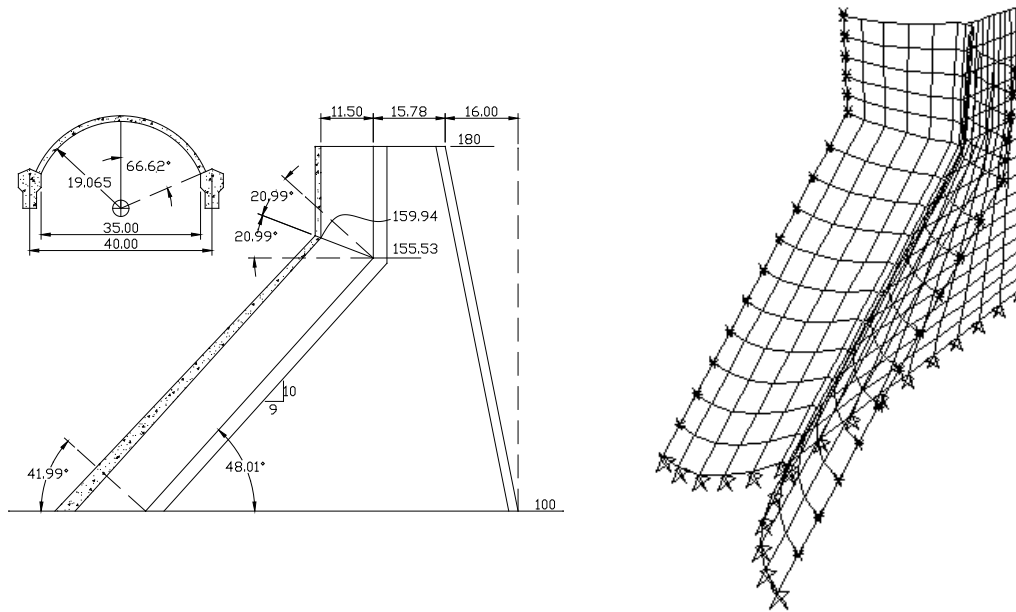


**Figure 5-4: Buttress dam finite element idealization.**

Dams may span entire valleys. Often, a buttress arch dam has dozens of buttresses. The analyst can often simplify the task by analyzing one representative bay. Boundary conditions for the idealized model must constrain degrees of freedom so that the effects of the bays on either side of the idealization are taken into account. A simplified model may not be appropriate in the cross-valley direction during seismic analyses because adjacent buttresses provide restraint somewhere between a fixed and free conditions.

For loading in the downstream direction, one would expect that rotations about the crown of each arch would be zero; therefore, rotation vectors in the downstream and upward planes must be fixed. Also, at the crowns, deflection in the cross-valley direction should be fixed since it is resisted by the neighboring bays. If cross-valley loading is to be considered, translation in the downstream and the upward directions should be fixed, and cross-valley axis translation should be free. Rotation in the downstream and the upward directions must also be free. If both the downstream axis and cross-valley axis loading are to be considered, it may be better to model the entire dam, since boundary conditions can become mutually exclusive.

The base of the buttress should be fixed with respect to all translation; however, the analyst has a choice about rotational fixity. If rotation about the upstream/downstream axis is fixed, bending moments at the foundation can develop. If the buttress has no physical means of transmitting moments into the foundation (i.e., if it is not doweled in), rotational fixity should not be assumed.

Boundary conditions at the bottom of the arches are similar to those at the bottom of the buttresses. Rotational fixity in the downstream and cross-valley planes should only be assumed if the connection of the arch to the foundation is capable of significant moment transfer.

In general, boundary conditions must represent real field conditions as much as possible. Fixity should not be assumed in a model when it does not exist in the real dam. Freedom should not be assumed when it is inhibited.

### **5.1.1.2 Finite Element Mesh Density**

Poor mesh geometry can cause significant error in finite element analysis. An element's displacement field dictates how well it can assume the required deformed shape for a given loading condition. All finite element methods will converge to the theoretical deformed shape and corresponding stress field as element size approaches zero. It is tempting for the modeler to use extremely fine meshes. Postprocessors produce stresses and deflections in graphical form, so the analyst is no longer required to wade through hundreds of pages of numerical output. As computer speed and available memory increase, one could argue that "the finer the mesh, the better" since there is less and less of a penalty to be paid for models with a large number of degrees of freedom.

The analyst should still be aware of the way mesh geometry can affect results. In figure 5-5, a uniform tension is applied to a member. Constant strain triangles used in the model are not as compliant as higher order elements, but this will illustrate the point more vividly. In areas of very high stress gradient, elements need to be small. Where stress does not change much with respect to location, elements do not need to be small.

One would expect stress concentration near the reentrant corners; for this reason, the mesh near the corner is very fine. Results are as expected. Stress near the reentrant corner rises to about three times that of the applied stress (see figures 5-5 and 5-6). If a coarse mesh is used, the stress concentration near the corners is completely missed (see figure 5-7).

The effects and importance of mesh geometry, like any other parameter, should be understood before any analysis is performed. However, the appropriateness of the mesh density is only determined by comparing analyses with different mesh densities.

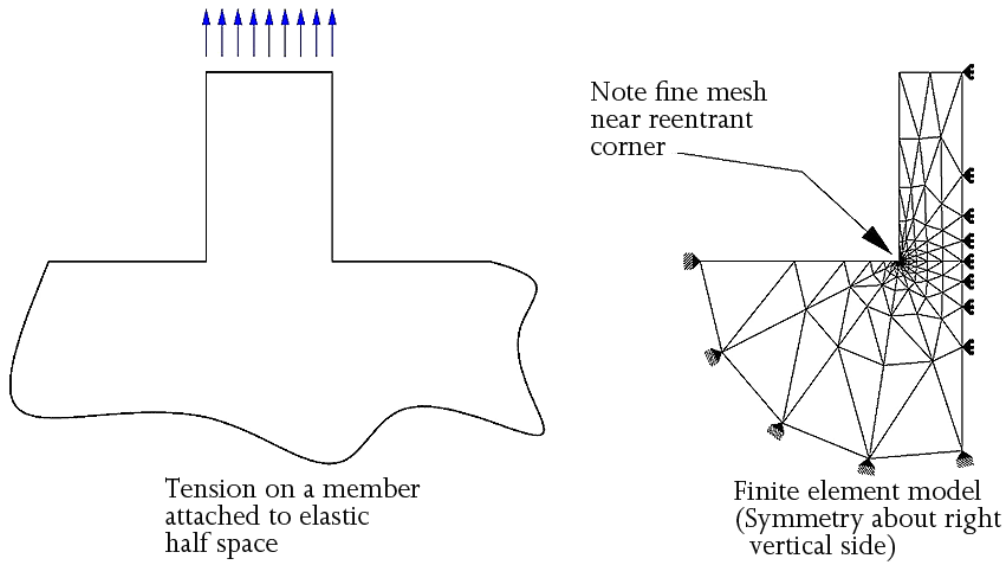


Figure 5-5: Fine finite element mesh at reentrant corner.

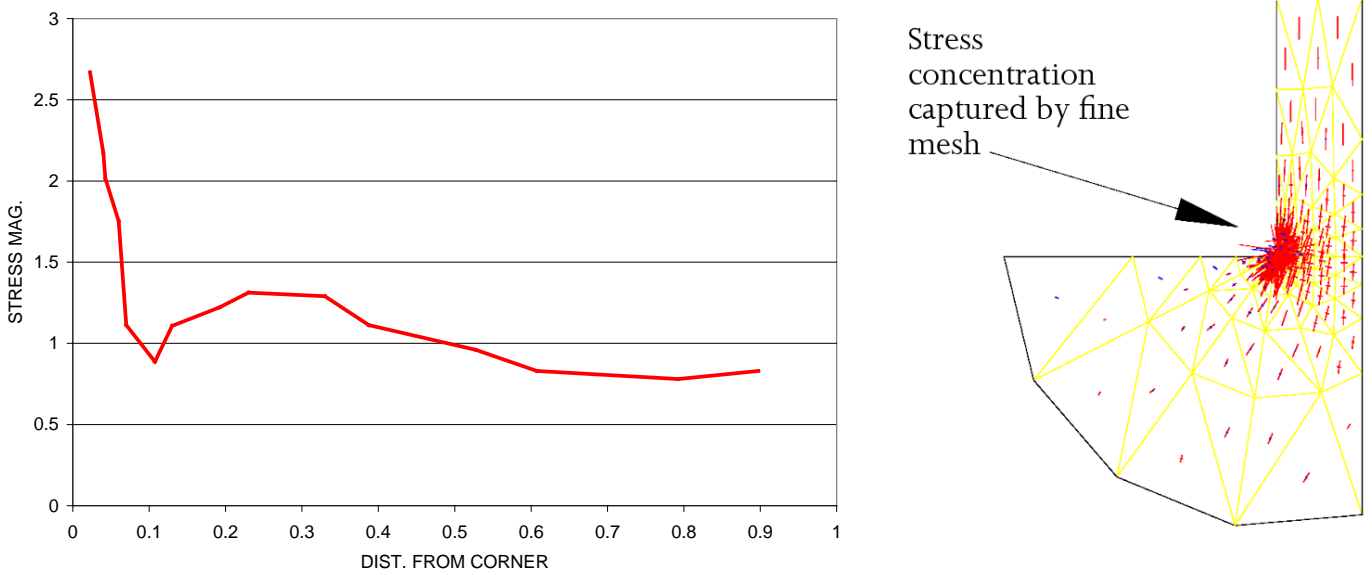


Figure 5-6: Stresses from the fine finite element mesh.

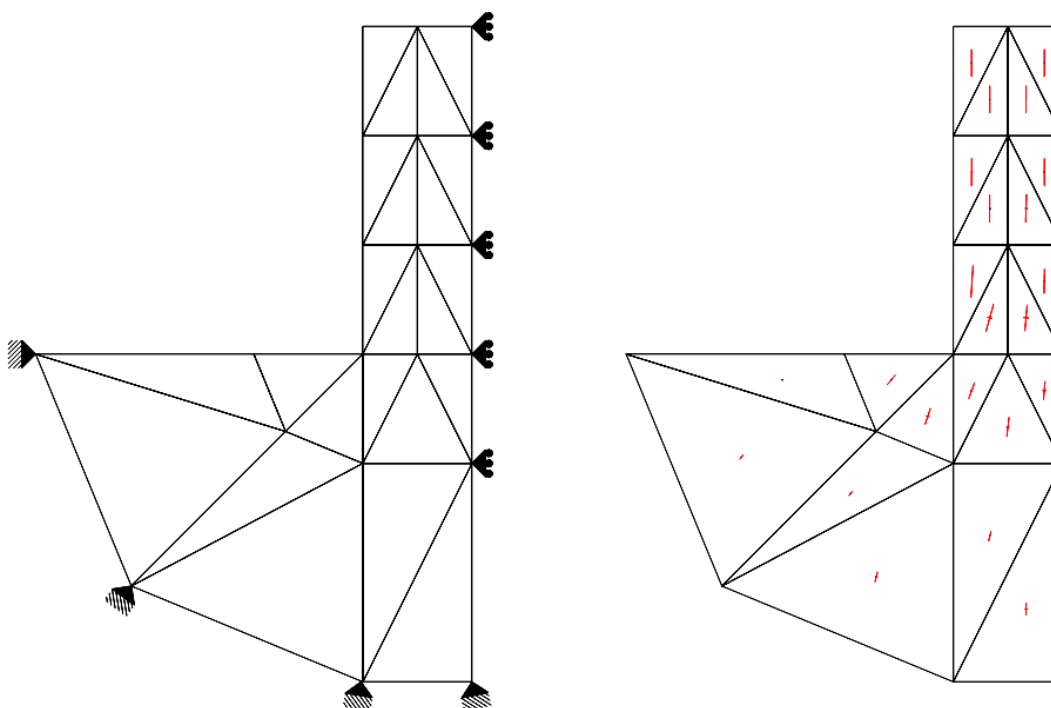


Figure 5-7: Coarse finite element model and stress results.

### 5.1.1.3 Damping

Damping in dynamic models is the result of energy dissipation due to several poorly understood physical effects. In mass concrete structures, these phenomena include wave radiation (back into the foundation and reservoir), sliding friction (along existing joints and cracks), and the complex process of material degradation (damage). Damping is mode-shape dependent, driving-force dependent, and a function of time as structural damage progresses through the seismic event. It has been shown that, for small vibrations, viscous damping in concrete dams is 5 percent or less. Small vibrations are defined as those producing stresses well within the linear range of the dam-reservoir-foundation system.

It is often tempting, when doing linear modeling, to use high damping values of 10 to 20 percent of critical. One rationale for using these damping values is based on a theoretical expectation of large radiation damping in the foundation rock materials. While this may be theoretically valid for a uniform, elastic half space, foundation nonuniformities and discontinuities, and increases in density and modulus with depth, can significantly reduce the amount of radiation damping that actually occurs. Large values of damping need to be justified and are normally not appropriate. Another argument for using excessive damping is based on the assumption that cracking and crushing of concrete and frictional sliding will dissipate large amounts of energy, justifying high damping assumptions. However, when large damping values are used, the dynamic response of the dam is so muted that the results do not show the potential for damage that was assumed to justify the high damping in the first place. This errant, circular reasoning must be avoided.



It is more appropriate to use low viscous damping of 5 percent or less and a rational basis of estimating damage when doing linear modeling. If the result of this assumption is the prediction of high stresses indicative of excessive damage, it may be appropriate to do a nonlinear time domain analysis. If the results of a linear analysis using higher levels of damping indicate low stresses, be aware that the use of higher levels of damping in linear analyses presupposes damage. The effect of energy dissipation due to damage accrual is automatically calculated in a nonlinear time domain analysis. Radiation damping is also directly accounted for if the foundation model includes the mass and the foundation boundaries are nonreflecting, thereby accounting for wave propagation.

#### **5.1.1.4 Failure Plane Tension/Cohesion**

Dam failures often involve cracking of concrete resulting in failure planes where sliding or overturning can occur. If the tensile strength of the concrete is not exceeded, no failure plane can form, and failure by this mechanism can be ruled out. Many analyses evaluate calculated tensile stresses with respect to published values of allowable tensile strengths of intact concrete. It is not uncommon for intact concrete to have significant tensile strength (several hundred lb/in<sup>2</sup>). However, the analyst must be aware that stress calculations only result in stresses produced by the applied loads. There are sources of stress that are not typically modeled, for example:

- Gravity load stress influenced by construction sequencing
- Stresses associated with concrete curing and cooling
- Stresses associated with differential foundation deformation

For this reason, the exact value of in situ tensile stress is often not knowable, and the difference between existing tensile stress and ultimate strength is not clear. In addition to the problem above, there is uncertainty due to the random variation of the material, and the fact that lift joints and preexisting cracks do not exhibit the same tensile strength as an intact laboratory specimen. Because of these uncertainties, the analysis should not rely on tensile strength perpendicular to a postulated failure plane for the stability of a dam. In the limit equilibrium analysis, the dam should be stable as a series of independent blocks.

#### **5.1.2 Summary**

In general, the following principles can be observed concerning choice of parameters:

- Understand how a parameter affects analysis conclusions. Parameters that have a big effect on the outcome need to be accurately determined or bounded. Parameters that do not have a big effect can be loosely assigned.

- If a parameter has a significant effect with a particular analysis type, and the required accuracy of the parameter is not realistically obtainable, consider a different type of analysis where the effect of this parameter is not as significant. For example, tensile strength of concrete is difficult to obtain. One could perform an analysis that assumes a no-tension criterion across a preexisting crack.
- Conservative assumptions need less verification unless they lead to expensive actions. If a dam can be shown to be stable with conservative parameters, there may be decreasing need to justify those parameters with testing. For example, the case of a gravity dam on a competent rock foundation, assuming 35-degree friction angle and no cohesion, would not require significant justification, whereas a 65-degree friction angle and 200-lb/in<sup>2</sup> cohesion would likely require more justification than reasonably obtainable.
- Analysis techniques that require few parameters are preferable.
- It is preferable for stability to be demonstrated using simple analysis techniques.
- The analyst needs to know how the data will be used and the effects of that data on the analysis before it is determined how much effort and cost to spend to get the data.

## **6.1 Uncertainty and Confidence**

### **6.1.1 Uncertainty**

Decisions about the safety of a dam are based on the understanding and perception at a point in time, knowing that the physical world has variability and knowing there are limits to our understanding and modeling of the physical world. Uncertainties about our understanding can result from the variability in the loads applied to the structure, the material properties of the structure, and in some cases, the geometry of the structure (Was the structure really built like it was shown on the drawings?). Many times, the level of uncertainty may not be explained to, or understood by, decisionmakers. Knowing the limitations and uncertainty will foster better decisions and increase the defensibility of the actions being taken.

Analyses are more valid if accompanied by a presentation of the degree of confidence in the results, as well as areas of possible uncertainties and consistency. Discussions would include the uncertainty associated with the parameters used in the structural analysis and how the parameters were obtained. The parameters might have been assumed based on, for example, material properties from dams with similar concrete characteristics, limited laboratory tests, construction records, or an extensive field exploration program. The analysis methods would be explained in terms of the simplifying assumptions used and their possible effect on the results and gaps in technology and the state of the art. The variability in the loads would be developed to show confidence bands around mean load levels. Consistency issues would be addressed, making sure that screening-level ground motions or assumed material properties were not used with state-of-the-art nonlinear finite element analysis.

Uncertainty comes in two forms: aleatory and epistemic. Aleatory uncertainty is attributed to inherent randomness, or natural variations. Aleatory uncertainty is what limits precision. Because there is random variability in a parameter, it cannot be assigned a specific value, but rather must be assigned a range of values. An example of aleatory uncertainty is shown in figure 6-1, showing a seismic hazard curve with uncertainty bands around the mean and how the bands get wider at longer return periods. The error bands show the magnitude of uncertainty that can be expected given the available data. Collecting more data might improve the estimated parameters and reduce the width of the error bands. However, expected error approaches a finite value as the sample size approaches infinity. Therefore, additional data can never eliminate aleatory uncertainty associated with random physical processes.

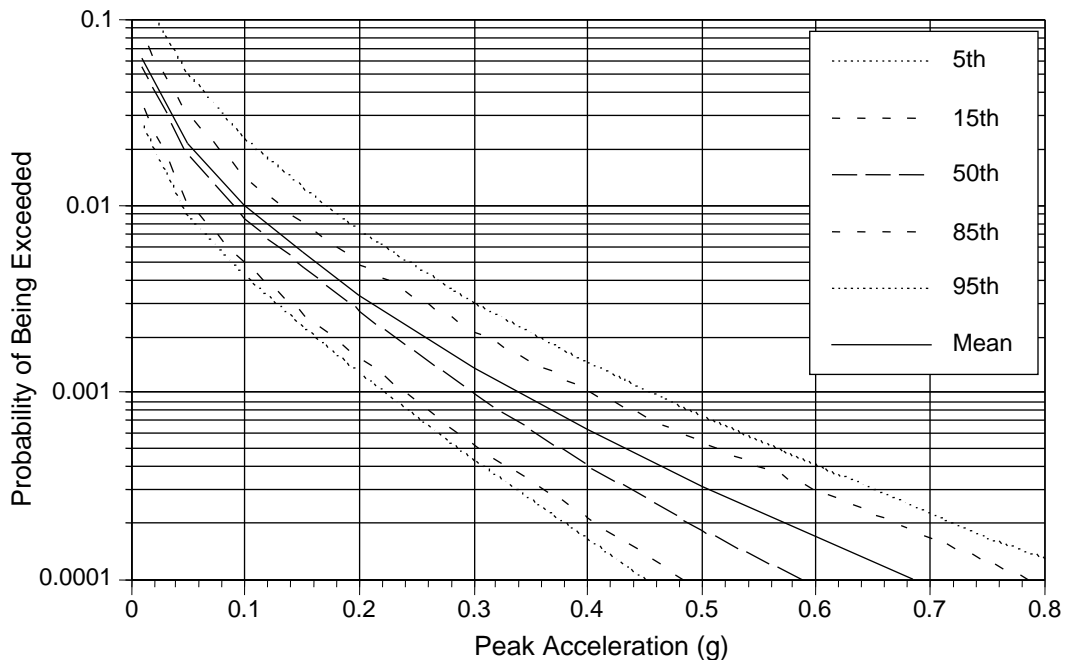


**Figure 6-1: Uncertainty bands around a seismic hazard curve (peak acceleration vs. exceedance probability).**

Epistemic uncertainty is attributed to lack of knowledge. The level of epistemic uncertainty cannot be quantified. It is unquantifiable because one does not know what one does not know. While aleatory uncertainty conditions precision, epistemic uncertainty affects accuracy. Epistemic uncertainty could, for example, be associated with the entire process of developing the curves being unknowingly flawed. Using the seismic hazard curve example, epistemic uncertainty would be that associated with the potential of omitting the governing seismogenic fault from the study, or epistemic uncertainty might be due to accelerometers in the field that are measuring the wrong parameter. As a result, statistical bounds drawn around data for the hazard curves are based on incorrect data. More seismic data to improve the aleatory estimation of uncertainty are useless based on the set of unknowingly bad data.

When epistemic uncertainty is suspected, the appropriate response of the analyst is to request more information. Unlike aleatory uncertainty, which is quantifiable but irreducible, epistemic uncertainty can be reduced. For example, the analyst may be uncertain if a low strength clay seam runs under the dam, which could present a failure mechanism. This example of epistemic uncertainty could be eliminated by a foundation coring program.

A systematic sensitivity and uncertainty analysis provides both the analyst and the decisionmakers the ability to judge the adequacy of the analysis and conclusions. Both Hartford and Baecher (2004) and Morgan and Hendron (1998) make a distinction between sensitivity studies and uncertainty analysis that is appropriate here. Sensitivity studies involve determining the change in response of a model to changes in either individual model parameters, more than one parameter, some key parameters across reasonable high and low ranges, or the model itself. They indicate how wide the spread of results can be if individual parameters vary within the bounds of their respective uncertainties. Sensitivity studies are a useful way of determining if some uncertainties significantly influence the results. For instance, the stability of a gravity dam could be computed for various uplift assumptions. The sensitivity of uplift on stability could then be determined.

Finally, a certain level of uncertainty may be tolerated depending on the degree of conservatism of the assumptions and results, and on the level of demand on the structure. High levels of uncertainty may be acceptable knowing the level of conservatism introduced in the analyses. Factors of safety are still viable benchmarks for analyses' results and decisionmaking given that there is an understanding of the parameters and procedures that produced those factors of safety.

### **6.1.2 Confidence**

A structural analyst should perform analyses appropriate to the level of study, focus on capturing the desired structural response at an event node associated with a potential failure mode, and portray the uncertainties and assumptions to decisionmakers. Choosing the appropriate analysis method is key to answering a desired question about the dam. The problem being solved should dictate the analysis method selected. Table 4-1 provides some guidance on selecting an analysis method. Once the analysis method is chosen, the accuracy or usefulness of the solution depends on the understanding of the material properties, boundary conditions, and loads input into the program. The many choices in analyses cause variability in the computed results. These might include, but are definitely not limited to, choices between:

- Average, generic material properties instead of site-specific material properties
- Using a massless foundation instead of a foundation with mass
- Viscous damping or Rayleigh damping
- Westergaard's added mass or compressible fluid elements for hydrodynamic interaction

- Modeling the dam as a homogeneous structure instead of modeling geometric nonlinearities in the dam such as contraction joints or unbonded lift joints
- Linear or nonlinear material properties
- A response spectrum analysis or a time-history analysis
- Modal superposition or direct time integration
- A coarse or a fine finite element mesh
- Various types of solid elements
- Ground motions generated at 0.02-second or at 0.005-second intervals
- Modeling 3D or only 2D canyon effects
- Applying ground motions in three orthogonal directions or in only one direction
- Using appropriate ground motions for the site including spatial variations

The analyst must be aware of the consequences of all of these modeling decisions. If known features are ignored or simplified, the analyst should include an explanation.

Analysis methods do not introduce uncertainty. They do what they do, and we know what they do because we created them. An analysis can introduce error, but this should not be confused with uncertainty. All analysis tools make simplifying assumptions, and it is the responsibility of the analyst to understand the effects of these limitations. No uncertainty band can cover a faulty analysis. In such a situation, the analysis can be incorrect or inappropriate with 100-percent certainty. Epistemic uncertainty may be why critical features are ignored in the analysis, but that uncertainty is not the result of the analysis itself. Choosing to ignore known critical features for the sake of simplification is not a case of uncertainty; it is a case of error.

Troubleshooting a numerical model, while important, is not an example of reducing uncertainty, but it does develop confidence in the analysis performed. Two effective techniques to troubleshoot models are to adjust parameters in the model until failure of the model can be reached or identify threshold levels for historic maximum loadings on the actual dam. For instance, in a nonlinear structural analysis of a potentially unstable foundation block, shear properties are reduced to the point where sliding commences for a historic maximum loading level. If the actual dam was stable for this historic loading but the finite element model shows movement with realistic shear properties, something is wrong with the analysis. If the analysis is run with zero cohesion and zero friction and the foundation blocks do not slide, something may be wrong with the analysis. The foundation block may be inadvertently held in place because of a modeling issue. Uncertainty analysis is an extension of sensitivity analysis, where probability

distributions are associated with the various parameters or models being varied. Thus, the output is in the form of a probability distribution that specifies the likelihood of each possible result across a full range of possible results.

Do the natural frequencies of the models match the field-measured frequencies? Do seasonal static deformations in the models match the measured deformations? Are static water pressures at locations on the upstream face of the dam in the finite element model the same before and after the earthquake? Do the friction forces developed along a contact surface match the computed normal force times the friction tangent? Do the velocities obtained by a potentially unstable rock block moving from a known constant force match the theoretical velocity? Are the results different with more finite element mesh density? Do the ground motions captured at the free-field surface of the model match the target motion provided by the seismologist? Are results of the progression of analyses, ranging from the simplest to the most complex, understandable? These checks of finite element models increase confidence in the models, help validate that the models are working correctly, and reduce doubt about how well the models are predicting reality.

## **7.1 Conclusions**

The process this document suggests is to first consider potential failure modes and the events for each mode that would lead to failure of a concrete dam, then select appropriate structural analysis methods to help quantify the response of the dam at desired events to determine the probability of failure, quantify the uncertainty, or prove that the failure process stops at an event. Field investigations, instrumentation, and testing can then be focused on the requirements of the analyses.

Potential failure modes start with some initiating event such as a flood, seismic event, or human operating error. These adverse changes can cause a sequence of interrelated and normally sequential events that must occur for failure to actually occur.

Event trees graphically represent event sequences. Event trees are available to the engineer conducting a risk or reliability analysis as an efficient way to organize the chronological sequence of failure mode development.

Structural analyses are then selected to determine the structural response at a given node. Structural analysis uses either limit equilibrium analysis or various types of finite element methods, namely 2D linear elastic, 2D nonlinear, 3D linear elastic, or 3D nonlinear. It must be realized that each of these analysis methods has a certain level of applicability and represents a certain level of reality. These methods also vary greatly in level of effort. The accuracy of the results depends on the accuracy of the material properties being used and the accuracy of the loading condition. However, more importantly, applicability of the analysis method being used depends on the question being asked. For instance, a linear analysis cannot be used to determine how far a crack progresses, because the linear elastic elements can carry tensile stresses higher

than the material strength. Nonlinear methods, or the limit equilibrium method, answer this question better. Examples showing various structural analysis methods and results are provided in the body of the report and in appendix A.

Evaluation of dam structures requires that the engineer make assumptions and use various parameters and structural analysis methods to develop a reasonably accurate representation of structural behavior. The impacts of particular parameters on analysis results vary based on the type of analysis.

Though many efforts are made during structural analysis to achieve high quality results, some analysis methods just cannot model the structural behavior as accurately as others. Many times, the analyst makes simplifying assumptions that greatly limit the accuracy of the analysis, yet decisions about the safety of a structure are made assuming the results of an analysis are more accurate than they actually are. This is because structural analyses have levels of uncertainty and levels of accuracy throughout the process.

There are uncertainties about the loads applied to the structure, the material properties used in the analysis, the analysis methods being used, and the interpretation of the results. Also, many times the level of uncertainty, level of accuracy, or level of reality may not be explained to or understood by decisionmakers as well as needed. It is important that decisionmakers understand the conservatisms, the accuracy, and limitations of the structural analyses so they can determine the safety of the dam and necessary actions to take. If they know the limitations, they might decide to update the loading, refine the structural analysis, or obtain actual material properties. Higher levels of effort may be needed in cases where risk is estimated to be near the agency's guidelines.





## Bibliography

Bureau of Reclamation, *Best Practices for Dam Safety Risk Analysis*, Technical Service Center, Denver, Colorado, 2012.

Bureau of Reclamation, *Public Protection Guidelines*, January 3, 2003.

Federal Energy Regulatory Commission (FERC), *Engineering Guidelines for the Evaluation of Hydropower Projects*, Chapter 14, “Dam Safety Performance Monitoring Program,” 2005.

Georgia Institute of Technology, *GT-STRUDL, Integrated CAE System for Structural Engineering Analysis and Design*, School of Civil and Environmental Engineering, Atlanta, Georgia.

Hartford, Desmond N.D. and Gregory B. Baecher, *Risk and Uncertainty in Dam Safety*, CEA Technologies Dam Safety Interest Group, 2004.

Itasca, *FLAC-3D*, Minneapolis, Minnesota.

Livermore Software Technology Corporation, *LS-DYNA*, Livermore, California.

Morgan, M. Granger and Max Hendron, *Uncertainty—A Guide to Dealing with Uncertainty in Quantitative Risk and Policy Analysis*, Cambridge University Press, 1990 with reprint in 1998.

Parametric Technologies Corporation, *MathCad 14*, PTC Corporate Headquarters, Needham, MA.

U.S. Army Corps of Engineers, *Ice Engineering*, 1110-2-1612, 2002.

University of Illinois at Urbana-Champaign, *CAST*, Version 0.9.11, 1998-2004.

Vose, David, *Risk Analysis—A Quantitative Guide*, second edition,” 2002.

Westergaard, H.M., *Handbook of Dam Engineering*, Chapter 8, Van Nostrand Reinhold Company Inc., 1977.

Westergaard, H.M., “Water Pressures on Dams during Earthquakes,” Alfred R. Golze, ed., *American Society of Civil Engineers Transactions*, Paper No. 1835, November 1931 Proceedings.



ICODS

Figure References for  
Selecting Analytic Tools for Concrete Dams to Address Key  
Events along Potential Failure Mode Paths  
Sept 12, 2014

Cover

Upper left	Reclamation aerial photograph
Upper right	Reclamation finite element model
Lower left	Figure developed by ICODES Committee in PowerPoint
Lower right	Figure developed by ICODES Committee in PowerPoint
Figure 2.1	Reclamation file photo of Grand Coulee Dam
Figure 2.2	Reclamation file photo of Roosevelt Dam
Figure 2.3	Reclamation file photo of Stony Gorge Dam
Figure 2.4	Reclamation file photo of Pueblo Dam
Figure 2.5	Reclamation file photo of Bartlett Dam
Figure 2.6	Reclamation file photo of Coolidge Dam
Figure 3.1	Reclamation file photo of Shasta Dam
Figure 3.2	Figure developed by ICODES Committee in PowerPoint
Figure 3.3	Figure developed by ICODES Committee in PowerPoint
Figure 3.4	Figure developed by ICODES Committee in PowerPoint
Figure 4.1	Figure developed by ICODES Committee in PowerPoint
Figure 4.2	Figure developed by ICODES Committee in FLAC
Figure 4.3	Figure developed by ICODES Committee in Spreadsheet
Figure 4.4	Figure developed by ICODES Committee in Spreadsheet
Figure 4.5	Figure developed by ICODES Committee in FLAC
Figure 4.6	Figure developed by ICODES Committee in Spreadsheet
Figure 4.7	Figure developed by ICODES Committee in PowerPoint
Figure 5.1	Figure developed by ICODES Committee in PowerPoint and FLAC
Figure 5.2	Figure developed by ICODES Committee in Spreadsheet
Figure 5.3	Figure developed by ICODES Committee in Spreadsheet
Figure 5.4	Figure developed by ICODES Committee in PowerPoint and FLAC
Figure 5.5	Figure developed by ICODES Committee in PowerPoint and FLAC
Figure 5.6	Figure developed by ICODES Committee in Spreadsheet and FLAC
Figure 5.7	Figure developed by ICODES Committee in FLAC
Figure 6.1	Figure developed by ICODES Committee in Spreadsheet
Figure A1.1	Figure developed by ICODES Committee in PowerPoint
Figure A1.2	Figure developed by ICODES Committee in PowerPoint
Figure A1.3	Figure developed by ICODES Committee in PowerPoint
Figure A1.4	Reclamation file photo of Shasta Dam

## Selecting Analytic Tools for Concrete Dams to Address Key Events Along Potential Failure Mode Paths

---

Figure A1.5	Reclamation file photo of Kortez Dam
Figure A1.5	Reclamation file photo of Kortez Dam looking downstream
Figure A2.1	Figure developed by ICODS Committee in PowerPoint
Figure A2.2	Figure developed by ICODS Committee in PowerPoint
Figure A2.3	Figure developed by ICODS Committee in FLAC
Figure A2.4	Figure developed by ICODS Committee in Spreadsheet
Figure A2.5	Figure developed by ICODS Committee in Spreadsheet
Figure A2.6	Figure developed by ICODS Committee in FLAC
Figure A2.7	Figure developed by ICODS Committee in FLAC
Figure A2.8	Figure developed by ICODS Committee in Spreadsheet
Figure A2.9	Figure developed by ICODS Committee in PowerPoint
Figure A2.10	Figure developed by ICODS Committee in FLAC
Figure A2.11	Figure developed by ICODS Committee in Spreadsheet
Figure A2.12	Figure developed by ICODS Committee in FLAC
Figure A2.13	Figure developed by ICODS Committee in FLAC
Figure A2.14	Figure developed by ICODS Committee in FLAC and Spreadsheet
Figure A2.15	Figure developed by ICODS Committee in Spreadsheet
Figure A2.16	Figure developed by ICODS Committee in Spreadsheet
Figure A2.17	Figure developed by ICODS Committee in Spreadsheet
Figure A2.18	Figure developed by ICODS Committee in PowerPoint
Figure A2.19	Figure developed by ICODS Committee in PowerPoint
Figure A3.1	Figure developed by ICODS Committee in PowerPoint
Figure A3.2	Figure developed by ICODS Committee in PowerPoint
Figure A3.3	Figure developed by ICODS Committee in PowerPoint
Figure A3.4	Reclamation file photo of Hungry Horse Dam
Figure A3.5	Reclamation file photo of Hungry Horse Dam foundation
Figure A3.6	Figure developed by ICODS Committee in EACD3D96
Figure A3.7	Figure developed by ICODS Committee in Spreadsheet
Figure A3.8	Figure developed at Reclamation in LSDYNA
Figure A3.9	Figure developed at Reclamation in LSDYNA
Figure A4.1	Reclamation file photo of Stony Gorge Dam
Figure A4.2	Reclamation file photo of Stony Gorge Dam
Figure A4.3	Figure developed by ICODS Committee in PowerPoint
Figure A4.4	Reprint of Corbel forces from ACI-318
Figure A4.5	Reprint from Reclamation file drawing of Stony Gorge Dam corbel
Page A-46	Reprint from Reclamation file drawing of Stony Gorge Dam buttress
Page A-47	Same as Figure A4.5
Page A-49	Reprint from Reclamation file drawing of Stony Gorge Dam buttress
Page A-51	Same as Figure A4.5
Page A-52	Figure developed by ICODS Committee in Computer Aided Strut and Tie
Page A-53	Figure developed by ICODS Committee in Computer Aided Strut and Tie
Page A-54	Figure developed by ICODS Committee in Computer Aided Strut and Tie

Page A-55	Figure developed by ICODS Committee in Computer Aided Strut and Tie
Figure A5.1	Upper figure developed by ICODS Committee in PowerPoint Bottom figures (verifying from Husein Hasan at TVA)
Figure A5.2a	Figure developed by ICODS Committee in PowerPoint
Figure A5.2b	Figure developed by ICODS Committee in PowerPoint
Figure A5.3	Same as Figure A4.5
Figure A5.4	Figure developed by ICODS Committee using GT-STRUDL
Figure A5.5	Figure developed by ICODS Committee using GT-STRUDL
Figure A5.6	Figure developed by ICODS Committee using GT-STRUDL
Figure A5.7	Reprint from Reclamation file drawing of Stony Gorge Dam
Figure A5.8	Figure developed by ICODS Committee using GT-STRUDL
Figure A5.9	Figure developed by ICODS Committee using GT-STRUDL
Figure A5.10	Figure developed by ICODS Committee using GT-STRUDL
Figure B.1	Figure developed by ICODS Committee in PowerPoint
Figure B.2	Figure developed by ICODS Committee in PowerPoint

Note: Original drawings by Committee members are listed as PowerPoint. There may have been another drawing program used such as AutoCAD, but these figures are originally developed by the committee.



## **Appendix A1**

# **Increased Reservoir Level Causes Sliding in a Gravity Dam**





# Appendix A1: Increased Reservoir Level Causes Sliding in a Gravity Dam

This potential failure mode is a sliding failure at the foundation contact or along an existing plane of weakness within a gravity dam due to reservoir loading in excess of original design conditions. These changes may be a result of operational changes (storing more water), updated hydrologic analyses, or operational errors (failure to operate gates in accordance with established plans, failure of gate equipment, plugging of gates or spillway by debris, etc.). Figure A1-1 shows the geometry of a typical gravity dam along with the free-body diagram of the portion of the dam above a plane of weakness. When the reservoir driving force exceeds the frictional resistance induced by the weight of the dam (reduced by the effect of uplift) the upper portion of the dam will slide in the downstream direction. Figure A1-2 is the event tree for this potential failure mode.

## A1.1 Node A: Reservoir Level Increases

An increase in reservoir loading will increase driving forces and uplift pressures, which reduce resisting forces. The combination of these effects may result in initiation of this potential failure mode.

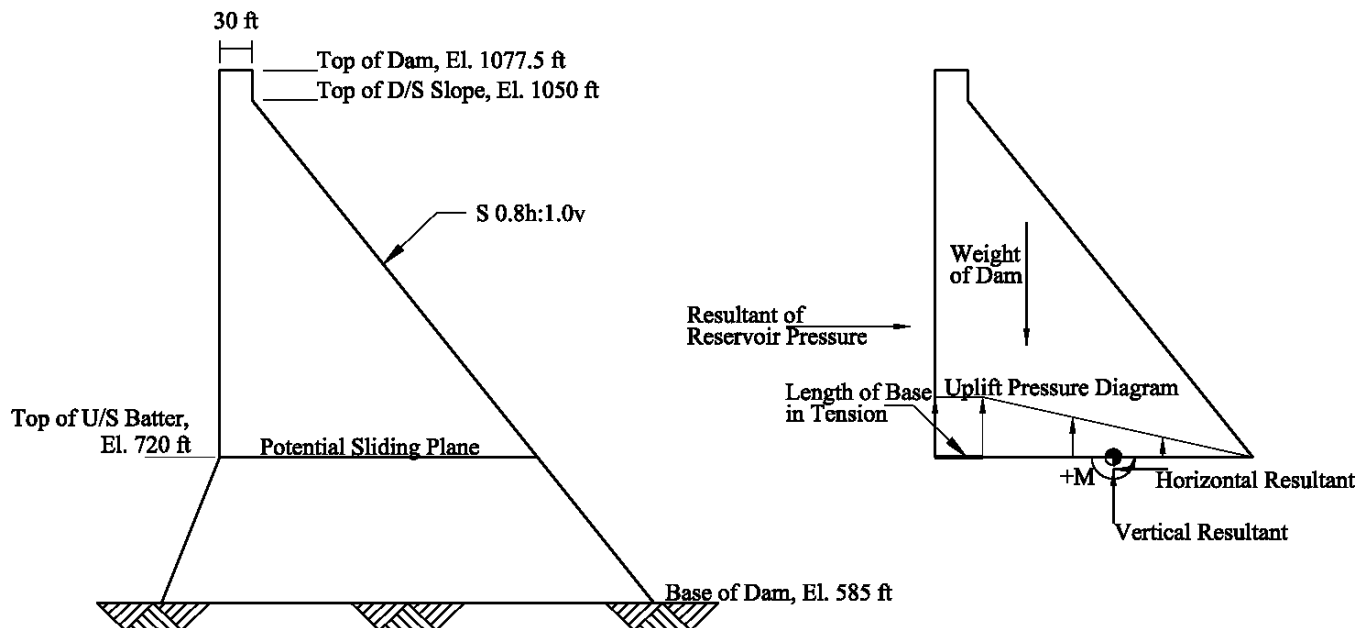


Figure A1-1: Geometry of a typical gravity dam (left) and free-body diagram above plane of weakness (right).

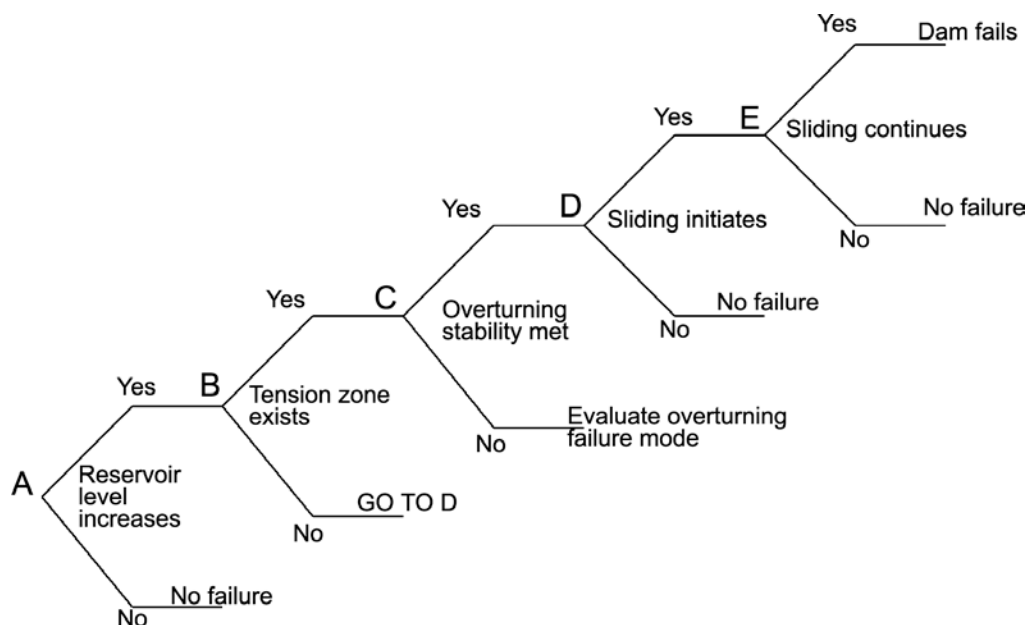


Figure A1-2: Event tree for a failure mode where increased reservoir load causes sliding instability.

If the dam has a drainage system that intersects the failure plane in question and the drainage system efficiency is reduced, the uplift forces will increase, and the portion of the failure surface upon which the resisting shear forces act may be reduced.

A thorough evaluation of the hydraulic loadings and evaluation of the drainage system is required prior to moving on to node B of the event tree.

## A1.2 Node B: Tension Zone Exists

To adequately address the sliding failure mode, an evaluation of the condition of the failure plane beginning at the location where the sliding plane intersects the upstream face is required. If the initiating event causes this location to enter into tension, or if the tensile stresses increase, a determination of the length of the resulting tension zone is required. If the upstream face is originally in tension, the initiating event will change the driving forces and/or the distribution of the uplift pressures causing the length of the tension zone to increase.

Node B of the event tree is where an evaluation of the condition of the failure surface is performed to determine how the failure mode would progress. Various methods exist to determine the portion of the failure surface that is cracked, including classical limit state “crack based” computations founded on force and moment equilibrium, nonlinear finite element methods, and fracture mechanics, which is based on the fracture energy required to advance a crack. Refer to section 4 of this report for a discussion on the applicability of the various methods.

Included in figure A1-3 is an example of the limit state computations for sliding on a plane within the dam. In this example, the length of the tension zone represents 15 percent of the width of the dam. The uplift diagram includes full reservoir head throughout the tension zone. In this example, drains are not present, so the uplift diagram is assumed to vary linearly from the point of zero total normal stress to the downstream face of the dam.

### **A1.3 Node C: Overturning Stability Met**

This node is an informational node for this sliding failure mode. In this case, overturning is not an issue because, as shown in the previous analysis, the resultant stays within the base. It is included to point out that, based on the initiating event and node B having occurred, the overturning failure mode needs to be evaluated.

In the example in figure A1-3, the location of the resultant based on the final iteration is outside the middle third but within the base of the dam. This indicates that the upstream face would be in tension and the dam would not overturn.

### **A1.4 Node D: Sliding Initiates**

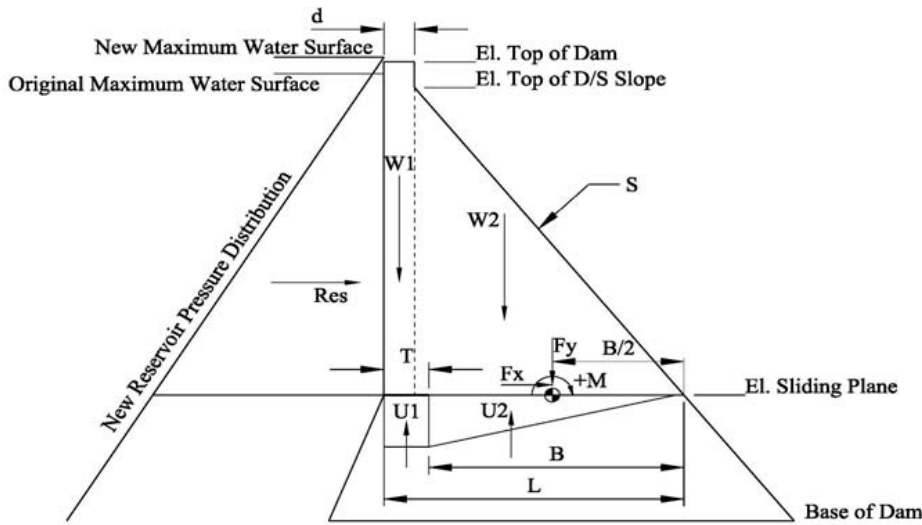
Sliding initiates when the driving forces exceed the resisting forces. The driving forces include the hydrostatic forces of the reservoir and any soil pressures (silt) acting on the upstream face of the dam. The resisting forces include soil conditions or tailwater that may exist on the downstream face, as well as frictional forces. The resisting forces are a combination of cohesion and friction. The frictional resistance is a function of the total forces normal to the sliding plane multiplied by the coefficient of friction ( $\tan \phi$ ). Uplift pressures offset the weight of the structure; therefore, the determination of the pressure diagram is important and should be compatible with the evaluation of the sliding plane as determined in nodes B and C. If cohesion is to be considered, it can only be applied to the portion of the base that is bonded and should be verified if critical by a coring and laboratory program.

Computations shown in figure A1-3 indicate that the factor of safety against sliding is less than 1.0; therefore, sliding is judged to begin based on a 2-dimensional (2D) study.

### **A1.5 Node E: Sliding Continues**

To this point, sliding stability has been evaluated based on the dam performing as a 2D structure. While stability computations can be applied to a 3-dimensional (3D) block, a 2D sliding stability analysis can be performed, and if 2D stability is met, failure will not occur. In the example, these computations suggest sliding will commence. Continuation of sliding is controlled by the 3D characteristics of the structure.

# Selecting Analytic Tools for Concrete Dams to Address Key Events Along Potential Failure Mode Paths



Geometry and Material Properties	
El. Top of Dam	1077.5 FT
Res. El	1082.5 FT
El Sliding Plane	720 FT
Crest Thickness	d 30 FT
D/S Slope	S 0.8
El. Top of D/S Slope	1050 FT
Width of Sliding Plane	L 294 FT
Density of Water	62.5 LB/FT <sup>3</sup>
Density of Concrete	150 LB/FT <sup>3</sup>

Iteration	Width of Base in Compression		Length of Tension Zone		Forces				
	B	T	Weight		Reservoir	Uplift			
	FT	FT	W1	W2	Res	U1	U2	Total	
1	294.000	0.000	1608750	6534000	4106445	0	3330469	3330469	
2	281.588	12.412	1608750	6534000	4106445	281204	3189867	3471071	
3	272.227	21.773	1608750	6534000	4106445	493284	3083827	3577111	
...									
25	249.977	44.023	1608750	6534000	4106445	997387	2831775	3829162	
26	249.977	44.023	1608750	6534000	4106445	997407	2831765	3829172	

Iteration	Moment Arms About Center of Uncracked Base					Moments					
	Weight		Reservoir		Uplift	Weight		Reservoir	Uplift		Total
	W1	W2	Res	U1	U2	W1	W2	Res	U1	U2	Total
1	-132.00	-29.00	120.83	147.00	49.00	-212355000	-189486000	496195475	0	163192969	257547444
2	-138.21	-35.21	120.83	147.00	46.93	-222338695	-230035161	496195475	41336919	149704848	234863386
3	-142.89	-39.89	120.83	147.00	45.37	-229868276	-260616846	496195475	72512721	139917065	218140139
...											
25	-154.01	-51.01	120.83	147.00	41.66	-247765684	-333307855	496195475	146615915	117979962	179717814
26	-154.01	-51.01	120.83	147.00	41.66	-247766381	-333310687	496195475	146618802	117979144	179716353

Iteration	Resultant			Estimate of Crack Length				
	FY	FX	e	LIMIT OF MIDDLE 1/3	DISTANCE FROM CL OF BASE	x'	Bnew	Tnew
	LBS	LBS	FT	FT	FT	FT	FT	FT
1	4812281	4106445	53.519	49.00	53.519	-134.588	281.588	12.412
2	4671679	4106445	50.274	49.00	56.480	-131.433	272.227	21.773
3	4565639	4106445	47.779	49.00	58.665	-129.255	265.369	28.631
...								
25	4313588	4106445	41.663	49.00	63.674	-124.988	249.977	44.023
26	4313578	4106445	41.663	49.00	63.675	-124.988	249.976	44.024

Where:  
 $x' = -1 * B * (B/12E)$   
 $B_{new} = 5 * B - x'$   
 $T_{new} = L - B_{new}$

Determine Factor of Safety Against Sliding:						
Driving Force (Reservoir) lb	Resisting Force					
	C psi	N lb	phi degrees	Tan(phi)	Total	F.S.
4106445.313	0	4313603	43	0.932515086	4022499.52	0.980

Figure A1-3: Example dam showing computation of length of base in compression, corresponding uplift distribution, and sliding factor of safety.

An evaluation of as-constructed conditions may suggest that there are 3D characteristics of the dam that would prevent continuation of the sliding failure. These may include, in the case of a curved gravity dam, individual monoliths that are narrower at the downstream face than the upstream face, thereby causing the blocks to wedge together if their 2D behavior would initiate downstream movement (figure A1-4).



**Figure A1-4: A curved gravity dam, Bureau of Reclamation.**

In the case of straight gravity dams, contraction joints may have been constructed with shear keys, which would require mobilization of adjacent monoliths prior to the monolith in question failing or shear failure of the concrete through the keys.

A monolith on an abutment will have a different height on one side of the monolith than the other. A 2D stability computation of the tallest section may indicate initiation of sliding, but a similar analysis of the shorter side may indicate no sliding. In this case, an evaluation of the entire monolith in 3D is required. Figure A1-5 shows a gravity dam constructed in a steep canyon where the structural height of each monolith varies along the axis of the dam.

The dam may be wedged in the canyon, which could add significant side resistance.

If these conditions exist, an evaluation is required to determine if the 3D effects are sufficient to prevent continuation of the sliding failure mode. In the case of keyed contraction joints, the shear key geometry and concrete shear strength may provide significant shear resistance.



**Figure A1-5: Looking upstream and downstream from a gravity dam in a narrow canyon, Bureau of Reclamation.**

However, the total driving forces on the monolith (not those from a 2D slice) must be considered. A complicating factor in this situation is that the block may want to slide longitudinally (parallel to the axis of the dam), thereby providing a normal force across the contraction joint, which, in turn, would provide a frictional resistance to downstream sliding. Also in the situation of a narrow canyon, a 3D finite element analysis may indicate that longitudinal stresses develop due to bending of horizontal cross canyon planes (beams). This also could lead to a determination that overall 3D stability should be evaluated similar to an arch dam. These examples are included to demonstrate the importance of a thorough evaluation of the failure mode and associated event tree.

## **Appendix A2**

# **Earthquake Causes Sliding in a Gravity Dam**





## Appendix A2: Earthquake Causes Sliding in a Gravity Dam

Consider the dam in figure A2-1. The potential failure mode being investigated in this example is a sliding failure only within the body of the dam on a potentially weak or unbonded lift joint at or about the location of the reentrant corner at elevation 720 feet. There are other failure modes that could be investigated, but it should be noted that potential failure modes have to be well described for analyses to be meaningful. That means that specific potential failure modes have to be considered independently. The event tree shown in figure A2-2 outlines the steps that must occur for an uncontrolled reservoir release as a result of a seismic induced sliding failure.

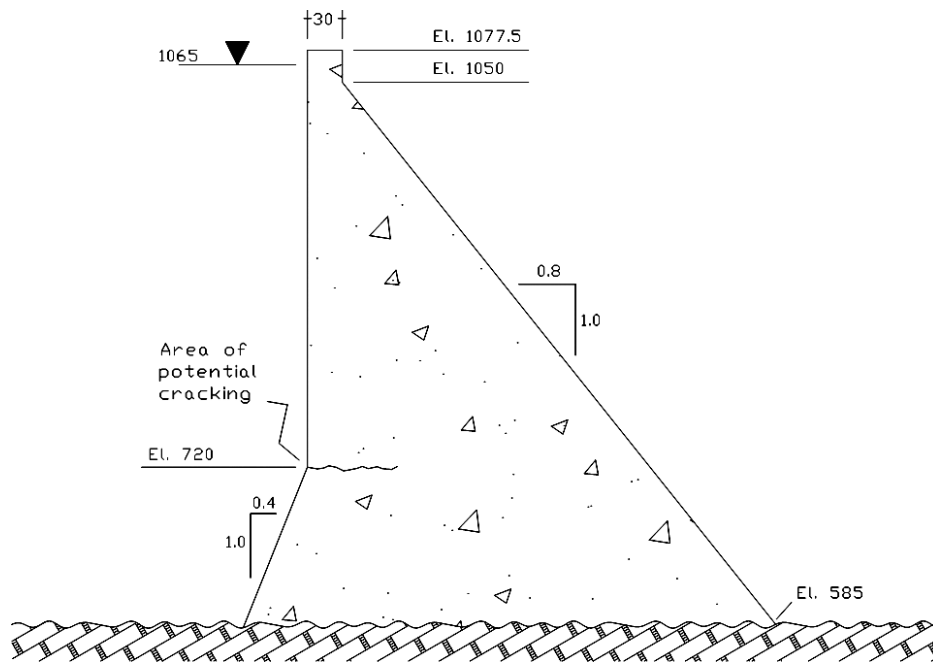


Figure A2-1: Concrete gravity dam.

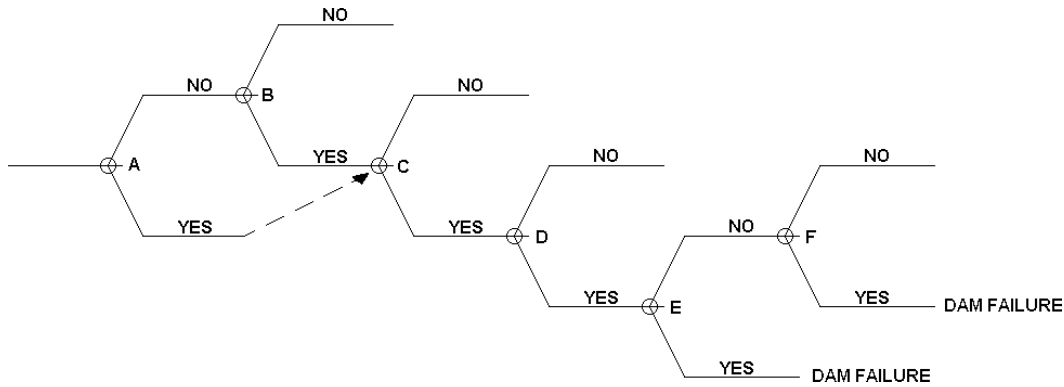


Figure A2-2: Event tree for earthquake causes sliding in a gravity dam.

Node key:

- A Preexisting crack or poorly bonded lift joint exists.
- B Earthquake sufficient to cause cracking.
- C Crack propagates through thickness of dam.
- D Removable block forms. Slide planes develop.
- E Duration and severity of shaking sufficient to cause failure.
- F Damage caused by earthquake results in the dam being unable to resist static loads.

## A2.1 Node A: Existing Crack or Poorly Bonded Lift Joint

The reentrant corner on the upstream face at elevation 720 feet is an area of potential cracking, and it is wise to investigate. The first branch point of the failure event tree is whether a crack or poorly bonded lift joint already exists in the area of concern. Whether a crack in this area is already present may be determined by underwater survey by remotely operated vehicle. It might also be possible to ascertain the condition of the area through borings. As this example will show, in many cases, it is more prudent to assume a crack than try to prove the tensile strength will not be exceeded.

If it is determined that the area of potential cracking is already cracked, or that the lift line is poorly bonded, the effect of the crack or line of weakness must be taken into account when evaluating the seismic response of the dam, and the analysis should proceed directly to node C. Linear elastic analyses are no longer appropriate if preexisting cracks have been identified.

## A2.2 Node B: Upstream Cracks

If it is determined that the area of the dam in question is not pre-cracked and that the concrete is intact, a linear elastic dynamic analysis can be done to determine if the induced seismic stresses are likely to produce a crack. If the stresses exceed the dynamic tensile strength of intact concrete, cracking is likely. Figure A2-3 shows a 2D linear elastic model of the dam/foundation/reservoir. Uplift was not applied in the postulated failure plane because the assumption is that there was no crack prior to the earthquake. This model has a

wave-propagating foundation with wave-radiating boundaries. Hydrodynamic effects are modeled directly through use of elastic wave-propagating elements with zero shear stiffness, as shown in figure A2-3.

The base of the foundation is excited with horizontal and vertical components of the 1999 Chi-Chi CHY006 record. The response spectrum is shown in figure A2-4. The method of application is to impose dynamic shear and normal stresses to the bottom of the foundation and allow them to propagate upward. The stress magnitudes are set to produce the desired free-field ground motion at the free surface of the foundation without the reservoir and dam.

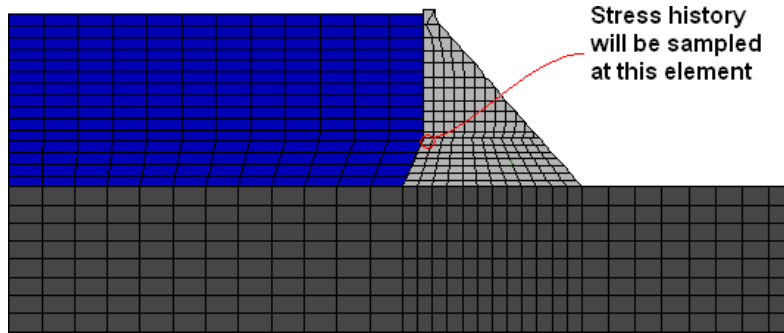


**Figure A2-3: Finite element model.**

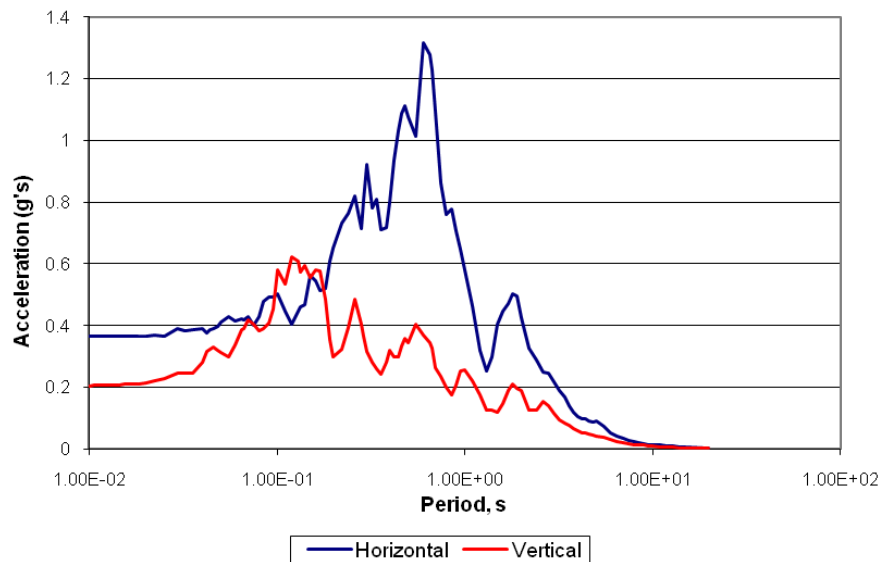


**Figure A2-4: Spectral acceleration (Chi-Chi CHY006) with 5-percent damping.**

## Selecting Analytic Tools for Concrete Dams to Address Key Events Along Potential Failure Mode Paths

---

The results of the analysis are shown below in figure A2-5. For the sake of this exercise, dynamic tensile strength is assumed to be 400 pounds per square inch (lb/in<sup>2</sup>). Note that several excursions exceed this stress limit; the most significant is 1,256 lb/in<sup>2</sup>.

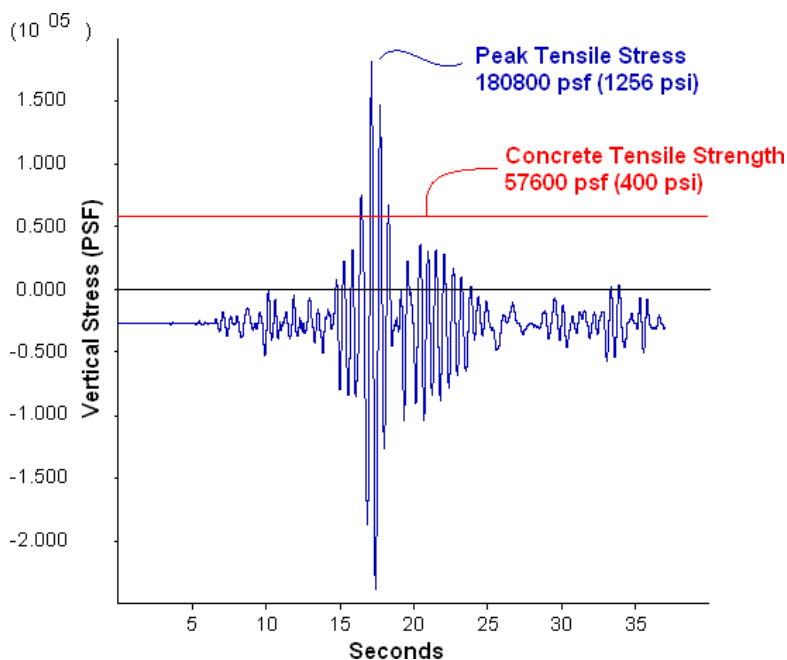


**Figure A2-5: Vertical stresses at reentrant corner, 2D model.**

It could be argued that the tensile strength is exceeded only a few times for short periods and, therefore, can be ignored. This argument is false. In a brittle material, cracking takes no time to initiate, and once initiated, cracks run through the material at sonic velocities. In addition to fast propagation, a stress concentration effect occurs at the crack tip, which allows the crack to propagate under a tensile stress that is much lower than the material's original uncracked tensile strength.

In reality, dams are not 2D structures. Gravity dams are capable of transferring load horizontally if the joints between monoliths are sufficiently keyed. If 3D behavior is factored into the analysis, induced dynamic stresses may be less than those indicated by the 2D model.

Figures A2-6 through A2-8 show the setup and results of a rigorous 3D linearly elastic finite element model. Material parameters and earthquake input are identical to those used in the 2D model, so there are no cross-canyon ground motion components.

Selecting Analytic Tools for Concrete Dams to Address Key Events Along Potential Failure Mode Paths

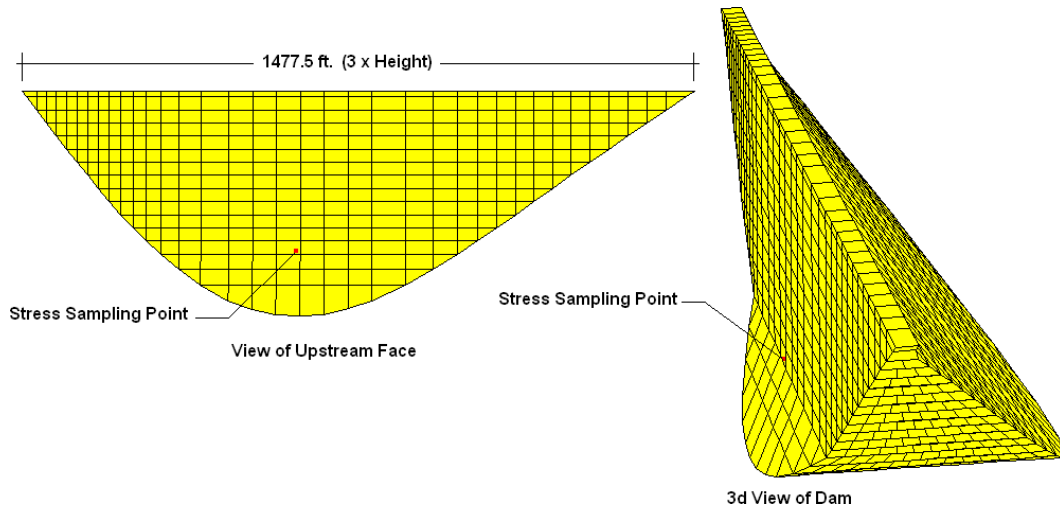


Figure A2-6: 3D linear finite element model.

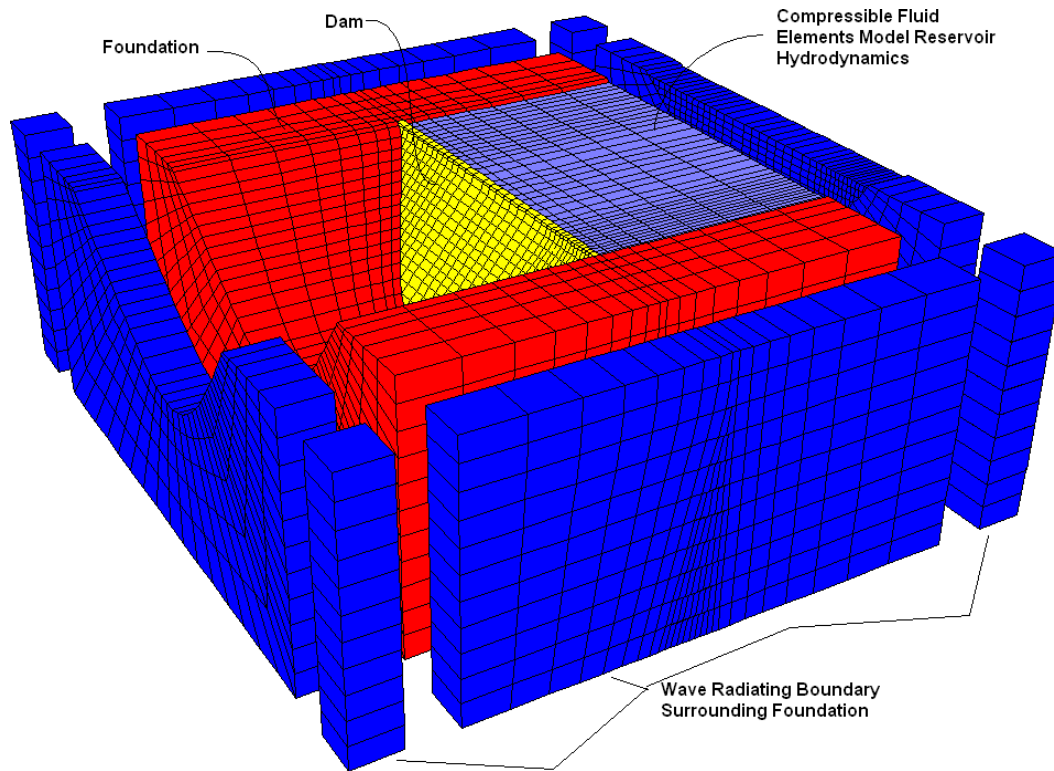


Figure A2-7: 3D linear finite element model with the dam, foundation, reservoir, and free-field boundaries.

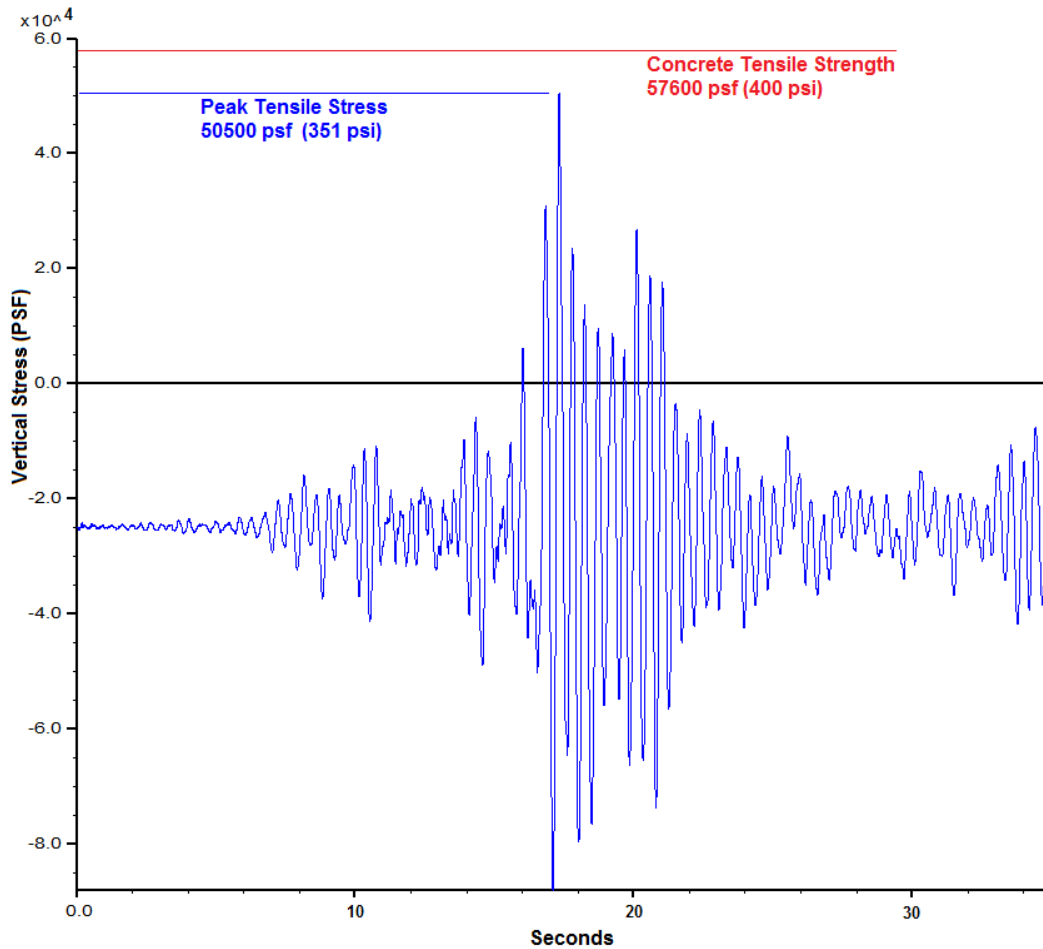


Figure A2-8: Vertical stress time history at reentrant corner, 3D model.

Note that the aspect ratio (crest length to dam height) of the dam is 3 (see figure A2-6). Gravity dams in narrow valleys are likely to exhibit more 3D behavior than dams in wide valleys. In a wide valley, a 3D analysis would not be expected to differ much from a 2D analysis; therefore, a 3D analysis would not be warranted. However in this case, it is not clear that 3D effects can be ignored.

The full dam, reservoir, and foundation model is shown in figure A2-7. Looking at the relative complexity of the model above, one can see why 2D analyses are preferable from an ease-of-modeling standpoint. Because of the desire to capture stress concentration effects at the upstream face near the reentrant corner at elevation 720 feet, the mesh of the dam must be sufficiently fine. This requirement for a fine mesh complicates the model and makes computation slower.

Because this model is linearly elastic, the effects of vertical contraction joints between dam monoliths are ignored. In this model, the dead load of the dam is allowed to be horizontally, as well as vertically, distributed. One can compare the initial stress in the 2D model (figure A2-5)

with that of the 3D model (figure A2-8) and note that the stresses are essentially the same (25,000 pounds per square foot [lb/ft<sup>2</sup>], 170 lb/in<sup>2</sup>); therefore, this error was not significant.

Figure A2-8 shows the vertical stress history at the sampling point shown in figure A2-6. Note that in the 3D analysis, unlike the 2D analysis, the tensile strength (400 lb/in<sup>2</sup>) is approached but not exceeded. The analyst now has somewhat of a dilemma. Which model is to be believed? It is likely that the 3D model shows lower dynamic stresses because there is another dimension available for energy loss. This wave radiation into the cross-canyon dimension is a real phenomenon; therefore, there is some cause to put more faith in the 3D model.

However, while the 3D model accounts for more physical reality than the 2D model, it does not take into account that the dam is actually separated by vertical contraction joints, which tend to diminish 3D behavior. It would not be advisable to accept the results of the 3D model as conclusive. Only one earthquake record was evaluated, and in that case, while the tensile limit was not exceeded, it was approached. Would another earthquake record cause the strength to be exceeded? To conclusively rule out cracking at elevation 720 feet, several earthquake records would have to be evaluated. In addition, the effects of vertical contraction joints would have to be accounted for.

The level of effort expended in evaluating this node on the event tree has been significant, and the results of the two analyses performed are contradictory. Rather than perform additional analyses to try to reconcile the conflicting results, it would be better to assume that a crack does form, but to try to rule out dam failure at another node on the event tree that may be evaluated more definitively. The question that then must be asked is: "If a crack does occur, how far will it run?"

### **A2.3 Node C: Crack Propagates through Thickness**

Once it is determined that the upstream face would crack at the reentrant corner as expected, it is necessary to evaluate what the effect of the crack would be. It must be determined whether the crack propagates through the dam.

How the crack propagation would be modeled is the first choice that must be made. Most analysis programs have what is called a gap friction element. This is a good choice for crack modeling because the element allows compression and frictional shear stress across the gap, but it disallows tension once a set tensile strength is exceeded. The problem with this approach is that gap elements have to be laid out before the analysis is performed. The analyst constrains the direction of crack propagation by the position of the gap friction elements. In the current problem, there are two probable directions for crack propagation.

The first possibility is that the crack would be roughly horizontal. Dams are constructed with horizontal lift joints between concrete placements. These joints are almost always weaker than the parent concrete above and below them. It is usually the case that these horizontal joints direct cracking.

## Selecting Analytic Tools for Concrete Dams to Address Key Events Along Potential Failure Mode Paths

---

The second possibility is that the crack would dive downward (see figure A2-9). This is because the forces that produce tension in this zone of consideration also produce shear stress. This shear stress tilts the major principal axis of stress in the area downstream. Since the crack would propagate perpendicularly to the major principal axis of stress, the crack would turn down. If the concrete is of uniform strength and not affected by lift joints, this second possibility is the most likely.

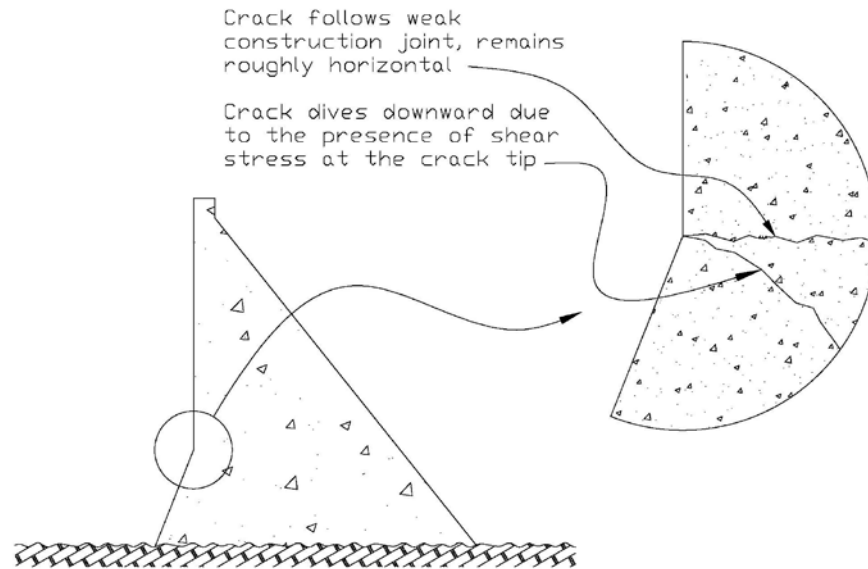


**Figure A2-9: Crack trajectories.**

It is possible to allow the analysis itself to determine the direction of crack propagation. There are concrete constitutive models that check for cracking on any plane within each element. Once an element is determined to have cracked, the orientation of the crack is stored, and the stress-strain characteristics of the cracked element are modified accordingly as the analysis progresses.

For the sake of this analysis, it was assumed that the lift joint at or near elevation 720 feet will control the direction of crack propagation. This assumption is reasonable and the more conservative of the two propagation assumptions. Horizontal propagation could eventually run all the way through the dam, enabling a sliding failure. A diving crack would not daylight, but rather turn down into the foundation. As a result, a sliding failure mechanism would not be enabled. Unless the analyst can be certain that lift joints would not provide planes of weakness, it should be assumed that they would control the direction of cracking.



Also for the sake of this analysis, crack propagation will be modeled with gap-friction, limited-tension elements. While these elements ignore some of the finer points of fracture mechanics, it must be remembered that the analysis must prove that cracking cannot propagate through the dam. More rigor is not expected to change the conclusion.

Figure A2-10 shows a 2D model with the addition of a gap-friction interface. For this example, this interface has been assigned the following characteristics:

- Tensile strength: 400 lb/in<sup>2</sup>
- Unbroken shear strength: No sliding allowed if bonded
- Broken shear strength: 55 degrees

All other properties of the model are identical to those in linear elastic model used for evaluation of node B. Earthquake excitation is also identical.

Figure A2-11 shows the results of the nonlinear analysis. The interface gap opening is plotted with respect to time. Note that the interface breaks at the upstream face at 16.35 seconds into the earthquake event. This corresponds to the first exceedance of tensile strength shown in figure A2-5. Note also that 0.45 second later, the crack has run all the way through the dam. This indicates that the crack has propagated at about 650 feet per second.

As a result of the analysis above, it is clear that cracking will start and propagate through the body of the dam for the given set of modeling assumptions and material properties. It should be noted that if a through-going crack were simply assumed in node A of the failure tree, the analyses for nodes B and C could have been avoided.

The question now is whether the dam can continue to resist static and dynamic loads in a cracked state. The potential for sliding on the plane induced by the crack will need to be evaluated.

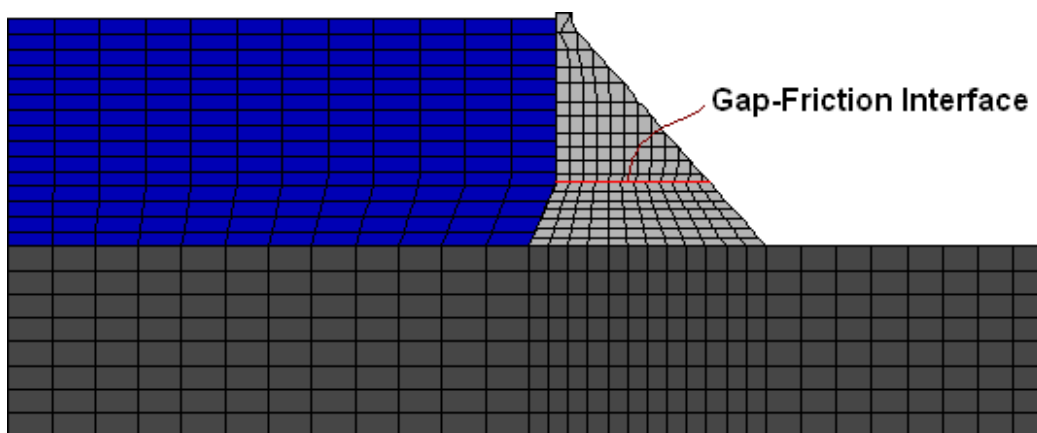


**Figure A2-10: 2D nonlinear finite element model.**

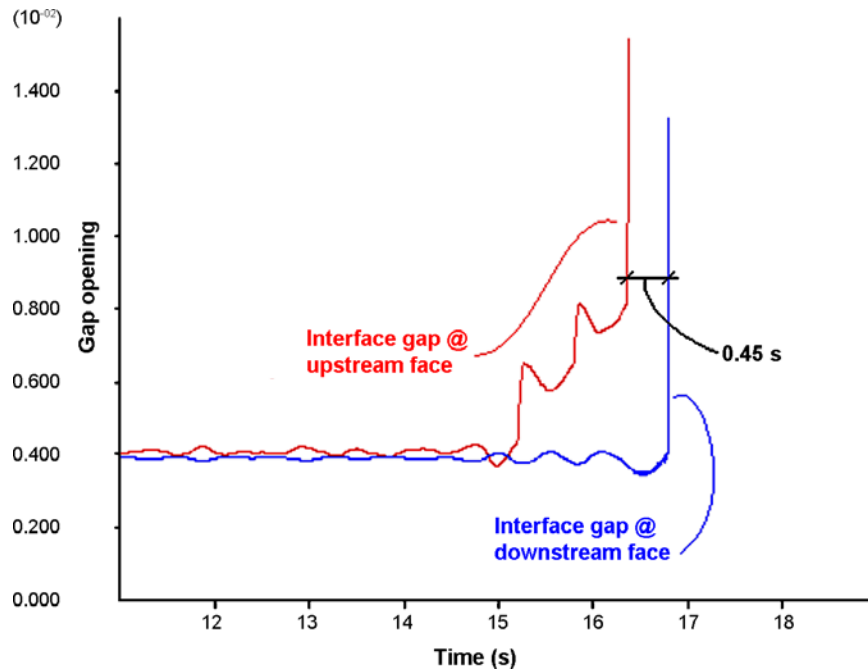


Figure A2-11: Crack propagation.

## A2.4 Node D: Removable Blocks Form and Slide Planes Develop

The dam is a 3D structure. The question that must now be considered is whether significant loads can be transmitted sideways, as well as directly downward to the foundation. If the dam can span from valley wall to valley wall above the crack, the cracking at elevation 720 feet will be less relevant. A nonlinear 3D model similar to the linear 3D model used in node B can be evaluated (see figure A2-12).

It is important to note that a real dam is divided by vertical monolith joints that can inhibit lateral load transfer (see figure A2-13). A realistic 3D model must account for the effect of these joints. Monolith joints can be keyed. If they are, they may be able to transmit significant shear forces; but if they are not, lateral load cannot be transferred. In either case, no tension can be transmitted across a vertical monolith joint. The gap-friction interface element is an effective way to model monolith interaction across joints. In addition, it is typically assumed that the concrete/foundation contact is a friction-only interface. Thus, the gap-friction interface is used to model the contact between concrete and rock above elevation 720 feet. It is the 3D analogue of the interface used in the 2D analysis performed for node C.

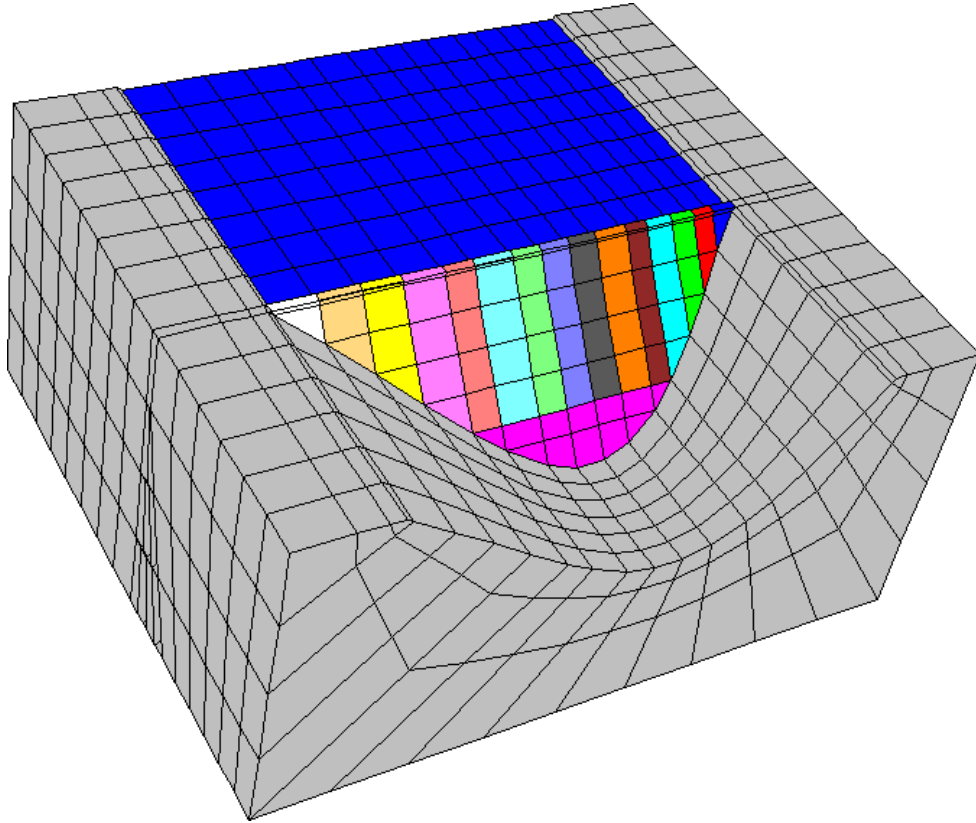


Figure A2-12: Coarse 3D nonlinear finite element model.

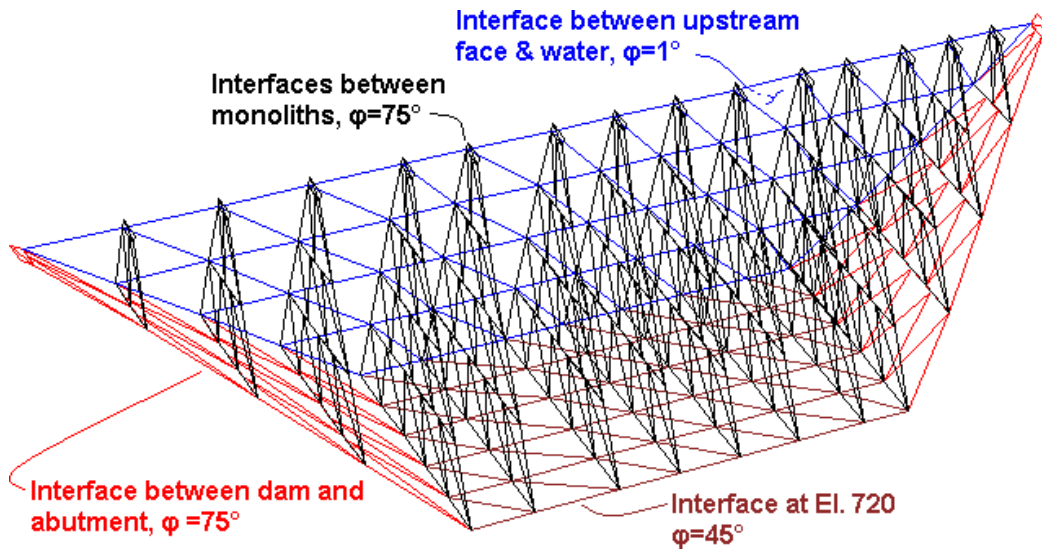


Figure A2-13: Interfaces.

Note the coarseness of the mesh used in this nonlinear model. In the linear elastic model used to evaluate node B, the dam alone consisted of 2,293 elements. In this nonlinear model, only 233 elements are used in the dam. This is almost a tenfold reduction. It may be necessary to perform parametric studies to arrive at the appropriate fineness of mesh size when stresses do not significantly change. The reason for this mesh coarsening is that we are no longer trying to evaluate stresses in the area of the reentrant corner at elevation 720 feet. Accurate determination of stress is no longer a concern because, from previous analyses, it is clear that cracking would start and propagate through the dam. The failure mode would be dominated by the rigid body motion of dam monoliths slipping and rocking on interfaces. Nonlinear models typically require quite a bit of time to run. Run times correlate roughly to the number of elements squared. It therefore behooves the analyst to not have an overly fine mesh when performing nonlinear analysis.

Interface parameters are reflective of the following assumptions:

- Vertical interfaces between monoliths have some keying. This is modeled by assuming a high friction angle of 75 degrees. If monoliths are in contact at all, they are capable of transmitting some shear between them. Keys could have been modeled directly with a significant increase in model complication.
- The interface between the abutments and the dam is assumed to be rough. Again, 75 degrees is used.
- The interface at elevation 720 feet is assumed to be broken concrete along a relatively smooth lift surface. A friction angle of 45 degrees is representative of this state.

Figure A2-14 tracks displacement of three points during the earthquake: (1) the motion of the base concrete below elevation 720 feet, (2) the motion of the base of monolith 7, and (3) the motion of the base of monolith 8.

At this history sampling point, the slip on plane 720 is about 0.1 foot (1.2 inches) at the end of strong shaking. Monoliths 7 and 8 are moving downstream with respect to the base.

The induced offset can be captured and plotted around the perimeter of the potential failure surface (see figure A2-15). In general, offsets are on the order of 1 inch over a significant portion of the failure surface.

The analysis performed above ignored the effects of uplift. If the crack at elevation 720 feet is not present until 15 seconds into the earthquake, it can be reasoned that there is insufficient time for the crack to be pressurized by the reservoir. This assumption may be reasonable, but it is somewhat unconservative. Figure A2-16 shows offsets produced when the effect of uplift is applied in the joint using concentrated forces at nodes. While offsets are several times greater than when uplift is ignored, they are still on the order of inches and not feet.

Selecting Analytic Tools for Concrete Dams to Address Key Events Along Potential Failure Mode Paths

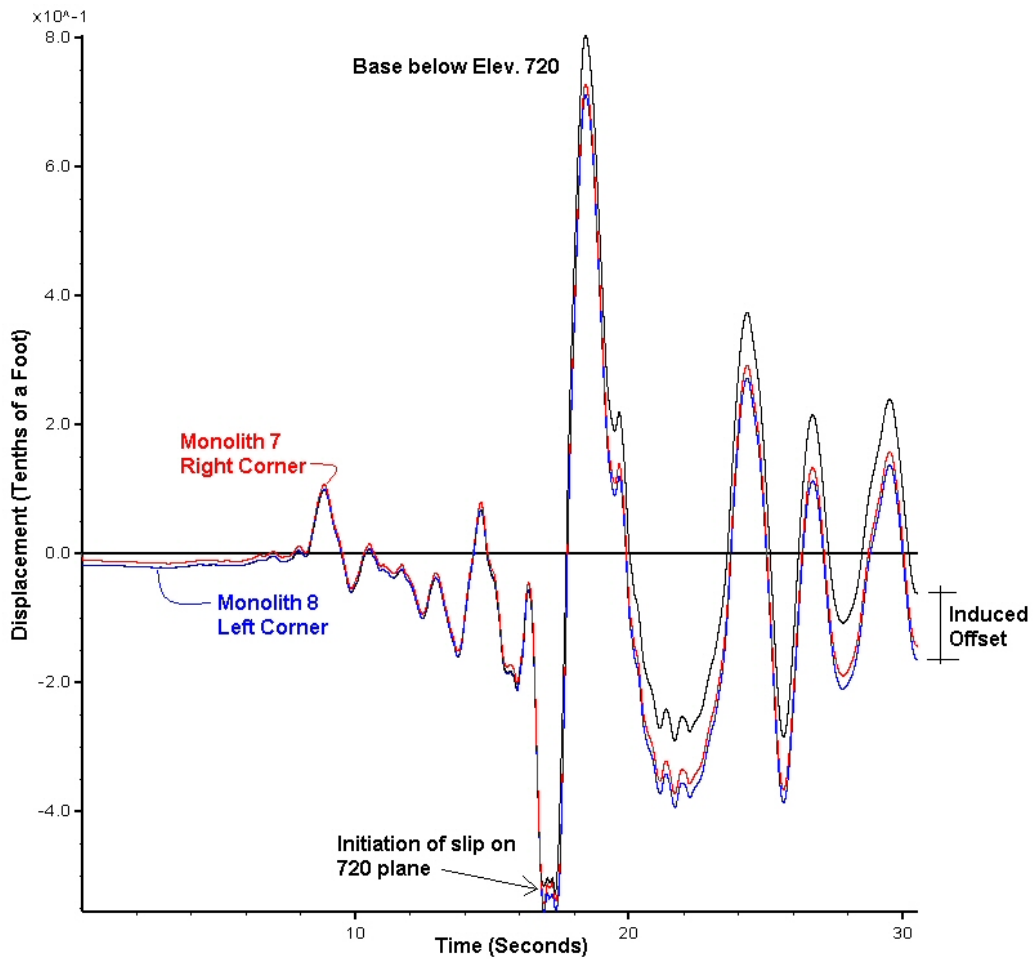
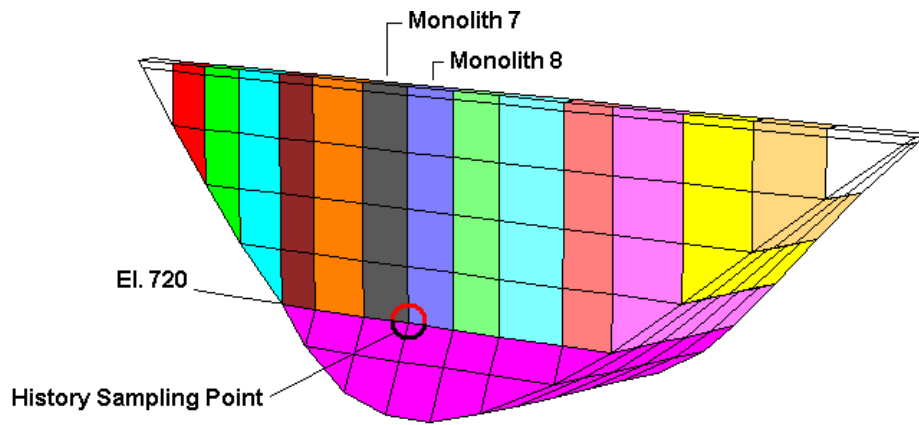


Figure A2-14: Induced offsets.

## Selecting Analytic Tools for Concrete Dams to Address Key Events Along Potential Failure Mode Paths

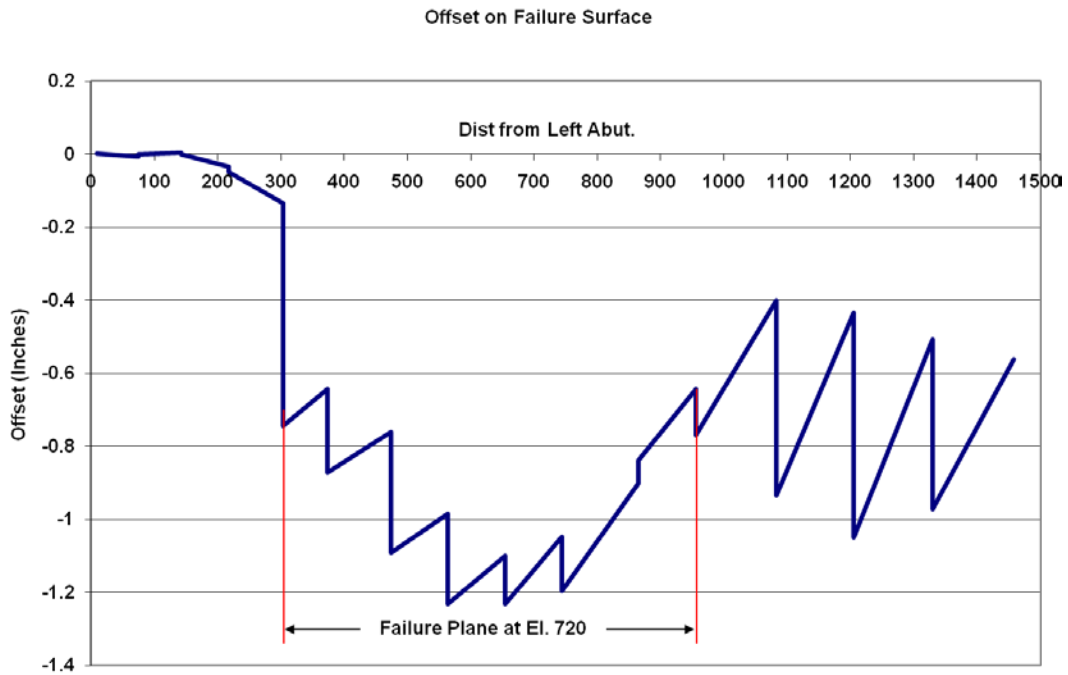


Figure A2-15: Without uplift, induced offsets at each contraction joint looking down at the model.

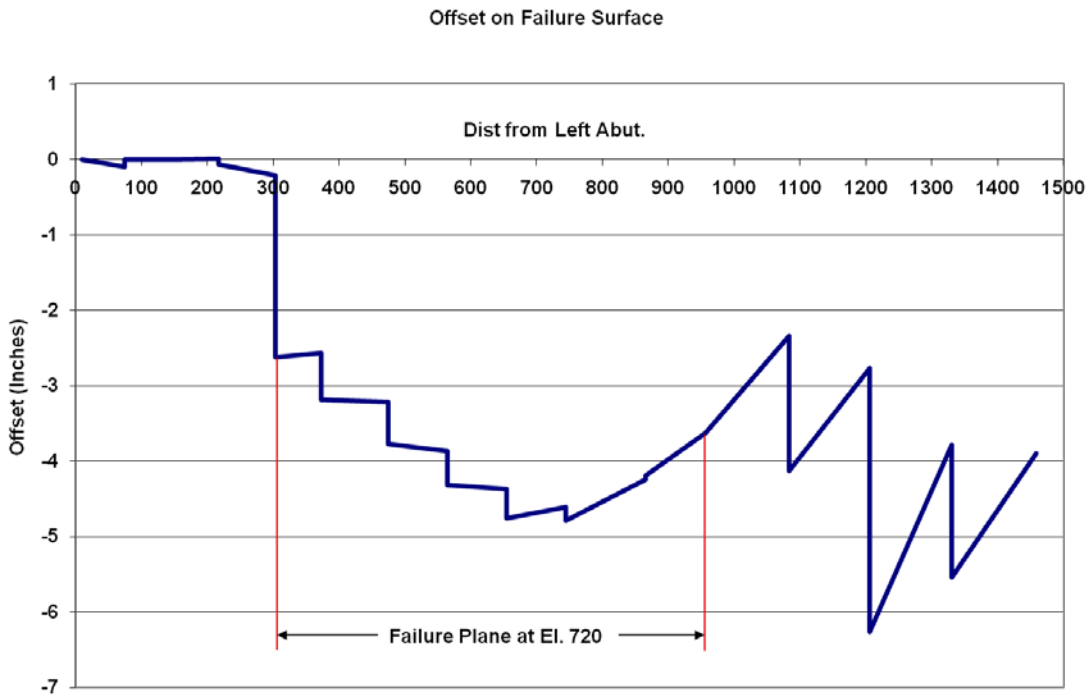


Figure A2-16: With uplift, induced offsets at each contraction joint looking down at the model.

One could argue that the 75-degree friction angle assumed on the right abutment interface is not appropriate considering the 6 inches of offset indicated in figure A2-16. It would be prudent to lower the friction angle to a residual value between 40 and 45 degrees and rerun the analysis. Certainly, larger offsets would result on the right abutment. However, this is technically a different failure mode and should be evaluated independently from the failure of blocks with a base plane at elevation 720 feet.

It is also possible that if abutment sliding were inhibited, sliding of blocks with a base plane at elevation 720 feet could be affected. Numerous parameters could be investigated through sensitivity analysis. However, each time a parameter is varied, a new run would have to be done. Judgment must be applied considering that each run takes considerable time.

## **A2.5 Node E: Duration and Severity of Shaking Sufficient to Cause Failure**

The analyses performed at nodes A through D have shown that cracking caused by the earthquake motions cannot be ruled out, and also that it is reasonable to expect that portions of the dam would slide downstream, but that the amount of displacement is on the order of inches. Is this induced offset cause for concern? The reservoir would not be released by blocks moving downstream a few inches. Was it necessary to progress through the entire failure tree, node by node, with ever more complicated analyses? It is probably not necessary. A simple Newmark style analysis could be done to estimate how big offsets would get.

The equation below, an expression of F=MA in finite difference form, can be solved iteratively using a simple program, or even a spreadsheet. As opposed to the 3D nonlinear analysis associated with node D, this computation can be performed in seconds rather than hours.

$$\begin{aligned}
 F_t &= M_s * A \\
 A &= \frac{D_{(t+\Delta t)} - 2 * D_{(t)} + D_{(t-\Delta t)}}{\Delta t^2} \\
 F_t &= M_s * \left( \frac{D_{(t+\Delta t)} - 2 * D_{(t)} + D_{(t-\Delta t)}}{\Delta t^2} \right) \\
 \frac{F_t * \Delta t^2}{M_s} &= D_{(t+\Delta t)} - 2 * D_{(t)} + D_{(t-\Delta t)} \\
 D_{(t+\Delta t)} &= \frac{F_t * \Delta t^2}{M_s} + 2 * D_{(t)} - D_{(t-\Delta t)} \qquad \text{eq. E1}
 \end{aligned}$$

where,

- D = downstream displacement.
- t = time.
- F<sub>t</sub> = total instantaneous force imbalance. This is the static and dynamic driving forces minus total frictional resistance.

$M_s$  = total system mass including the dam above the elevation 720 failure plane and the mass of participating water.

Inherent in this analysis is the assumption that the failure plane is fully cracked and that a residual friction angle is approached due to slipping along the failure plane. In this example, 45 degrees was assumed. Uplift was assumed to be acting on the failure plane.

Results are shown in figure A2-17. Note that this simple rigid body sliding model results in 8 inches of downstream offset, similar to the 6 inches of downstream offset indicated by the 3D nonlinear dynamic analysis done for node D.

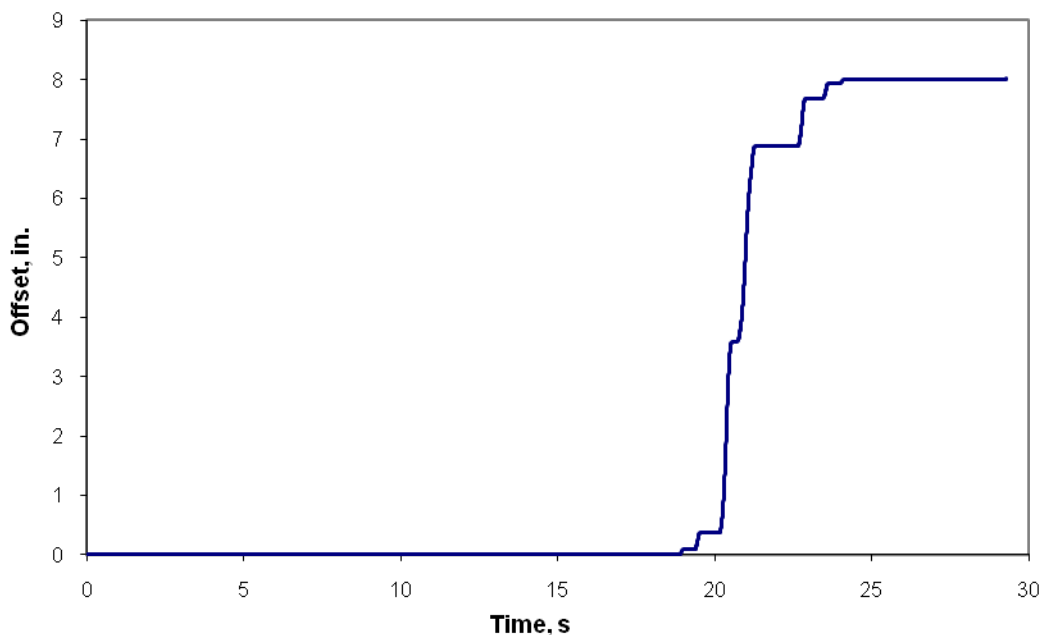


**Figure A2-17: Results of Newmark analysis.**

Whether offset is 1 inch or 10 inches, this is a small amount compared to the 294 feet of contact length on the failure plane; however, drain efficiency may be compromised if offsets are greater than drain diameter or dilation on the plane allows for large water inflows. In addition, joint shear strength would be reduced as a result of sliding.

## **A2.6 Node F: Damage Caused by Earthquake Results in the Dam Being Unable to Resist Static Loads**

The simple gravity analysis shown in figure A2-18 and accompanying results in table A2-1 reveal that with a friction angle of 45 degrees, there is a post-earthquake factor of safety of 1.34. The block above elevation 720 feet is stable.



**Selecting Analytic Tools for Concrete Dams to Address  
Key Events Along Potential Failure Mode Paths**

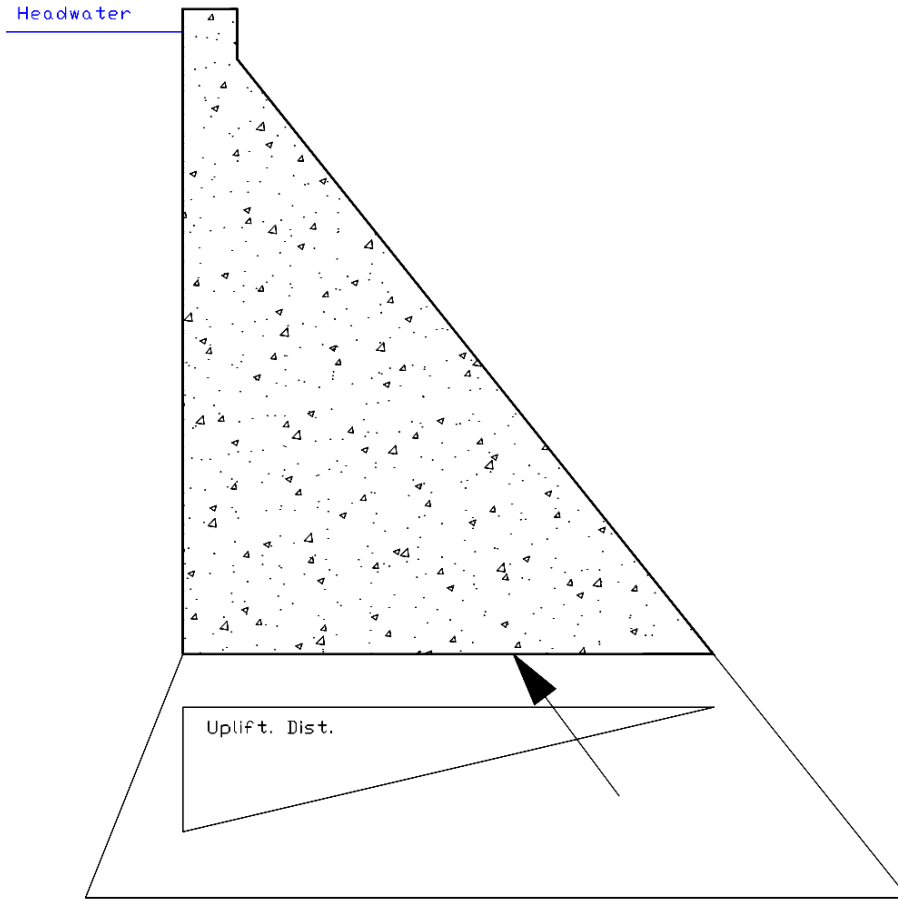


**Figure A2-18: Post-earthquake analysis.**

**Table A2-1: Results**

Forces	Fx (kip)	Y= (feet)	Fy (kip)	X= (feet)	Moment (0,0) (kip-ft)
Dam weight	0.00	0.00	-8,142.75	97.65	795,143.31
Headwater	3,713.58	835.00	0.00	0.00	3,100,839.00
Uplift	0.00	0.00	3,164.62	98.00	-310,132.38
Totals	3,713.58		-4,978.13		3,585,850.00
Resultant location at X= 183.216 ft, Y= 720 ft, sliding safety factor = 1.34					

Note: kip = 1,000 pounds, kip-ft = 1,000 pound-feet

## Selecting Analytic Tools for Concrete Dams to Address Key Events Along Potential Failure Mode Paths

---

Input parameters:

- Concrete unit weight = 150 pounds per cubic feet (lb/ft<sup>3</sup>)
- Slide plane phi = 45 degrees
- Head elevation = 1065 feet
- Tailwater elevation = 720 feet

One point that must be understood is that if the failure process is interrupted at any node, failure will not occur. It is not necessary to progress through the failure tree from the first node to the last. If failure can easily be ruled out at any node, it is most prudent to concentrate efforts on that node and ignore other nodes. Figure A2-19 illustrates this point.

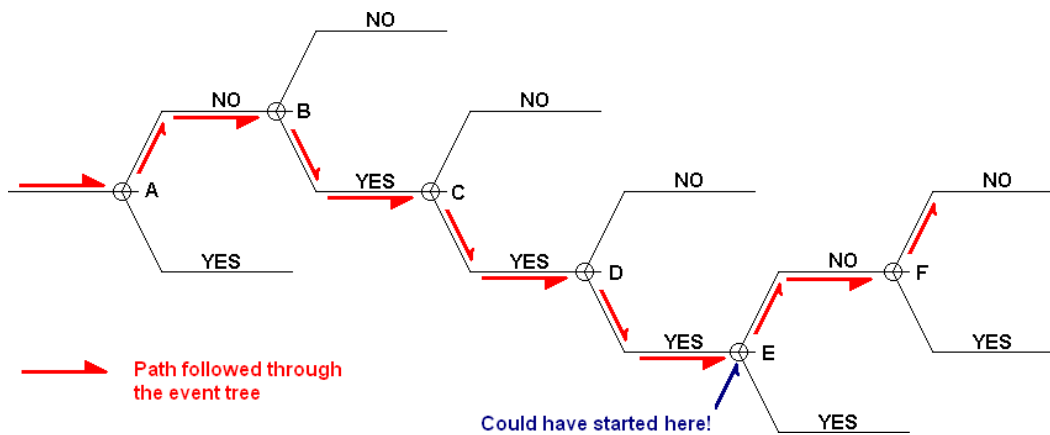


Figure A2-19: Path through event tree.

## **Appendix A3**

# **Earthquake Causes Sliding in Foundation Leading to Dam Failure**



## Appendix A3: Earthquake Causes Sliding in Foundation Leading to Dam Failure

This potential failure mode is due to a seismic event with sufficient energy to displace a removable rock block of sufficient size in an abutment causing loss of foundation support for a curved gravity dam (see figure A3-1). With loss of abutment support, sections of the dam may not be stable. The dam and foundation blocks may slide together and fail as a unit.

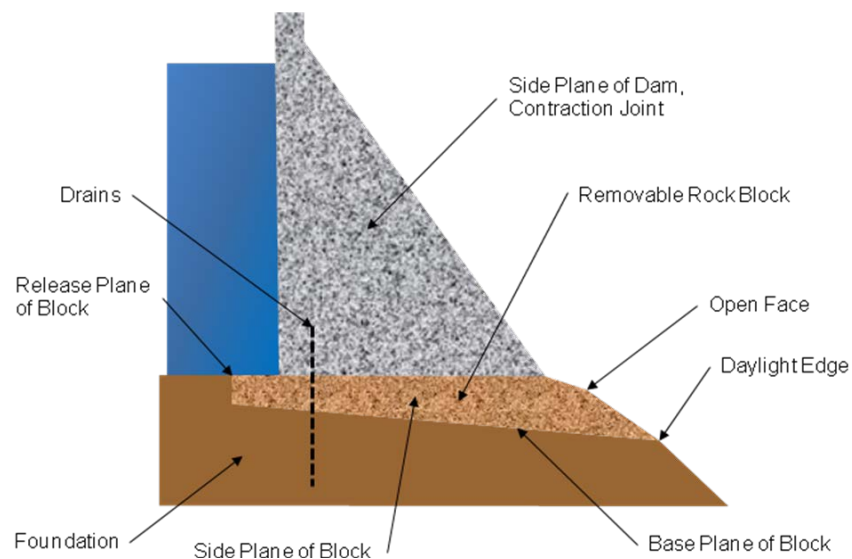


**Figure A3-1: Schematic of a dam built on a removable rock block in the foundation of sufficient size to affect dam stability if the block moves.**

The key point in the description of this potential failure mode is that the rock block is potentially removable and is of sufficient size to affect the stability of the dam. For this example, it is assumed that no potential failure mode is associated with rock blocks if there is no removable block in the foundation. A removable block has a base plane, side plane(s), and a release plane, as well as a free surface for the block to slide toward (see figure A3-1). The base plane of the block is a relatively horizontal surface forming the bottom of the block. The side planes of the block are steeply sloping, diverging surfaces oriented in the stream direction. The release plane is a steeply sloping surface oriented in the cross-canyon direction and positioned at the upstream extent of the block. Movement of the rock block would slide on both or either of the base and side planes and would pull away from the release plane. An open face is an unrestrained face. There is also no potential failure mode if the block is too small to affect the stability of the dam. In this case, the dam can bridge across the block. Considerable field work may be necessary to determine the likelihood that a block exists and that this potential failure mode is possible in the foundation. Movement of the rock block is a function of the driving forces on the block and the resisting forces as described below. Figure A3-2 shows graphically what might happen if the

rock block slides, the loading path changes, the shearing resistance changes, the concrete fractures, and the drainage system undergoes disruption. In addition, dilation of the foundation planes may result in increased seepage and a change in water pressures including the development of full hydrostatic pressure on the release plane.

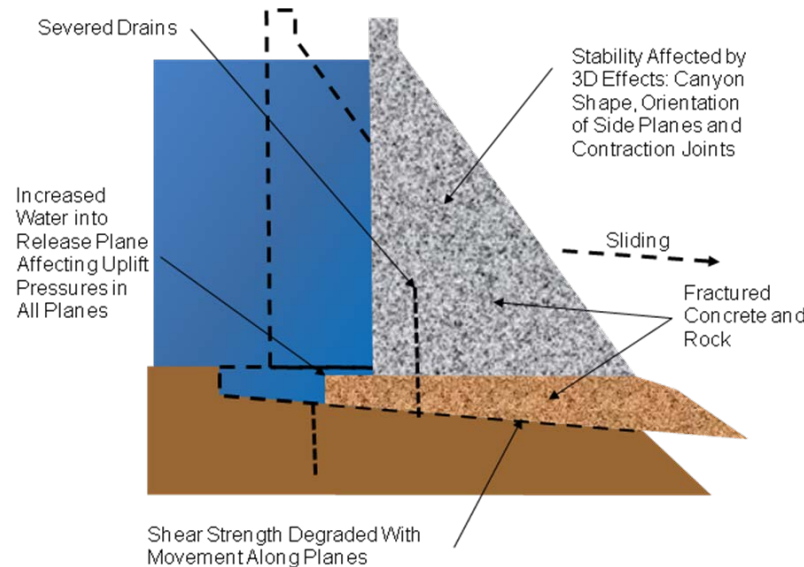


**Figure A3-2: Potential failure mode of sliding of a removable block in the foundation induced by a seismic event and post-seismic considerations.**

The event tree for this potential failure mode is shown in figure A3-3 and has five nodes along the tree. In this case, it has been determined that there is a removable block in the foundation and the potential failure mode exists. The analyst could start at any point along the event tree to attempt to disprove failure, but in this example, the following sequence was used.

### **A3.1 Node 1: Initiating Event: Earthquake Load with Normal Operating Loads**

Node 1 of the event tree considers if the earthquake has sufficient magnitude along with the corresponding static loads to potentially cause movement of the foundation block. When appropriate, static operating loads include gravity, reservoir, ice, tailwater, silt, temperature, uplift, and other loads during normal operations. The dynamic loads include inertial forces of the dam onto the foundation block, inertial forces of the foundation, and the hydrodynamic interaction of the reservoir. Some loads (typically temperature, ice, and silt loads) apply an initial state of stress in the dam and foundation but are relieved once movement occurs.

## Selecting Analytic Tools for Concrete Dams to Address Key Events Along Potential Failure Mode Paths

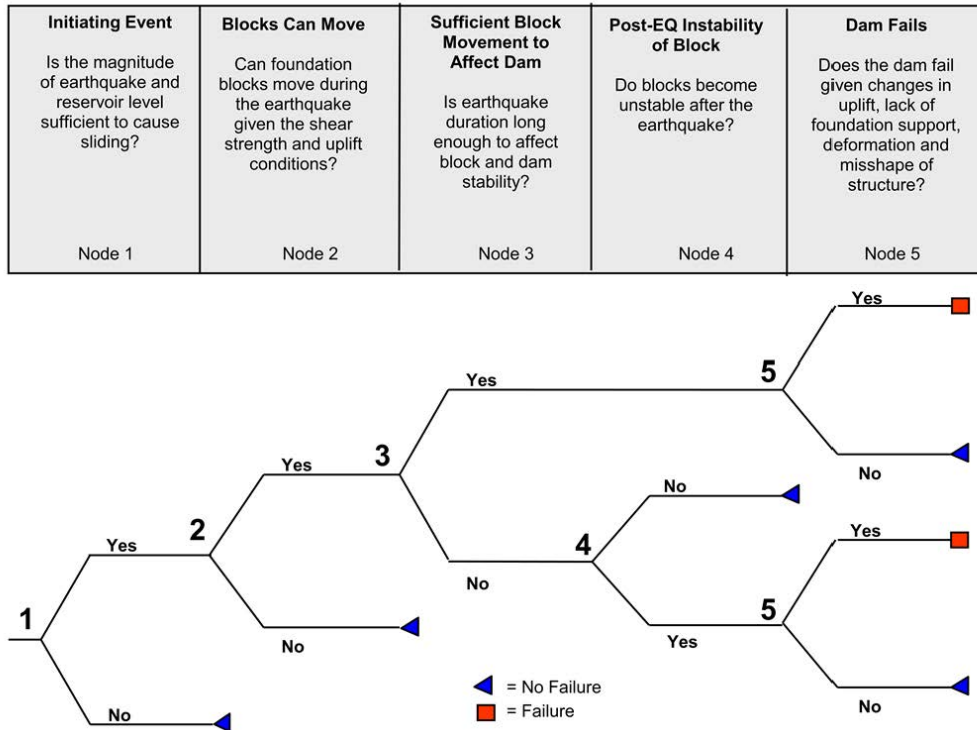


**Figure A3-3: Event tree for this potential failure mode.**

Conversely, follower loads (typically gravity, hydrostatic (reservoir, tailwater, and uplift), hydrodynamic, and seismic loads) continue to load the dam and foundation block even after movement occurs. These loads may change in magnitude as movement occurs. Static loads on the dam and foundation could be significantly different after the earthquake compared to the start of the earthquake. The dam may become unstable not from the seismic loads but from the new post-seismic static loads and material strengths.

Following the earthquake, other potential failure modes not associated with the seismic event, such as increased reservoir elevation on the damaged structure, could develop and should be checked.

### A3.2 Node 2: Movement of Foundation Block Commences

Node 2 of the event tree considers if the driving forces on the foundation blocks are sufficient to overcome the sliding resistance and sliding initiates. Movement of foundation blocks is a function of the magnitude and orientation of the applied loads, the cyclical nature and frequency content of the ground motion, the shear strength along sliding planes, and the orientation of the sliding planes. Shear strength along sliding planes is a function of joint roughness and infilling material. Depending on the orientation of the joints and the orientation of the loading, sliding can be along a single plane or along the intersection between two planes.

### **A3.3 Node 3: Sufficient Block Movement Affects Dam**

Node 3 of the event tree determines if the earthquake lasts long enough to cause sufficient sliding of the foundation blocks to affect the stability of the dam. The earthquake must have sufficient duration to induce sufficient movements in the foundation to have the potential to cause a dam failure. One large pulse of the earthquake may cause initial foundation block movement, but if the movement is too small and not sustained, redistributed loads within the dam may prevent failure. Longer duration earthquakes can cause larger movements in the foundation such that loads cannot be redistributed in the dam and thus might cause failure during the earthquake. For this reason, the event tree splits into two possible scenarios at node 3. If the earthquake has sufficient duration to move the foundation block enough to affect the stability of the dam, the tree progresses to node 5, where the stability of the dam is evaluated during the earthquake. If the earthquake does not have enough duration to fail the dam during the earthquake, the event tree progresses to node 4, where the post-earthquake stability of the foundation block is evaluated due to possible changes in static load and sliding resistance.

### **A3.4 Node 4: Foundation Block Slides After the Earthquake (Post-Earthquake)**

Node 4 of the event tree deals with post-seismic stability if the foundation blocks do not slide enough during the earthquake to adversely affect dam stability. Movements of the foundation block may change stability conditions, increasing uplift and waterflow around the block, crushing or fracturing rock blocks, or reducing shear strength from sliding. Post-seismic stability considerations might include aftershocks. Uplift might increase around the block from: (1) opening of the release plane, allowing full hydrostatic reservoir head to penetrate to the full depth of the block; (2) dilating of block planes, allowing more water to penetrate along the planes; or (3) severing or disruption of foundation drains, impairing their ability to relieve seepage pressures.

### **A3.5 Node 5: Dam Fails**

Node 5 of the event tree considers the stability of the dam given post-earthquake instability of the foundation block. The movement of the block has occurred either during the earthquake (node 3) or after the earthquake (node 4). Questions that could be asked are: How stable is the dam given a certain amount of movement in the foundation? How stable is the dam given a certain lack of foundation support? Are there other 3D mechanisms that might come into play that could stabilize the dam? Is the dam too deformed or damaged to be stable? Is the dam large enough to stabilize the foundation block and prevent large releases of the reservoir?



### A3.6 Case Study of a Foundation Stability Study

The following case study describes the process of progressing through an event tree multiple times. The potential failure mode is sliding of a large block in the foundation under a curved gravity concrete dam (see figure A3-4). Each assessment through the event tree represented more focused attention to a node in the tree, reducing uncertainty (associated with the seismic loading, geology, and material properties) and increasing understanding of the dam response by using more advanced analysis methods to remove known limitations of simpler methods, making a **No** failure decision at any of the nodes more defensible.

The dam is generally in good condition and has performed well for over 50 years. Great attention was paid to the geology of the foundation during original construction, but little was understood at that time regarding potential failure modes related to sliding of foundation rock blocks. The primary dam safety issue had to do with potential sliding on weak bedding plane partings within the dolomitic limestone of the left abutment. The entire left abutment of the dam was founded on a 30-degree “dip slope” in the dolomitic limestone foundation rock (continuous bedding plane partings parallel the abutment contact at various depths (base planes) and daylight just downstream from the dam (open face)) (see figure A3-5). Faults and joints form additional discontinuities (side and release planes) within the rock mass potentially allowing movement of large foundation blocks. It was determined that the foundation blocks were removable and large enough to affect the stability of the dam. Block sliding in the foundation is definitely a potential failure mode.



**Figure A3-4: Aerial view of curved gravity dam,  
Bureau of Reclamation.**



**Figure A3-5:** This photograph, taken during construction, shows dam-to-foundation contact and the continuous nature of slide planes on the left abutment; the side plane is the fault just below workers, the base plane is parallel to dam contact, and the release plane is vertical along the upstream face of the dam, Bureau of Reclamation.

### **A3.6.1 Node 1: Seismic Load and Normal Loads**

Node 1 relates to the initiating event: an earthquake. The dam is in a relatively high seismic area, so a sufficiently large earthquake is of concern. Hydropower generation at the dam requires a constantly high reservoir level, making static driving forces and post-seismic stability a concern and generating hydrodynamic forces that would increase seismic loads. The dam is a massive curved gravity dam, so temperature loads, ice loads, and silt loads are of lesser concern.

### **A3.6.2 Node 2 and Node 3: Block Movement Commences and Affects the Dam:**

#### **Assessment 1**

Node 2 considers if movement of a foundation block occurs, and node 3 considers how much movement occurs. The first time through the event tree was based on simplified and preliminary assessments, based on existing knowledge about the foundation, screening-level seismic ground motions, assumed material properties, forces generated from the dam to foundation with linear elastic finite element models (see figure A3-6), assumed uplift pressures, approximated plane orientations, and simplified, linear, uncoupled rigid block Newmark analysis (see figure A3-7). Uncoupled analysis means that the dam analysis and the foundation stability analysis are separate computations. Forces from the dam are applied continuously on the foundation and do not change as the foundation moves. Also, any rotation of the foundation blocks is not considered.

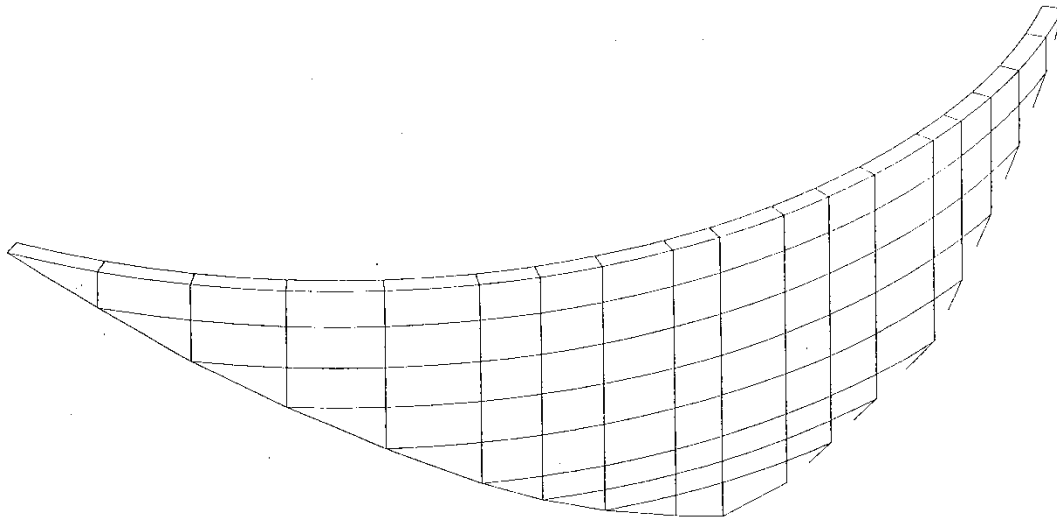


**Figure A3-6: EACD3D96 finite element model of the dam computed forces from the dam into the foundation for an uncoupled rigid block Newmark foundation stability analysis.**

The computed maximum displacement of the foundation block was 180 feet (see figure A3-7). Because of the large magnitude of predicted displacements, the responses to nodes 2 and 3 were **Yes**.

The alarming prediction of 180 feet of deformation needs to be tempered with the realization that because of 3D effects, the failure mode analyzed is probably impossible. If this analysis had concluded that the displacements were small, it could have been reasoned that failure could not occur. The fact that the simplified analysis predicted very large movements does not mean the converse, and further analysis is required.

### **A3.6.3 Node 2 and Node 3: Block Movement Commences and Affects the Dam: Assessment 2**

The results of the first study had large uncertainties based on available information and simplified analysis. At this point, one could choose to refine the material properties and loads or change the analysis technique. The decision was made to reduce uncertainties, refining seismology with site-specific field investigations, performing site-specific geologic investigations, extracting core and performing laboratory testing of the block slide planes and concrete within the dam, including large scale roughness effects to increase sliding resistance, and conducting vibration testing of the dam. The cost of creating a nonlinear, coupled finite element model was significant, so this was not done during the second study. Uncertainty associated with the simpler, uncoupled analyses was known and accepted for this assessment. It was known at the start of studies 1 and 2 that the simplified, uncoupled rigid block Newmark method had limitations and would probably overpredict sliding displacements of the rock blocks. However, the analyses could be easily rerun, inputting new material properties.

**Selecting Analytic Tools for Concrete Dams to Address Key Events Along Potential Failure Mode Paths**

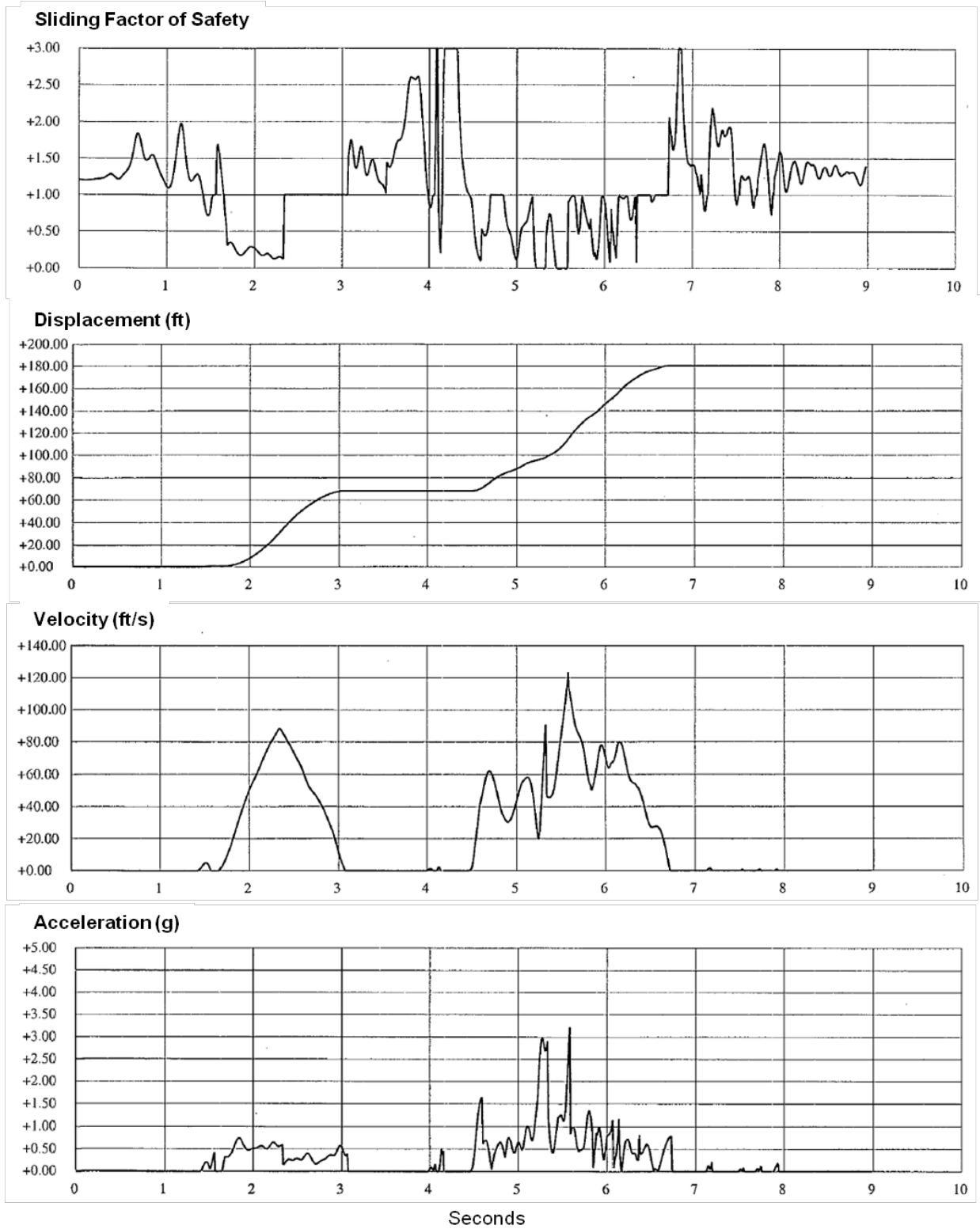


**Figure A3-7: Results from the uncoupled Newmark rigid block sliding study.**

No further studies would be necessary if the uncoupled analyses using the best available data showed acceptable displacements. Unfortunately, the displacements computed in this assessment were still significant enough to affect the stability of the dam, and the responses to nodes 2 and 3 were still **Yes**.

#### **A3.6.4 Node 2 and Node 3: Block Movement Commences and Affects the Dam: Assessment 3**

It was decided that the third assessment through the event tree would be based on more advanced analyses. A nonlinear, coupled dam-foundation-reservoir, dynamic, structural analysis using LS-DYNA was the next step. A coupled analysis includes both the dam and a critical foundation block in the same finite element model so that the forces on the blocks change as movements occur and redistribution of loads and dam-foundation interaction takes place (see figures A3-8 and A3-9). Nonlinear aspects of the analyses included contact surfaces to model the contraction joints in the dam and foundation sliding planes, and reservoir water modeled with finite elements.

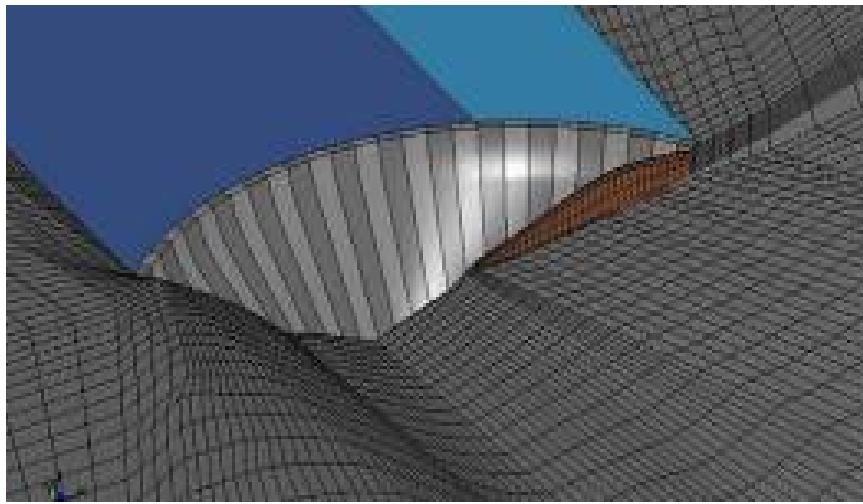


**Figure A3-8: Closeup of LS-DYNA model showing dam, contraction joints, foundation, reservoir, and potentially unstable rock blocks, Bureau of Reclamation**

The LS-DYNA results indicated significantly smaller foundation block displacements of 3.3 inches, depending on the magnitude of the earthquake (a few inches compared to tens of feet) for low Rayleigh damping levels (about 2 percent of critical), frictional damping, and radiation damping on the order of 0.4. This is, in large part, due to the 3D effects of the vertical contraction joints in the dam in controlling the mode of sliding. Contraction joints in the dam forced sliding of the blocks in an oblique, uphill direction along the theoretical intersection of the contraction joint and base plane, resulting in higher static safety factors and, thus, smaller seismic displacements. There also was a small clockwise rotation of the block not computed in the uncoupled analysis. The response for node 3 was now **No**. However, the response at node 4 could not be a **No** because with 3.3 inches of movement, the foundation drains could be pinched shut, permitting increased uplift pressures, and the release plane was now open and joints dilated

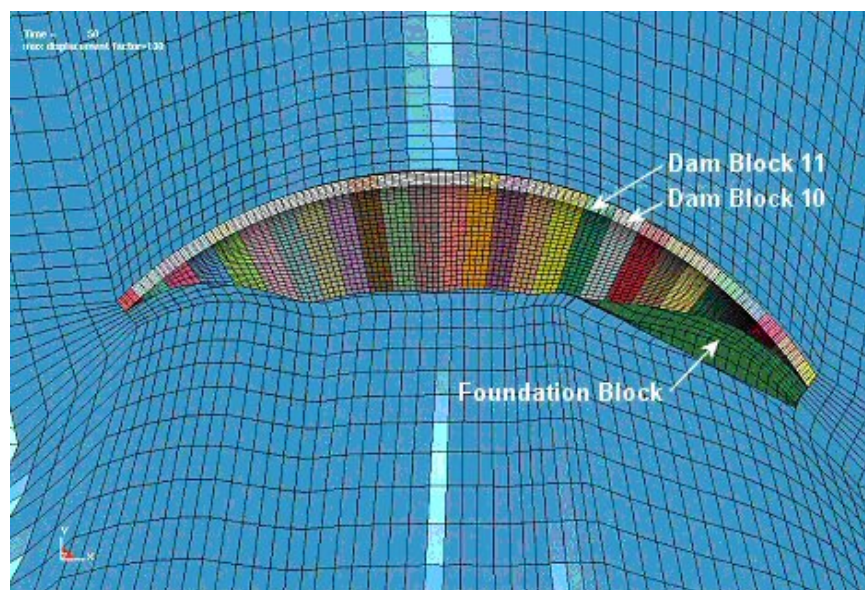


Figure A3-9: Plan view of LS-DYNA model showing dam, contraction joints, foundation, reservoir, and potentially unstable rock block, Bureau of Reclamation.

to permit direct inflow of reservoir water into the planes. Post-seismic stability would be in question. Although it is difficult to predict exactly how the foundation water pressures would change following earthquake movement, they are likely to increase as a result of the release plane opening up along the upstream dam contact. Post-earthquake foundation stability with increased uplift is, therefore, a concern. The results of the modeling indicated that the dam and foundation were likely to be stable during a large earthquake, but post-earthquake stability was still questionable. This prompted additional studies addressing nodes 4 and 5 and to further reduce some uncertainties.

#### A3.6.5 Node 4: Post-earthquake Stability of the Foundation Blocks

For the reasons just stated, a fourth time through the event tree for post-seismic stability was performed using an additional validation of the nonlinear finite element model and including post-seismic stability analyses. There is considerable uncertainty in the assumed uplift profiles. It was assumed an increase in uplift would be nearly certain if the dilation along the planes approached the maximum value of about 2.5 inches. For dilations less than an inch, increases in uplift were thought to be unlikely. If the horizontal displacement from LS-DYNA was calculated to be more than half the drain diameter of 3 inches, it was thought likely that the uplift would tend toward the linear case of full reservoir head on the upstream side to zero at the downstream point (point above tailwater). If the displacement was less than this, it was thought that drain effectiveness would likely remain, and the case of 50-percent drain effectiveness (drain factor  $K=0.5$ ) was chosen to represent this condition.

The post-seismic static sliding factors of safety were greater than one, showing stability even with inoperable foundation drains, varied uplift profiles, and reduced shear strengths, indicating that post-earthquake instability is unlikely in any case. So the response for node 4 was **No**.

### **A3.6.6 Node 5: Dam Fails**

Because the response at node 4 was **No**, the event tree sequence stopped and did not lead to a plausible failure of the dam.

## **A3.7 Addressing Uncertainty**

This case study shows the process of approaching an assessment of a potential failure mode in phases from simple analyses with large uncertainties and known limitations to more complex analyses with reduced limitations and uncertainties. Because this process involved multiple analyses building on one another, it is important not to take conclusions from initial analyses that were superseded. The first phase assessment for nodes 2 and 3 resulted in significant sliding, using known limitations in the simplified Newmark rigid block analysis with accepted uncertainty in the available and assumed material properties and loading. The assessment was that the block could slide too far to maintain dam stability. The second phase assessment also focused on nodes 2 and 3 with the intent of reducing the uncertainties on the loads and material properties. Again, the assessment was that the block could slide too far to maintain dam stability. The third phase also focused on nodes 2 and 3 with the intent of reducing the limitations of the simplified analyses with nonlinear analyses. The nonlinear analyses eliminated some limitations of the uncoupled analysis because it modeled additional features. The assessment was that the block would slide but not far enough to fail the dam during the earthquake. This moved the assessment along the event tree to node 4 and, to a smaller degree, still in node 3. The additional uncertainties in the nonlinear analyses were addressed, and the post-seismic stability analyses determined that the dam would be stable after a large earthquake.

Nonlinear analyses provide valuable insight into the nonlinear response of the dam and foundation block. The geometric nonlinearities in the model required numerous validation studies to gain confidence in the model and demonstrate it was correctly working. This would also be true if the material nonlinearities of the concrete or foundation rock were modeled. Nonlinear analyses require additional considerations for element size, load path, wave travel through the finite elements, time step, rate effects, effects of damage, and damping. There needs to be a demonstration of the model's ability to replicate stress-strain paths and failure along strain paths not used in the fitting procedure. The evolution of damage needs to be represented. The rate effects attributable to inertial resistance to crack opening may also be an important parameter.

Uncertainties were reduced by several means. Strength properties used in the Newmark and nonlinear models were based on a detailed, laboratory, direct shear testing program to determine the basic friction angles (with dilation removed) of the various bedding plane partings and detailed photogrammetric roughness profile evaluation to estimate the waviness component to shear strength. Concrete properties were determined from detailed laboratory testing and vibration testing. Foundation water pressures were determined from a series of permanent and temporary piezometers (placed in existing foundation drain holes). The approximate average displacements of the block from the finite element analyses were used to estimate the amount of probable dilation and resulting friction based on the roughness studies.

## Selecting Analytic Tools for Concrete Dams to Address Key Events Along Potential Failure Mode Paths

---

Some uncertainties were not addressed or still remained. First, a friction angle of 55 degrees was assigned to the contraction joints in the dam model. The contraction joints are keyed, providing higher shear strength than included in the finite element model. Second, full uplift was included on the back release surface in the analyses, which is unlikely to exist under current predisplacement conditions based on piezometric measurements and the tightness of the foundation.

An understanding of the geometric interaction between the faults in the foundation and the contraction joints in the arch dam was vital when assessing results from the nonlinear coupled dam/foundation analysis. The contraction joints converge in the downstream direction, making their wedge shape inherently stable. The block planes diverge in the downstream direction, but the likely direction of sliding is controlled by a dam contraction joint at the downslope limit of the foundation block. This resulted in a more favorable condition and reduced sliding displacements. In essence, the dam helps stabilize the foundation. This may be acceptable for a massive dam such as a gravity dam.



## **Appendix A4**

# **Increased Silt Load Causes Failure of Reinforced Concrete Corbels of a Buttress Dam**



## **Appendix A4: Increased Silt Load Causes Failure of Reinforced Concrete Corbels of a Buttress Dam**

This potential failure mode considers increased loads due to silt buildup on the slabs of the buttress dam. Increased silt loading takes place when the elevation of silt buildup is higher than the anticipated height for design. The increased elevation of the silt would cause an increase in lateral and vertical earth pressures that act on the slabs of the buttress dam which are supported by the corbels. Most dams are designed to resist the forces of silt up to a certain elevation, at which time the silt would be removed to a lower level and the silt buildup process would start over again. Silt buildup can occur more rapidly than expected due to occurrences upstream of the dam such as heavy construction or poor land management techniques. The situation is compounded by a lack of maintenance or a disregard for the level of silt. Figures A4-1 and A4-2 show a typical slab and buttress dam.

The event tree for this potential failure mode is presented in figure A4-3. The resulting overstressing and failure of the corbels could lead to loss of support of the buttress slabs which could lead to loss of storage and instability of the buttress dam system. Several failure mechanisms of the corbel must be investigated to determine the mechanism with the least strength associated with it. Figure A4-4 presents the possible failure mechanisms that must be investigated to determine the strength of the corbel system. The four potential failure mechanisms are: (1) direct shear failure at the interface between bracket or corbel and supporting member; (2) yielding of the tension tie due to moment and/or direct tension; (3) crushing of the internal compression “strut;” and (4) bearing or shear failure under the loaded area.

The analysis addresses all four mechanisms of failure of the corbel that could lead to the failure of the slab that could release the reservoir, constituting failure of the dam. This example assumes failure of the corbel results in failure of the dam. Analysis was accomplished without load factors because actual failure states were of interest. The concrete compressive strength, originally at 3,000 lb/in<sup>2</sup>, was assumed to deteriorate to 2,500 lb/in<sup>2</sup>, and the yield strength of the steel was assumed to be 40,000 lb/in<sup>2</sup>.

**Selecting Analytic Tools for Concrete Dams to Address  
Key Events Along Potential Failure Mode Paths**

---



**Figure A4-1: Downstream side of a slab and buttress dam, Bureau of Reclamation.**

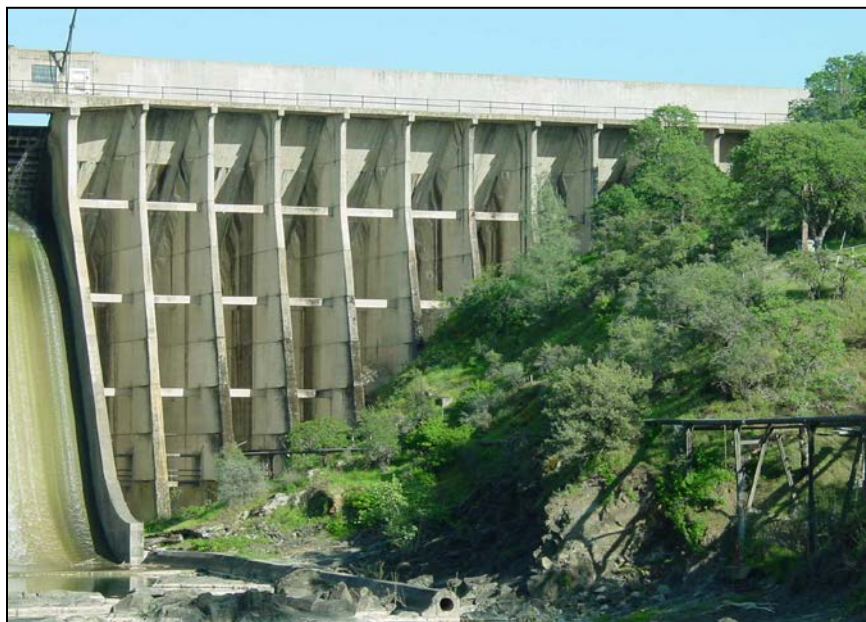


**Figure A4-2.—Closer photograph of the downstream side of the dam showing buttresses, struts, corbels, and upstream slab. This example looks at silt accumulation on the upstream side of the dam and the effect on the corbels, Bureau of Reclamation.**

**Selecting Analytic Tools for Concrete Dams to Address Key Events Along Potential Failure Mode Paths**

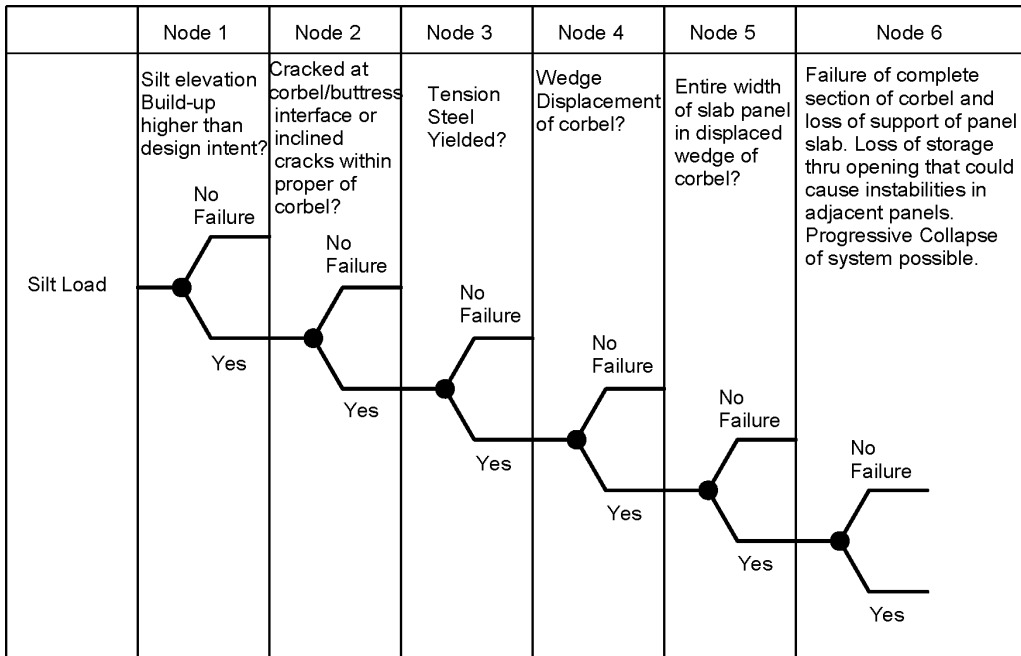


**Figure A4-3: Event tree.**

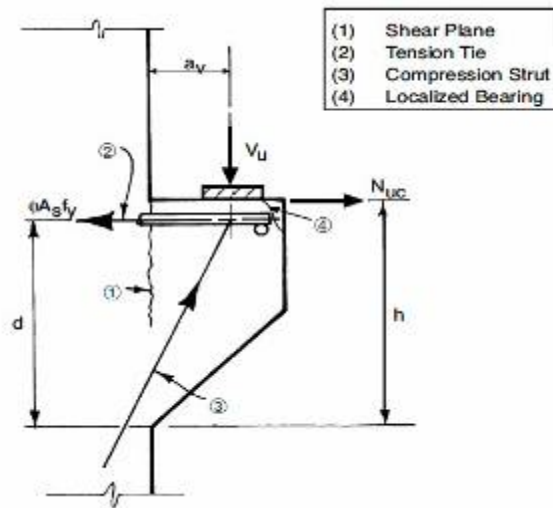


**Figure A4-4: Structural action of corbel.**

### **A4.1 Node 1: Initiating Event: Silt Buildup with Normal Loads**

This node investigates whether the design elevation for silt buildup has been exceeded in the presence of normal loads. The original design documents should be reviewed to determine the level of silt buildup accounted for in the original design, if any. Obviously, if the level of silt

buildup is less than allowed in the original design and the strength level of the concrete is adequate to support the design silt buildup level, failure of the corbel is unlikely due to silt buildup. Figure A4-5 shows the area of the corbel/buttress system being investigated.

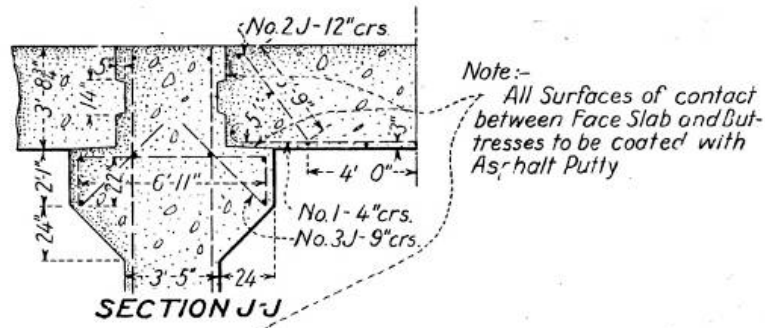


Figure A4-5: Corbel/buttress section.

## A4.2 Node 2: Crack Initiation at Corbel/Buttress Interface

Destructive and/or nondestructive tests on the concrete and reinforcing steel of the structural elements of the buttress dam should also be performed, depending on the age of the structure, to determine compressive strength levels of the concrete and condition of the reinforcing steel. Obviously, destructive testing needs to be done at a structurally inconsequential area. Information can be gleaned from the current conditions and construction records. Cracking at the interface between the corbel and buttress would indicate that service level loading has increased beyond the uncracked flexural capacity of the corbel and can also mean that the strut and tie phenomenon of the corbel system has been engaged. Further evidence of the strut and tie phenomenon would be diagonally oriented cracking within the corbel and buttress. The tension reinforcement near the top of the corbel will be engaged to balance the strut action of the strut and tie system being developed.

Analysis computations based on the silt and water levels, as well as the compressive strength of the in situ concrete, can predict the strength level of the various failure mechanisms. All failure mechanisms would involve various levels of cracking of the corbel and buttress. Because cracking would commence at the upstream side of the corbel, the presence of cracking could not be seen and could only be determined by nondestructive testing. Nondestructive testing would have to be capable of detecting interior delaminations as this would be the type of cracking involved. Access to the top side of the corbel is not possible due to the presence of the slabs, silt, and water from the reservoir.

### **A4.3 Node 3: Yielding of Tension Steel at Corbel/Buttress Interface**

Yielding of the tension steel at the top of the corbel would occur in conjunction with the compressive action of the inclined compression struts. Initially, the tension in the steel is due to flexural actions of the corbel just after first cracking at the interface between the corbel and buttress. Additional cracking, along with rotations of the formed struts, would cause additional tensioning of the steel until it reaches its yield strength. Actually, it is most desirable for the steel to reach its yield strength before the compressive struts crush since a brittle failure situation would exist if the concrete crushes before the steel yields. Analysis computations can determine the strength level of the corbel/buttress system at yield of the steel. An example of a corbel analysis is provided after section A4.6.

### **A4.4 Node 4: Wedge Displacement of Corbel**

This node describes the final stages of failure of the corbel. Signs of failure would be visible from the downstream face of the corbel/buttress. The wedge displacement would be characterized by a pair of inclined to nearly vertical cracks, with a horizontal crack running between the two cracks that is located near the intersection of the corbel and buttress face. Since the corbel is integral to the top of a sloping buttress wall, the loading on the corbel is variable, and the loading is reduced as the elevation of the corbel increases. The failure wedge could be less than the width of a slab panel; thus, there would not be a loss of support for the entire width of the slab.

### **A4.5 Node 5: Entire Slab Panel Width of Corbel in Wedge Displacement**

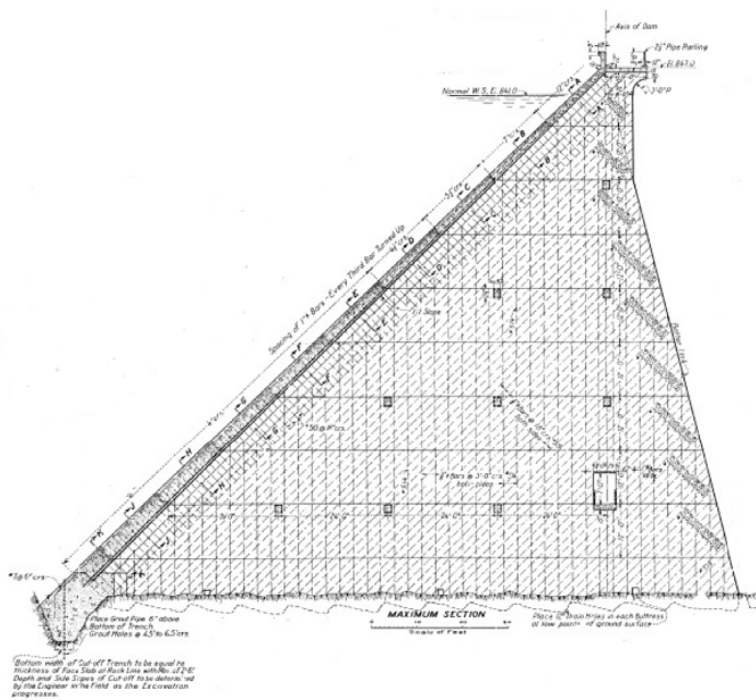
This node deals with a length of failed corbel that is equal to the width of slab. Without corbel support, the slab would displace downward, allowing water to leak from the reservoir. Damage to the bearing ends of the slab panels could eventually occur that would allow the slab to be completely dislodged. Overall instability of the slab and buttress system could result.

### **A4.6 Node 6: Corbel Fails Leading to Dam Failure**

This node deals with the loss of corbel support for the slab for the complete width of a slab panel. Loss of storage through the resulting opening could lead to instabilities of the adjacent panels. Progressive collapse of the system of slabs and buttresses could result.

**Summary of Variable Definitions for Example**

$L_{\text{slab}}$	Span length for slab panels, ft
H	Head of water above the section being analyzed, ft
$\gamma_{\text{water}}$	Unit weight of water, pcf
$v_{c\_plans}$	Originally calculated shear stress at corbel, psi
$f_{c\_plans}$	Originally calculated flexural compressive stress at corbel, psi
$f_{s\_plans}$	Originally calculated flexural steel stress at corbel reinforcing, psi
$f_c$	Calculated or allowable concrete flexural stress, psi
$f_s$	Calculated or allowable flexural steel stress, psi
b	Unit width used for analysis, ft
$h_R$	Corbel height at "R" position at wall, in
$d_R$	Depth to tension reinforcing for corbel, in
$A_s$	Effective area of tension steel for corbel, in <sup>2</sup>
$f_{c\_original}$	Compressive strength of corbel for original design, psi
$f_{y\_original}$	Reinforcement yield strength for original design, psi
$n_{original}$	Modular ratio used for the original design
Reaction <sub>water</sub>	Reaction on corbel due to water head only, lbf
Reaction <sub>water_silt</sub>	Reaction on corbel due to water and silt, lbf



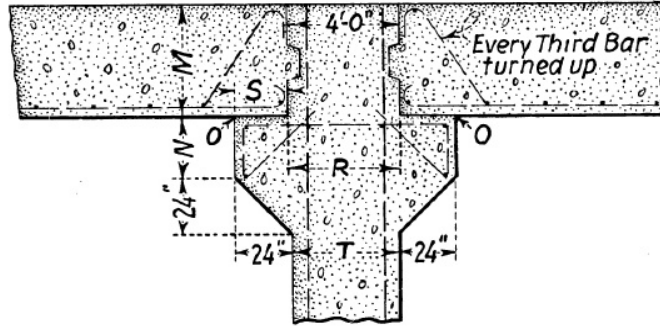
MAXIMUM SECTION AT BUTTRESS DAM



**Selecting Analytic Tools for Concrete Dams to Address  
Key Events Along Potential Failure Mode Paths**

The actual stresses presented in the design documents (as-builts) for slab section J-J, which is at El. 739.0, of Figure A4.5 are now calculated. Shear is calculated at end of slab which is designated as R in the Typical Section for water at El 841.0:

- $L_{slab} = 14ft$
- $H = 102ft$
- $\gamma_{water} = 62.4pcf$
- $v_{c\_plans} = 98psi$
- $f_{c\_plans} = 286psi$
- $f_{s\_plans} = 15300psi$
- $b = 1.0ft$



**TYPICAL SECTION THRU FACE SLAB**

$h_R = 44in$      $d_R = 40.5in$     Dimensions at "R" in Typical Section above.

$A_s = 0.79in^2 \cdot \frac{12}{9}$      $A_s = 1.053 \cdot in^2$     This is based on the size and spacing of the steel presented in the design documents.

$f_{c\_original} = 3000psi$     Concrete compressive strength used for original design

$f_{y\_original} = 40000psi$     Assumed value. Actual value could be 36000 to 40000 psi.

$n_{original} = 12$      $j_{original} = 0.932$

$v_{c\_calculated} = \frac{H \cdot \gamma_{water} \cdot L_{slab} \cdot b}{b \cdot j_{original} \cdot d_R \cdot 2}$      $v_{c\_calculated} = 98 \cdot psi$

$v_{c\_plans} = 98psi$

$Reaction_{water} = \frac{H \cdot \gamma_{water} \cdot L_{slab} \cdot b}{2}$      $Reaction_{water} = 44554 lbf$

H	SECTION	DIMENSIONS				FACE SLAB					BUTTRESS CORBEL			
		M	N	S	T	REINFORCING STEEL		CONCRETE			REINFORCING STEEL		CONCRETE STRESSES	
						Spacing of 1"Ø bars	$f_s$ psi	U psi	$f_c$ psi	$v@"0"$ psi	Spacing of 1"Ø bars	$f_s$ psi	$f_c$ psi	$v@"R"$ psi
102'	J-J	3'-8¾"	2'-1"	20½"	3'-5"	4"	17,000	149	513	78	9"	15,300	286	98

**Selecting Analytic Tools for Concrete Dams to Address Key Events Along Potential Failure Mode Paths**

---

Determine the design moment from a given steel stress,  $f_s$ , and concrete stress,  $f_c$ ,  $b$ , and  $d$  at face of buttress taken from the original corbel design documents. These computations were performed to determine/confirm the basis of the original design:

$$f_c = 0.288\text{ksi} \quad f_s = 15.3\text{ksi} \quad b_w = 12\text{in} \quad d = 45.5\text{in} \quad f_y = 40\text{ksi}$$

$$w = 145\text{pcf} \quad A_s = 1.053 \cdot \text{in}^2 \quad f_{c\_original} = 3 \cdot \text{ksi}$$

$$\rho = \frac{A_s}{b_w \cdot d} \quad n = 12$$

$$k = \sqrt{(\rho \cdot n)^2 + 2 \cdot \rho \cdot n} - \rho \cdot n \quad k = 0.1933$$

**Allowable Stress Design Principles based on ACI 318-63**

$$j = 1 - \frac{k}{3} \quad j = 0.936$$

$$R_{\text{steel}} = \left( \frac{A_s}{b_w \cdot d} \right) \cdot f_s \cdot j \quad R_{\text{steel}} = 0.028 \cdot \text{ksi}$$

Resistance factor due to steel stress for original design.

$$R_{\text{concrete}} = \frac{f_c \cdot j \cdot k}{2} \quad R_{\text{concrete}} = 0.026 \cdot \text{ksi}$$

Resistance factor due to concrete stress for original design

$$R = \min(R_{\text{steel}}, R_{\text{concrete}}) \quad R = 0.026 \cdot \text{ksi}$$

Design controlled by the smaller of the two resistance factors.

$$M_{\text{design}} = R \cdot b_w \cdot d^2 \quad M_{\text{design}} = 647 \cdot \text{kip} \cdot \text{in}$$

Design moment of original design.

$$a_{v\_orig} = \frac{M_{\text{design}}}{\text{Reaction}_{\text{water}}} \quad a_{v\_orig} = 14.52 \cdot \text{in}$$

Moment arm used in original design.

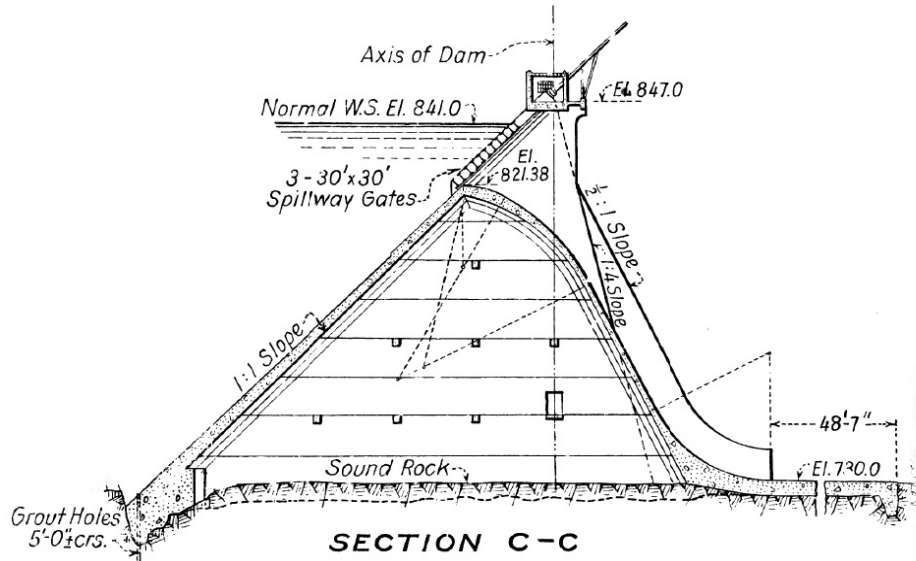
$$a_{v\_actual} = 5\text{in} + \frac{2}{3} \cdot 19\text{in}$$

$$a_{v\_actual} = 17.67 \cdot \text{in}$$

More appropriate moment arm to be used in failure analysis.

The original design also ignored the weight of the slab and any silt loading. The moment arm, normal water surface loading, and the silt loading will be utilized in the assessment of the adequacy of the slab and buttress system.

**Selecting Analytic Tools for Concrete Dams to Address  
Key Events Along Potential Failure Mode Paths**



Check reaction on corbels due to Normal Water Surface plus Silt Loading. Water at elevation 841.0 and silt at elevation 758.0. Buttress to be analyzed at Section J-J, Elevation 739 ft.

$$EL_{\text{water}} = 841.0\text{ft}$$

$$EL_{\text{Sect}_J} = 739\text{ft}$$

$$EL_{\text{Silt}} = 758.0\text{ft}$$

$$H_{\text{silt}} = EL_{\text{Silt}} - EL_{\text{Sect}_J} = 19\text{ft}$$

$$H_{\text{water}} = EL_{\text{water}} - EL_{\text{Sect}_J} = 102\text{ft}$$

$$\gamma_{\text{silt}} = 120\text{pcf} \quad K_{\text{silt}} = 0.4 \quad t_{\text{slab}} = 3.73\text{ft} \quad \gamma_{\text{conc}} = 150\text{pcf} \quad b = 1\text{ft}$$

$$R_{\text{water\_silt}} = \frac{H_{\text{water}} \cdot \gamma_{\text{water}} \cdot L_{\text{slab}} \cdot b}{2} \dots$$

$$+ \frac{H_{\text{silt}} \cdot K_{\text{silt}} \cdot (\gamma_{\text{silt}} - \gamma_{\text{water}}) \cdot L_{\text{slab}} \cdot b}{2} \cdot \sin(45\text{deg}) \dots$$

$$+ \frac{H_{\text{silt}} \cdot (\gamma_{\text{silt}} - \gamma_{\text{water}}) \cdot L_{\text{slab}} \cdot b}{2} \cdot \cos(45\text{deg}) + \frac{t_{\text{slab}} \cdot \gamma_{\text{conc}} \cdot L_{\text{slab}} \cdot b}{2} \cdot \cos(45\text{deg})$$

$$R_{\text{water\_silt}} = 54907 \cdot \text{lbf}$$

Reaction on corbel due to water, silt, and concrete slab loading. This is the magnitude to be safely resisted by the strut and tie system of the corbel.

## Selecting Analytic Tools for Concrete Dams to Address Key Events Along Potential Failure Mode Paths

---

The following analysis is based on limit states of ACI Code based design strengths for bearing, plain (un-reinforced), and reinforced concrete members. The analysis is provided because the original design of the corbel was based on beam theory. Current guidance does not recommend this type of analysis for the geometry of the corbel. A strut and tie analysis will be provided that is a more appropriate analysis method for the corbel.

$$\begin{aligned}
 f'_c &= 2.5\text{ksi} & \phi_{\text{brg}} &= 0.65 & b_w &= 12\text{in} & L_{\text{brg}} &= 19\text{in} & h &= 49\text{in} \\
 \phi_{\text{plain\_shear}} &= 0.6 & \phi_{\text{plain\_bend}} &= 0.6 & A_s &= 0.79\text{in}^2 \cdot \frac{12}{9} & A_s &= 1.053 \cdot \text{in}^2 \\
 a_v &= \frac{2}{3} \cdot L_{\text{brg}} + 5\text{in} & a_v &= 17.667 \cdot \text{in} & d &= h - 3.5\text{in} & d &= 45.5 \cdot \text{in} & \phi_{\text{flex}} &= 0.9 \\
 f_y &= 40\text{ksi} & \mu &= 1.4 & \phi_{\text{shear}} &= 0.75
 \end{aligned}$$

Assuming the maximum bearing stress is reached at the edge of the corbel under a triangular pressure distribution, the maximum reaction using strength reduction factors can be computed as:

$$\phi P_{\text{nbrg}} = \phi_{\text{brg}} \cdot 0.85 \cdot f'_c \cdot \frac{1}{2} \cdot b_w \cdot L_{\text{brg}} \quad \phi P_{\text{nbrg}} = 157.5 \cdot \text{kip} \quad h = 49 \cdot \text{in}$$

Using principles of plain concrete (un-cracked), the maximum reaction can be calculated

$$\phi P_{\text{bend\_plain}} = \frac{\phi_{\text{plain\_bend}} \cdot 5 \cdot \sqrt{f'_c \cdot \text{psi}} \cdot b_w \cdot (h - 5\text{in})^2}{6 \cdot L_{\text{brg}}} \cdot \frac{3}{2} \quad \phi P_{\text{bend\_plain}} = 45.9 \cdot \text{kip}$$

$$P_{\text{bend\_plain}} = \frac{5 \cdot \sqrt{f'_c \cdot \text{psi}} \cdot b_w \cdot (h - 5\text{in})^2}{6 \cdot L_{\text{brg}}} \cdot \frac{3}{2} \quad P_{\text{bend\_plain}} = 76.4 \cdot \text{kip}$$

Reinforced Section Flexure Limit State

$$d = 45.5 \cdot \text{in}$$

$$\phi M_n = \phi_{\text{flex}} \cdot A_s \cdot f_y \cdot \left( d - \frac{A_s \cdot f_y}{0.85 \cdot f'_c \cdot b_w \cdot 2} \right) \quad \phi M_n = 1694 \cdot \text{kip} \cdot \text{in}$$

$$\phi P_{\text{nflex}} = \frac{\phi M_n}{a_v} \quad \phi P_{\text{nflex}} = 95.9 \cdot \text{kip} \quad \text{Moment taken at face of buttress}$$

$$P_{\text{nflex}} = \frac{\phi P_{\text{nflex}}}{\phi_{\text{flex}}} = 106.5 \cdot \text{kip}$$

Shear Friction Limit States:

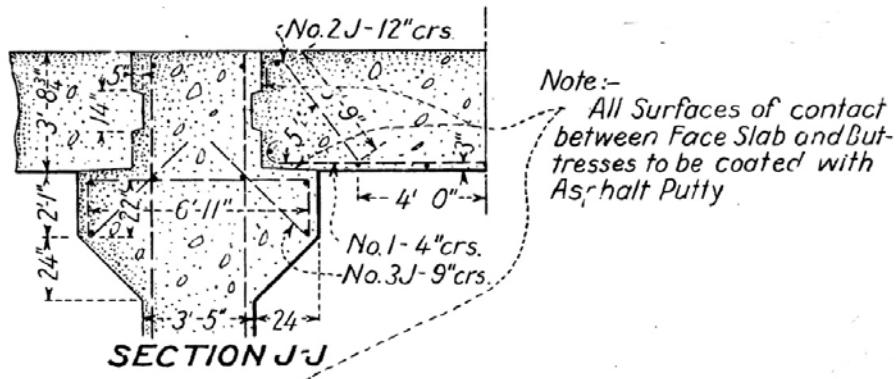
$$\phi_{\text{shear}} = 0.75 \quad \mu = 1.4 \quad A_s = 1.053 \cdot \text{in}^2 \quad f_y = 40 \cdot \text{ksi}$$

$$\phi P_{\text{nshear\_frict}} = \phi_{\text{shear}} \cdot \mu \cdot A_s \cdot f_y \quad \phi P_{\text{nshear\_frict}} = 44.2 \cdot \text{kip}$$

$$P_{\text{nshear\_frict}} = \mu \cdot A_s \cdot f_y \quad P_{\text{nshear\_frict}} = 59 \cdot \text{kip}$$

As can be seen, the 54.9 kip load due to the combined water and silt loading is less than the smallest of the limit states investigated when the phi-factors are taken as 1.0. The shear friction limit state has the lowest value, 59 kips, which is only slightly larger than the 54.9 kip loading. This gives a safety factor of 1.07. Again, these strengths are based on beam behavior and not deep beam behavior. The strut and tie method will now be used to assess the strength of the corbel.

The forces in the struts and ties due to the reactions from the slabs will now be calculated. The shear span to depth ratio,  $a/d$ , for the corbel places it in the deep beam action category. The geometry of the strut and tie system will be as shown in the figure below. The maximum reaction will be determined by the smallest capacity of the the individual components of the strut and tie system. The strut and tie analysis is based on the principles of ACI 318 and AASHTO.



$$a_v = 17.667 \cdot \text{in}$$

$$d = 45.5 \cdot \text{in}$$

See strut and tie model of Section J-J below.

$$\frac{a_v}{d} = 0.388$$

Shear span to depth ratio

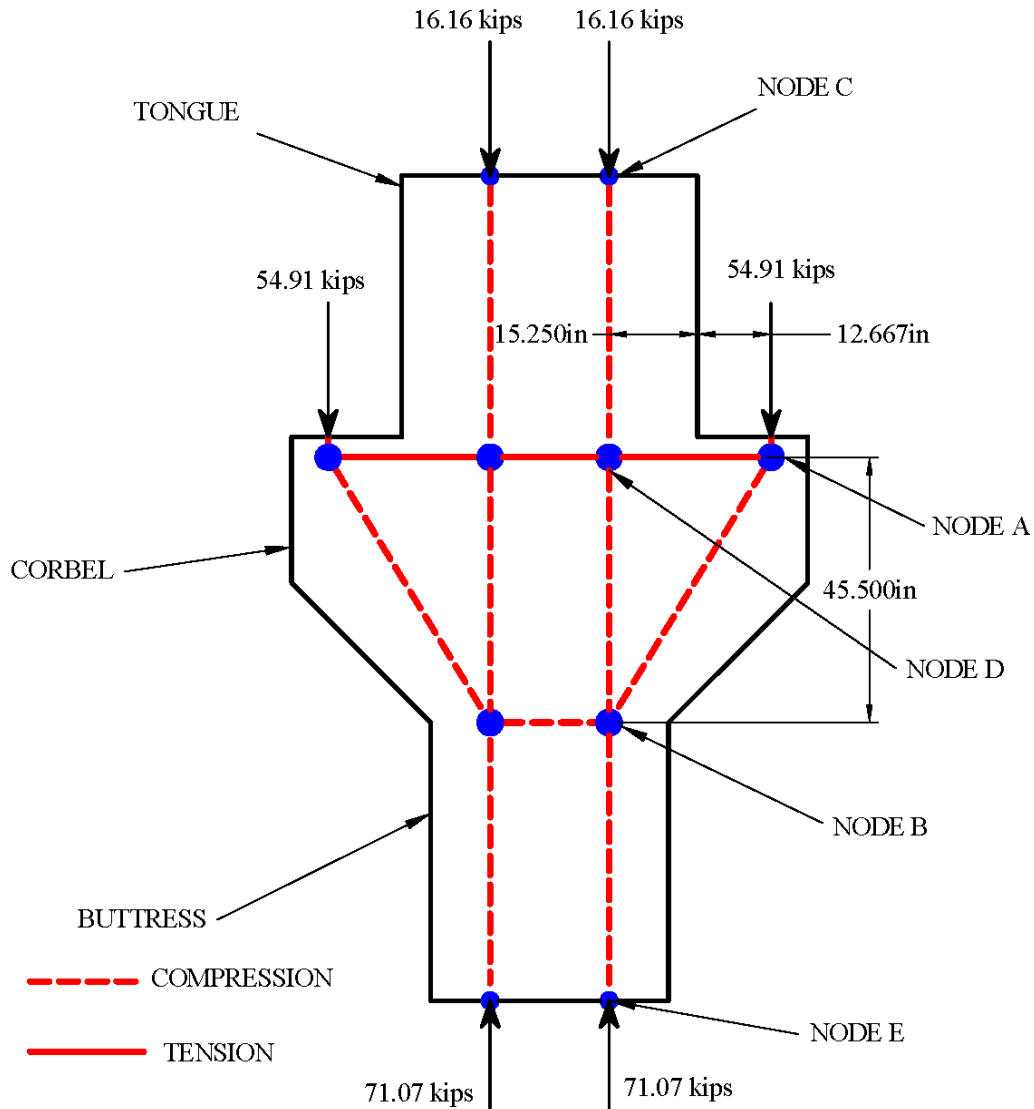
Shear span-to-depth ratio is less than 1.0, which places the corbel in the deep beam category where non-linear stress distribution will govern the analysis. ACI 318 has a specific procedure for corbels that have a shear span-to-depth ration less than 1.0; however, the amount of steel provided for this corbel design does not meet the minimum requirements of ACI 318, so the strut and tie methodology will be used to assess the adequacy of this corbel system to resist the loads.

**Selecting Analytic Tools for Concrete Dams to Address Key Events Along Potential Failure Mode Paths**

---

A graphical representation of the strut and tie system is shown below. Forces in the various elements will be calculated by hand and verified by Computer Aided Strut and Tie System. The software checks the strength of the struts, ties, and nodes based on ACI 318 principles.

**STRUT AND TIE ANALYSIS**



**CORBEL AND BUTTRESS STRUT & TIE MODEL**

Analysis of the truss will be accomplished by the method of joints.

NODE A Analysis

$$\Sigma F_y = 0 \text{ kip}$$

$$F_{BA} \cdot \sin(58.47 \text{ deg}) - 54.91 \text{ kip} = 0 \text{ kip}$$

$$F_{BA} = \frac{54.91 \text{ kip}}{\sin(58.47 \text{ deg})}$$

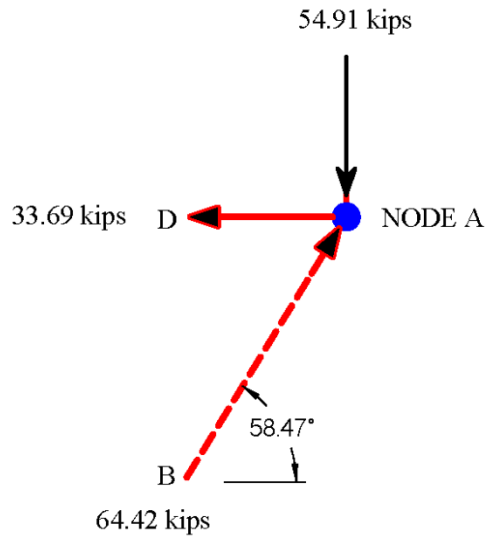
$$F_{BA} = 64.42 \cdot \text{kip}$$

$$\Sigma F_x = 0 \text{ kip}$$

$$F_{BA} \cdot \cos(58.47 \text{ deg}) - F_{AD} = 0 \text{ kip}$$

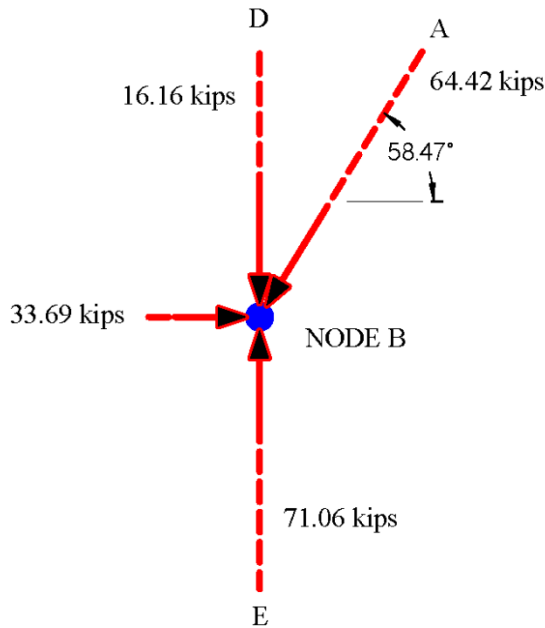
$$F_{AD} = F_{BA} \cdot \cos(58.47 \text{ deg})$$

$$F_{AD} = 33.69 \cdot \text{kip}$$



$$\theta = \text{atan}\left(\frac{45.5 \text{ in}}{15.25 \text{ in} + 12.6667 \text{ in}}\right)$$

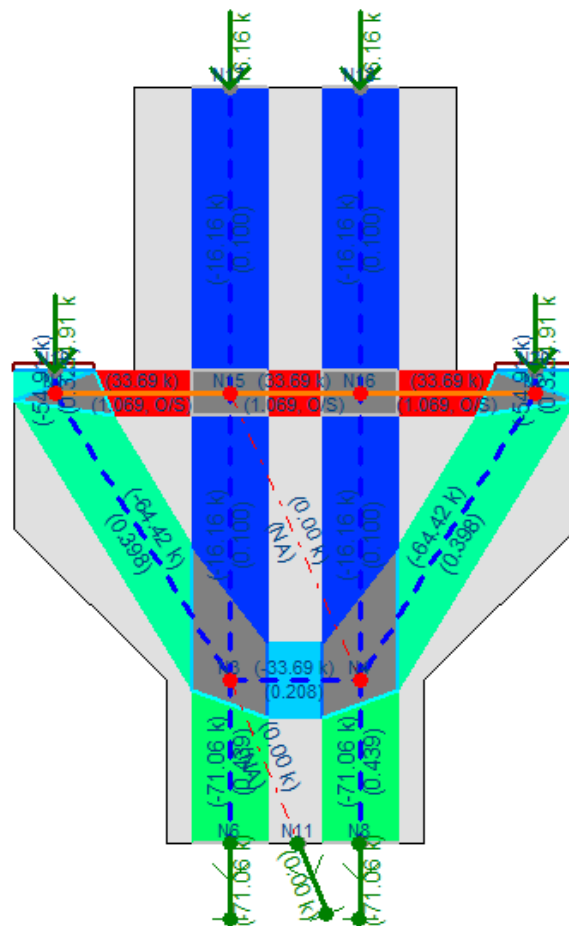
$$\theta = 58.47 \cdot \text{deg}$$



Forces at Node B are determined by inspection. Forces in all elements of the truss have now been established.

## Selecting Analytic Tools for Concrete Dams to Address Key Events Along Potential Failure Mode Paths

The results of an analysis of the strut and tie system using Computer Aided Strut and Tie System (CAST) software is presented below in graphical form. The various struts and ties are color coded in accordance with the interaction ratio of the actual force to the force based on the design strength of the strut or tie. The actual interaction value is given below the value of the force in each element of the truss. The red color indicates the interaction ratio is one or greater and represents impending failure of the element. The dark blue color represents a low interaction ratio and a very safe level of stress. As mentioned above, the design strength includes ACI recommended phi-factor of 0.75. Which means the nominal strength of the struts and ties have been reduced by 25%. If the concrete strength and steel yield strength is verified, it would seem that the assesment could be based on nominal strength values. The results of a nominal strength comparison is presented on the next page.

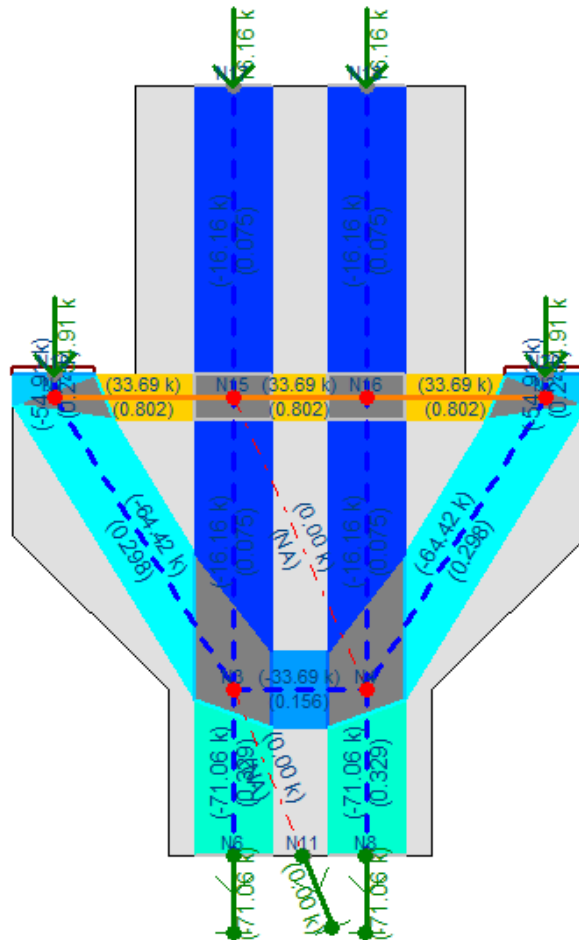


RESULTS OF CORBEL AND BUTTRESS STRUT AND TIE ANALYSIS  
LOAD VERSUS DESIGN STRENGTH (phi-factors included)



## Selecting Analytic Tools for Concrete Dams to Address Key Events Along Potential Failure Mode Paths

Results of an assessment based on nominal strength is presented graphically below. The element with the highest interaction ratio value controls the results. The tension tie has an interaction ratio of 0.802 which represents a safety factor of approximately 1.25 for this loading condition. This is based on a steel yield strength of 40,000 psi. This indicates that a failure condition does not exist for the additional silt loading. However, there could be significant cracking associated with this loading. Measures should be taken to reduce the silt loading or strengthen the corbel.



RESULTS OF CORBEL AND BUTTRESS STRUT AND TIE ANALYSIS  
LOAD VERSUS NOMINAL STRENGTH (phi-factors not included)

## Selecting Analytic Tools for Concrete Dams to Address Key Events Along Potential Failure Mode Paths

---

Analysis/assessments such as the one just completed should be based on procedures that will address the ultimate strength limit state of the system involved. The stresses computed should be accurate representations of those actually occurring in the structure. Analysis results that are not reflective of the actual conditions have a low level of confidence associated with them and must be revised to take in account all the major factors attributing to the strength of the system being evaluated. The role of material specific codes plays a vital role in this process by presenting acceptable levels of strength based on material properties. The corresponding commentaries of material specific codes provide insight into the testing and theory behind the procedures prescribed in the codes. It is also important to obtain copies of the prevailing material specific codes at the time of design and construction of the concrete dam. This is especially true for elements of slab and buttress dams since they have components that are similar to the traditional elements of buildings.

## **Appendix A5**

# **Freeze-Thaw Deterioration Removes Concrete Cover and Causes Upstream Slab to Fail**



## Appendix A5: Freeze-Thaw Deterioration Removes Concrete Cover and Causes Upstream Slab to Fail

Buttress dam concrete slabs subjected to freezing and thawing cycles/action may experience deterioration (figure A5-1). This deterioration could lead to significant loss of concrete surface, as well as corrosion of reinforcing steel. Deterioration of concrete by freeze thaw action needs to be evaluated to determine the buttress dam slab adequacy. The following example shows the process by which the slab may be evaluated (see the event tree in figure A5-2a and the analysis tree in figure A5-2b). While codes are cited in this example, we are evaluating failure limits; therefore, load factors are not applied.

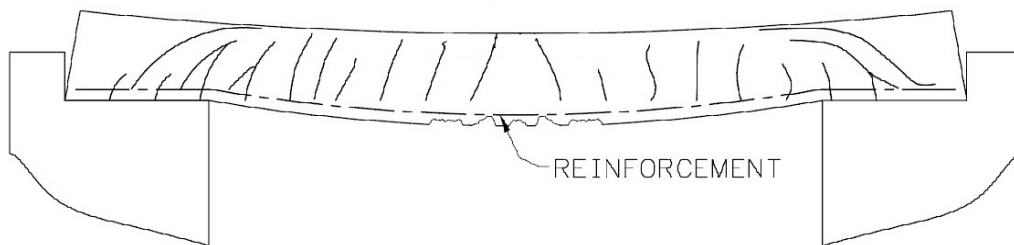


**Figure A5-1: Depiction of failure mode and example of freeze-thaw in a buttress dam, Bureau of Reclamation.**

# Selecting Analytic Tools for Concrete Dams to Address Key Events Along Potential Failure Mode Paths

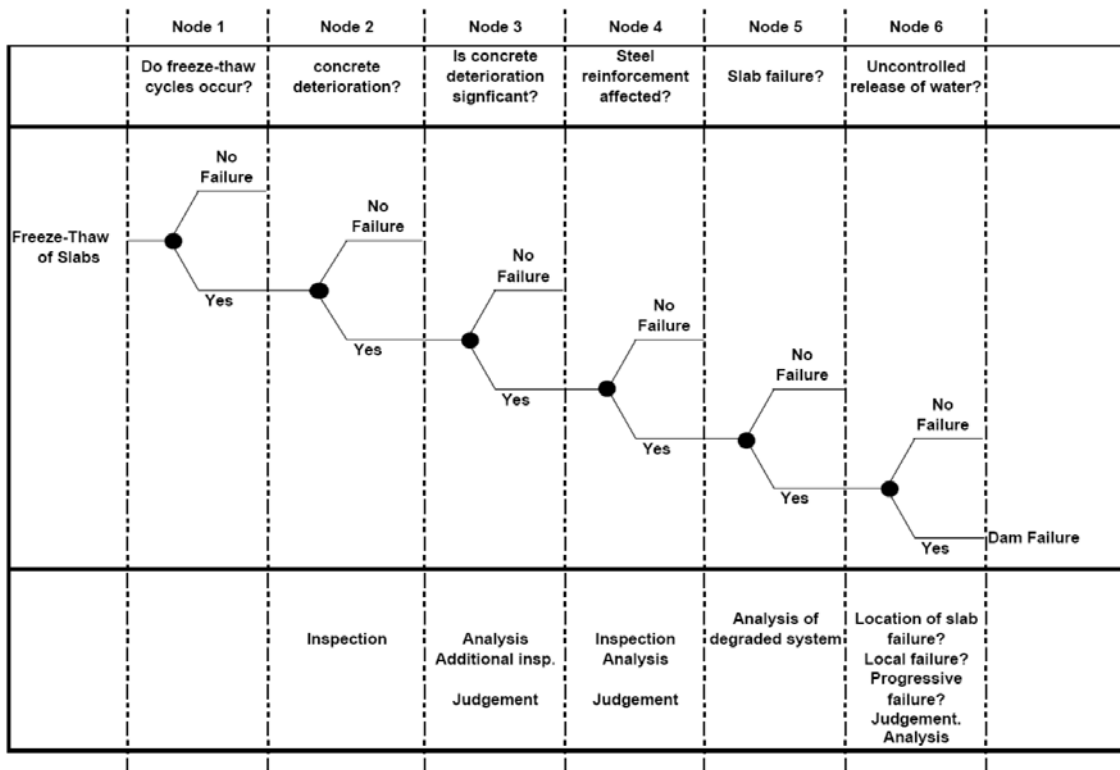


Figure A5-2a: Event tree.

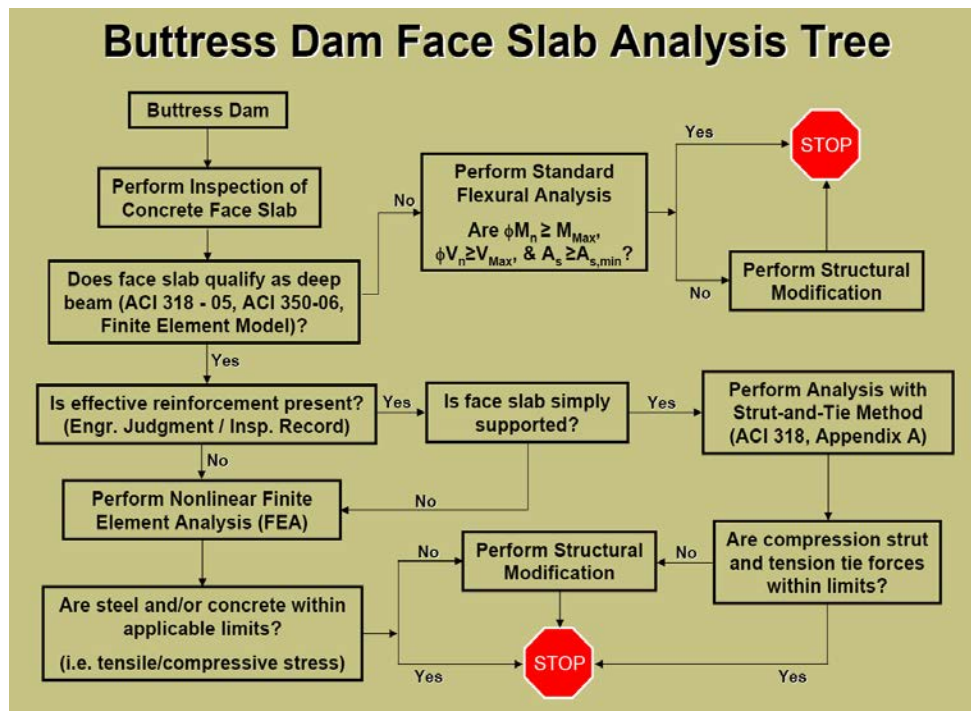


Figure A5-2b: Analysis tree.

## **A5.1 Node 1: Freezing and Thawing**

Hydraulic structures are especially susceptible to freeze-thaw damage because they are more likely to be critically saturated. Older structures are also more susceptible to freeze-thaw damage since the concrete was not air entrained.

Deterioration of concrete from freeze-thaw actions may occur when the concrete is critically saturated, which is when approximately 91 percent of its pores are filled with water. When water freezes to ice, it occupies 9 percent more volume than when it is water. If there is no space for this volume expansion in a porous, water containing material like concrete, freezing may cause distress in the concrete.

## **A5.2 Node 2: Inspection for Freeze-Thaw Damage**

High water content and non-air-entrained concrete were commonly used in older buttress type dams, which contributed significantly to their potential for freeze-thaw damage. Particular attention must be paid to the concrete in face slabs. Because of their relative thinness, they cannot withstand excessive scaling or spalling, which decreases the strength of the slab structure.

Typical signs of freeze-thaw damage are:

- Spalling and scaling of the surface
- Large chunks (inches size) are coming off
- Exposing of aggregate and/or reinforcing
- Surface parallel cracking

## **A5.3 Node 3: Extent of Deterioration**

Distress to critically saturated concrete from freezing and thawing would commence with the first freeze-thaw cycle and continue throughout successive winter seasons, resulting in repeated loss of concrete surface. An inspection for freeze-thaw deterioration should include determination of extent of spalling, scaling, and cracking. The visual inspection should serve to examine and record the condition of the slabs and buttress structure.

## **A5.4 Node 4: Steel Reinforcement**

Corrosion of reinforcing steel produces iron oxides and hydroxides, which have a volume much greater than the volume of the original metallic iron. This increase in volume causes local radial cracks, formation of longitudinal cracks (parallel to the bars), and spalling with loss of cover

concrete. This cracking and/or spalling, if significant enough, can result in delamination of the surface (a well-known problem in bridge decks). Corrosion of reinforcing steel also results in loss of tension steel area, which reduces the strength of the slab (structure). Corrosion also reduces the ability of reinforcing steel to develop a bond between bars at splice locations.

### **A5.5 Node 5: Slab Evaluation for Structural Adequacy**

Based on an inspection/testing program of the buttress slab(s), determine if a strength evaluation of the slab(s) is required. This determination should consider the amount of concrete deterioration and loss of reinforcing steel area that have occurred. To illustrate this approach, a typical buttress slab will be analyzed for strength as shown in the example below.

### **A5.6 Introduction**

The buttress dam face slab analyzed in this exercise was constructed in the 1920s. The face slab thickness varies from approximately 3 feet 8 inches at elevation 738 to approximately 1 foot 5 inches at elevation 847. The face slab is reinforced with 1-inch-diameter bars in the downstream face of the slab with a 3-inch clear cover. The bar spacing varies from 4 inches on center to 12 inches on center. The normal water surface is at elevation 841, and for this exercise, sediment up to elevation 758 will be included. The 14-foot-long face slab was poured in place and has shear keys at the buttress walls as shown in figure A5-3.

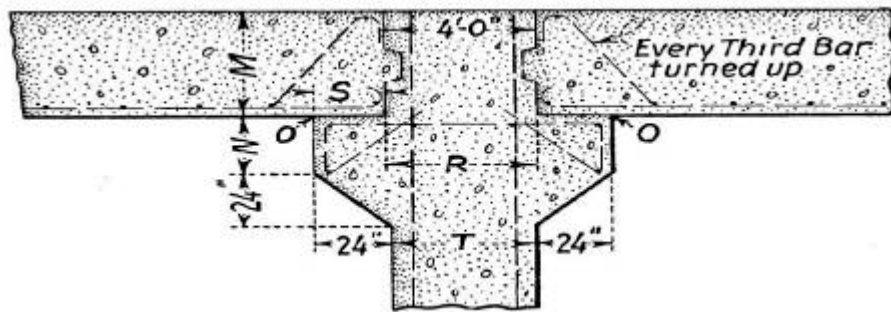


**Figure A5-3: Typical section at buttress wall.**

#### **A5.6.1 Event Tree Node 1**

For the purposes of this exercise, the buttress dam is assumed to be in an area susceptible to subfreezing temperatures. Since air-entrained concrete was not used at the time of construction, the buttress dam face slab could potentially experience freeze-thaw damage.



### **A5.6.2 Event Tree Node 2**

The following inspection scenario was developed for this exercise: An inspection of the buttress dam face slab revealed a concrete spall at approximately the center of the face slab span, extending from elevation 738 to elevation 742. The concrete spall is approximately 6 inches wide and 2 inches deep. Additional cracking was noted in the damaged area.

### **A5.6.3 Event Tree Node 3**

Due to the depth of the concrete spall (only 1 inch of reinforcement cover remaining) and the location of the damage (near the center of the slab span), the concrete deterioration is determined to be significant and could potentially impact the safety of the structure.

### **A5.6.4 Event Tree Node 4**

The additional cracking noted in the concrete spall area indicates that the reinforcement has likely been exposed to moisture and has been degraded to some extent. The degrading reinforcement would have a larger volume, which could have caused the cracking documented in the inspection.

In the event that the reinforcing development length does not comply with current American Concrete Institute (ACI) code requirements, assume the section is unreinforced (because inspections have revealed that the steel is exposed and unbonded) and evaluate for structural integrity as a plane concrete section. Boundary conditions at the end of the slab should be carefully considered in modeling the slab to take advantage of any provided restraint. The conservative assumption of no effective steel will not result in slab failure, as will be seen. However, the horizontal thrust that will appear at the supports must be resisted.

### **A5.6.5 Event Tree Node 5**

Analysis is required at node 5 to determine if a slab failure is imminent. Under the provisions of ACI 318-05 section 10.7, the face slab section analyzed in this exercise is classified as a deep beam because the loads are applied to the face opposite the face that is supported, and the slab depth to span ratio is greater than 0.25. Since the slab is classified as a deep beam, the analysis must account for the nonlinear strain distribution in the slab. Therefore, a 3D finite element analysis of the face slab was performed using GTStrudl Version 28. Since the reinforcement has potentially been impacted and the deep beam behavior would likely result in arching action, the slab was modeled as plain concrete. The concrete stresses will be compared to the plain concrete tensile and compressive strength in ACI 318-05. ACI 350-06 was not used because it addresses reinforced concrete design of environmental engineering structures and does not address the tensile and compressive strength of plain concrete.

The deep beam analysis of the face slab described above is necessary due to the ratio of the slab depth to the clear span. However, the face slab thickness decreases at higher elevations of the dam from 48 inches thick at the base to 16.75 inches at the crest. Since the loads on the slab are not concentrated, once the ratio of the face slab thickness to the clear span is less than 0.25, the face slab is no longer classified as a deep beam and the finite element analysis is no longer necessary. The face slab must be analyzed as a reinforced concrete beam in accordance with chapter 10 of ACI 318-05 and meet the minimum reinforcement requirements.

## A5.7 Finite Element Model Description

A 12-inch-wide section of the face slab extending from elevation 738 to elevation 738.71 was modeled. However, to simplify the model geometry and load application, the slab was not inclined as it is actually constructed. Because both the hydrostatic pressure and the sediment pressure vary with the depth, they were decreased across the width of the model. This simplification is conservative because the full dead weight of the slab in the model is supported by the buttress walls, which results in higher bending stresses in the slab. The actual inclined orientation of the slab would result in lower bending stresses due to dead load because a portion of the dead load would be transmitted to the foundation at the base of the face slab. The face slab in the finite element model has a thickness of 41.75 inches after removing the concrete cover on the reinforcement. The face slab was loaded with three independent load cases and one dependent load case. Table A5-1 shows a summary of the loads applied to the model.

**Table A5-1: Loads applied to the model**

Load name	Load description
Case 1	Dead load of the concrete slab.
Case 2	Hydrostatic pressure on the slab with the water surface at elevation 841.
Case 3	Pressure due to the buoyant weight of sediment up to elevation 758. It was assumed that the saturated unit weight of the sediment is 120 lb/ft <sup>3</sup> .
Case 4	Dependent load case including independent load cases 1, 2, and 3. The load factors for the independent load cases were taken as 1.0.

The portion of the face slab modeled is 14 feet long and has a clear span of 12 feet 7 inches. The face slab supports were modeled by restraining the translational degrees-of-freedom and releasing the rotational degrees-of-freedom at the model joints located where the slab rests on the support corbels. Compression only nonlinear springs oriented perpendicular to the ends of the slab to model the slab interaction with the buttress wall. A second support configuration that locates the supports only at the middle of the slab thickness was used to model a theoretical simple beam for model calibration using flexural analysis.

Based on the age of the buttress dam, the concrete is assumed to be a normal weight concrete with a compressive strength of 2,500 lb/in<sup>2</sup>. The modulus of elasticity of the concrete is 2.85 x 10<sup>6</sup> lb/in<sup>2</sup> (57,000 (f<sub>c</sub>')<sup>0.5</sup>).

### A5.7.1 Finite Element Load Calculation

Calculate hydrostatic pressure:

$$w_{\text{hydro}_{738}} = 62.4 \text{ pcf} (841 \text{ ft} - 738 \text{ ft}) = 6,427 \text{ psf}$$

$$w_{\text{hydro}_{738.71}} = 62.4 \text{ pcf} (841 \text{ ft} - 738.71 \text{ ft}) = 6,383 \text{ psf}$$

Calculate buoyant sediment pressure:

$$w_{\text{sediment}_{738}} = (758 \text{ ft} - 738 \text{ ft})(120 \text{ pcf} - 62.4 \text{ pcf}) = 1,152 \text{ psf}$$

$$w_{\text{sediment}_{738.71}} = (758 \text{ ft} - 738.71 \text{ ft})(120 \text{ pcf} - 62.4 \text{ pcf}) = 1,111 \text{ psf}$$

### **A5.7.2 Finite Element Model Calibration**

To calibrate the model, the stress in the extreme tension and compression fibers of the face slab was calculated based on a 14-foot simple span beam as shown below.

Calculate Slab Section Modulus

$$S = \frac{bh^2}{6} = \frac{12''(41.75'')^2}{6} = 3486 \text{ in}^3$$

Calculate Hydrostatic Pressure

$$w_{\text{hydro}} = 62.4 \text{ pcf}(1 \text{ ft})(841 \text{ ft} - 738 \text{ ft}) = 6427 \text{ plf}$$

Calculate Bouyant Sediment Pressure

$$w_{\text{sediment}} = (758 \text{ ft} - 738 \text{ ft})(120 \text{ pcf} - 62.4 \text{ pcf}) = 1152 \text{ plf}$$

Calculate Distributed Load on Slab

$$w = 41.75'' \left( \frac{1 \text{ ft}}{12 \text{ in}} \right) (1 \text{ ft}) * 150 \text{ pcf} + 6427 \text{ plf} + 1152 \text{ plf}$$

$$w = 8,101 \text{ plf}$$

Calculate Maximum Moment

$$M_{\text{max}} = \frac{wl^2}{8} = \frac{8101 \text{ plf} * (14.0 \text{ ft})^2}{8} = 198,475 \text{ lb} - \text{ft}$$

$$M_{\text{max}} = 2,381,964 \text{ lb} - \text{in}$$

Calculate Stress

$$F_b = \frac{M_{\text{max}}}{S} = \frac{2,381,964 \text{ lb} - \text{in}}{3486 \text{ in}^3}$$

$$F_b = 683.2 \text{ psi}$$

The maximum tensile and compressive stresses in the calibration model were 683 lb/in<sup>2</sup> and 693 lb/in<sup>2</sup>, respectively. The maximum variance between the calculated stress and model results was only 1.4 percent. This variance shows that the model geometry and load applications are accurate.

### A5.7.3 Finite Element Analysis Results

The supports were relocated to the bottom edge of the face slab, and the compression only nonlinear springs were added to model the actual support configuration. Since the slab was analyzed as an unreinforced elevated slab, the tensile stress was compared to the reduced modulus of rupture of the concrete in accordance with ACI 318-05. The reduced modulus of rupture for the concrete ( $\phi 7.5 (f'_c)^{0.5}$ , where  $\phi = 0.55$ ) was calculated to be 206 lb/in<sup>2</sup>. However, an elevated plain concrete slab is only permitted by ACI 318-05 if the slab exhibits arch action. Therefore, an iterative process was used to run the model and remove any elements where the tensile stress exceeded that calculated tensile strength of 206 lb/in<sup>2</sup>. Figure A5-4 shows the final model geometry once the elements exceeding the tensile strength were removed.

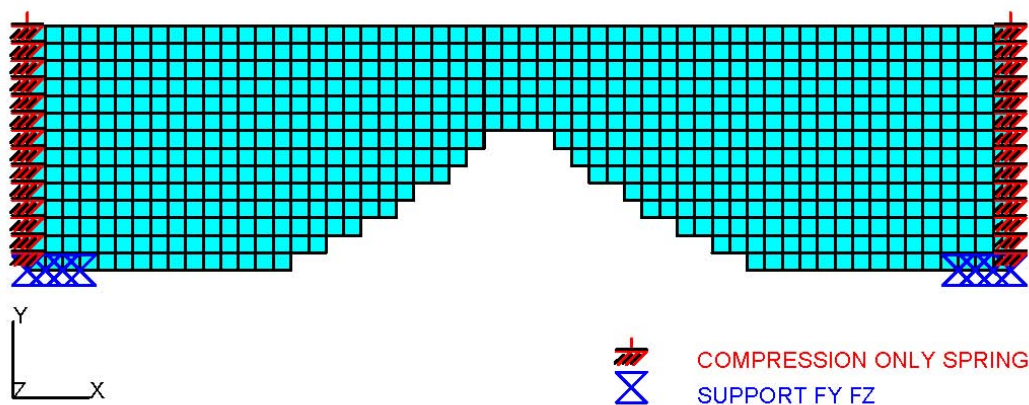


Figure A5-4: Final model geometry once the elements exceeding the tensile strength were removed.

The stress contours in the face slab under the load case 4, shown in figure A5-5, demonstrate the arch action in the slab. The maximum tensile stress in the model was 20.4 lb/in<sup>2</sup>, which is well below the tensile strength of 206 lb/in<sup>2</sup>. Since the slab develops arch action, the compressive stress in the concrete was compared to the compression limit for plain concrete in accordance with chapter 22 of ACI 318-05. The compression limit ( $\phi P_n = 0.6f'_c[1-(l_c/32h)^2]$ , where  $\phi = 0.55$ ) was calculated to be 815 lb/in<sup>2</sup>. The maximum compressive stress at mid-span was 571 lb/in<sup>2</sup>, and the maximum compressive stress at the edge of the corbel was 1,037 lb/in<sup>2</sup>. However, the stress at the edge of the corbel diminishes to less than 800 lb/in<sup>2</sup> within 1.5 inches of the joint. The corbel was modeled as a perfectly rigid support and, as shown in figure A5-6, a sharp change in the deformed shape occurs at this location. In reality, the corbel would have some flexibility and deformation, which would relieve some of the stress at this location. Therefore, the localized stress concentrations at the edge of the corbel were discounted.

## Selecting Analytic Tools for Concrete Dams to Address Key Events Along Potential Failure Mode Paths

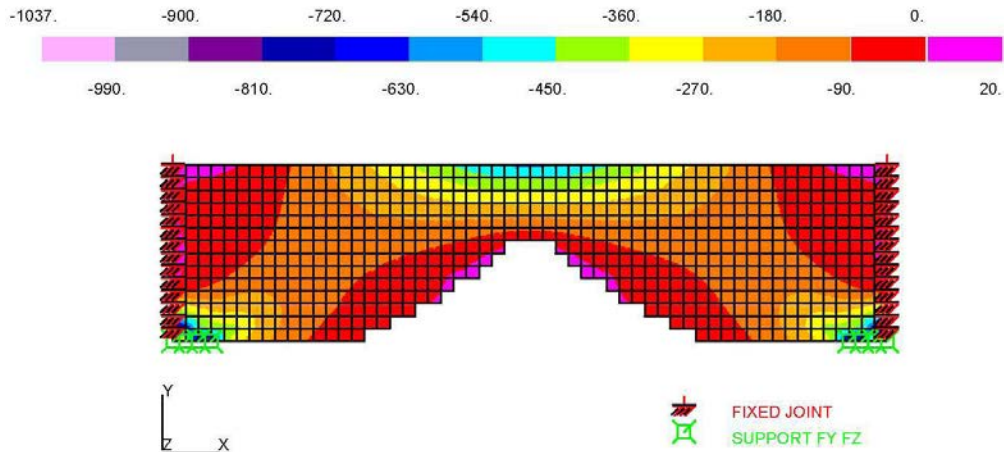


Figure A5-5: Face slab stress ( $S_{xx}$ ) contours.

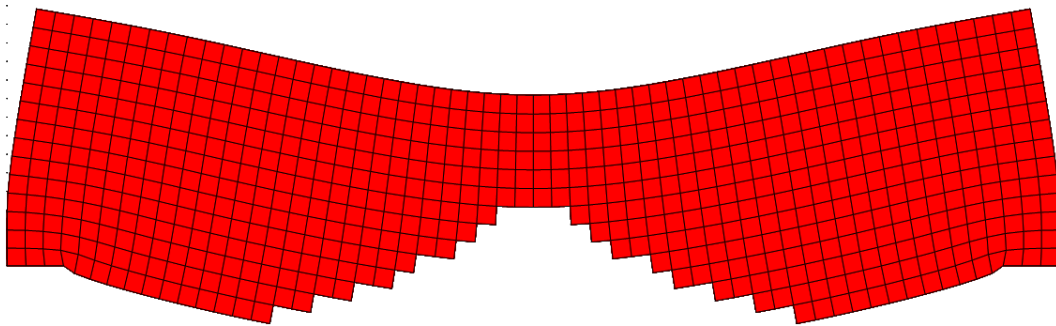


Figure A5-6: Deformed shape.

Based on the results of the finite element analysis, the determination can be made that the deteriorated face slab in this exercise does not fail. Therefore, the slab does not fail in its current state. If deterioration is allowed to continue, its effects would have to be considered.

In this example, phi factors were used to address material uncertainty and brittleness of the failure mechanism. If the conclusions of the analysis had been that the slab had failed, one would have to question whether or not failure was falsely indicated by excessive phi factors. In this case however, the analysis results without factors would indicate the same conclusion (see figure A5-7).

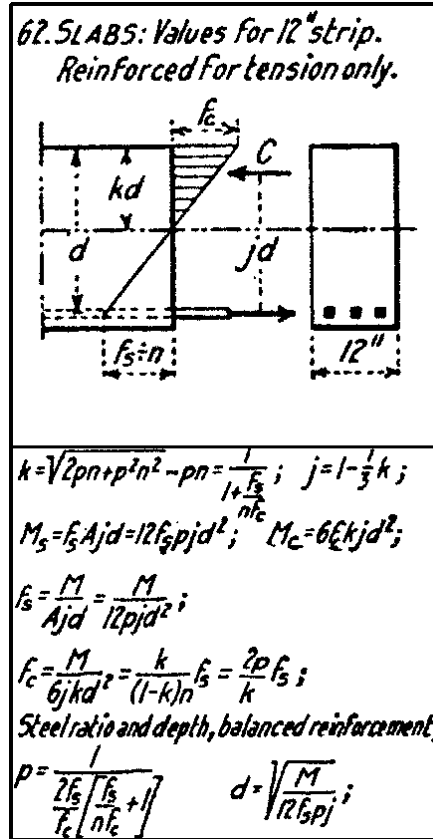


Figure A5-7: Slabs: values for 12-inch strip. Reinforced for tension only.

Calculate Hydrostatic Pressure at Center of 12" Wide Strip

$$w_{\text{hydro}} = 62.4 \text{ pcf} (1 \text{ ft})(841 \text{ ft} - 738.35 \text{ ft}) = 6,405 \text{ plf}$$

Calculate Maximum Moment

$$M_{\text{max}} = \frac{wl^2}{8} = \frac{6,405 \text{ plf} * (12.583 \text{ ft})^2}{8} = 126,767 \text{ lb} - \text{ft}$$

$$M_{\text{max}} = 1,521,206 \text{ lb} - \text{in}$$

$$A_s = 3 \times \frac{\pi(1'')^2}{4} = 2.356 \text{ in}^2$$

$$b = 12''$$

$$d = 41.75''$$

$$\rho = \frac{A_s}{bd} = \frac{2.356 \text{ in}^2}{(12'')(41.75'')} = 0.005$$

$$E_c = 57,000 \sqrt{2500 \text{ psi}} = 2,850,000 \text{ psi}$$

$$E_s = 29,000,000 \text{ psi}$$

$$n = \frac{E_s}{E_c} = \frac{29,000,000 \text{ psi}}{2,850,000 \text{ psi}} = 10.18$$

$$n\rho = 10.18(0.005) = 0.0509$$

$$k = \sqrt{(n\rho)^2 + 2n\rho} - n\rho$$

$$k = \sqrt{0.0509^2 + 2(0.0509)} - 0.0509 = 0.272$$

$$j = 1 - \frac{k}{3} = 1 - \frac{0.272}{3} = 0.909$$

Calculate steel stress :

$$f_s = \frac{M_{\text{max}}}{A_s jd} = \frac{1,521,206 \text{ lb} - \text{in}}{2.356 \text{ in}^2 (0.909)(41.75'')} = 17,057 \text{ psi} \approx 17,000 \text{ psi}$$

$$f_s = 17,057 \text{ psi} \approx 17,000 \text{ psi}$$

Calculate concrete stress :

$$f_c = \frac{M_{\text{max}}}{6 jkd^2} = \frac{1,521,206 \text{ lb} - \text{in}}{6(0.909)(0.272)(41.75'')^2} = 588.3 \text{ psi} \approx 513$$

$$f_c = 588.3 \text{ psi} \approx 513$$

## A5.8 Uncertainty

The boundary conditions of the mathematical model are typically a major uncertainty in the development of the model. For example, three different boundary conditions were applied to the buttress dam face slab finite element model to demonstrate the effect on the stress results under the same load application. The support conditions included the following: restraint of the translational and rotational degrees-of-freedom at the center of the slab thickness, generating traditional beam behavior; restraint of the translational degrees-of-freedom where the face slab bears on the corbel, generating deep-beam arching behavior; and restraint of the translational degrees-of-freedom where the face slab bears on the corbel and along the end of the face slab. Figures A5-8 through A5-10 show the stress contours for each boundary condition, respectively, and table A5-2 shows a summary of the stress results at center span.

The second boundary condition most closely models the actual boundary conditions of the buttress dam face slab being modeled. As shown in table A5-2, modeling the support conditions as a traditional fixed beam overstates the tensile stresses by 194 percent and the compressive stresses by 73 percent. While completely restraining the ends of the fixed beam only overstates the tensile stress by 2.5 percent, the compressive stress is underestimated by 40 percent.

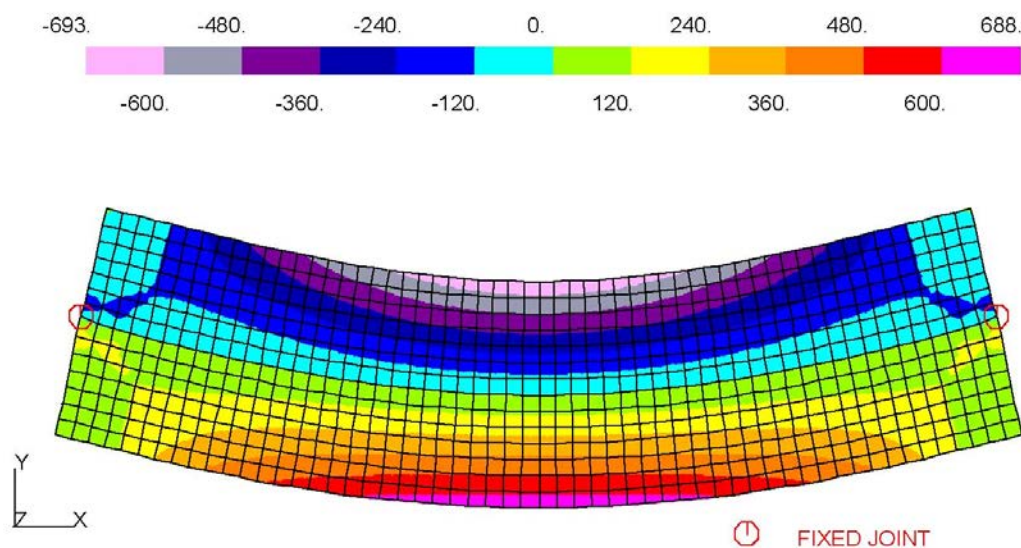


Figure A5-8: Stress contours for restraint of the translational and rotational degrees-of-freedom at the center of the slab thickness.



Selecting Analytic Tools for Concrete Dams to Address Key Events Along Potential Failure Mode Paths

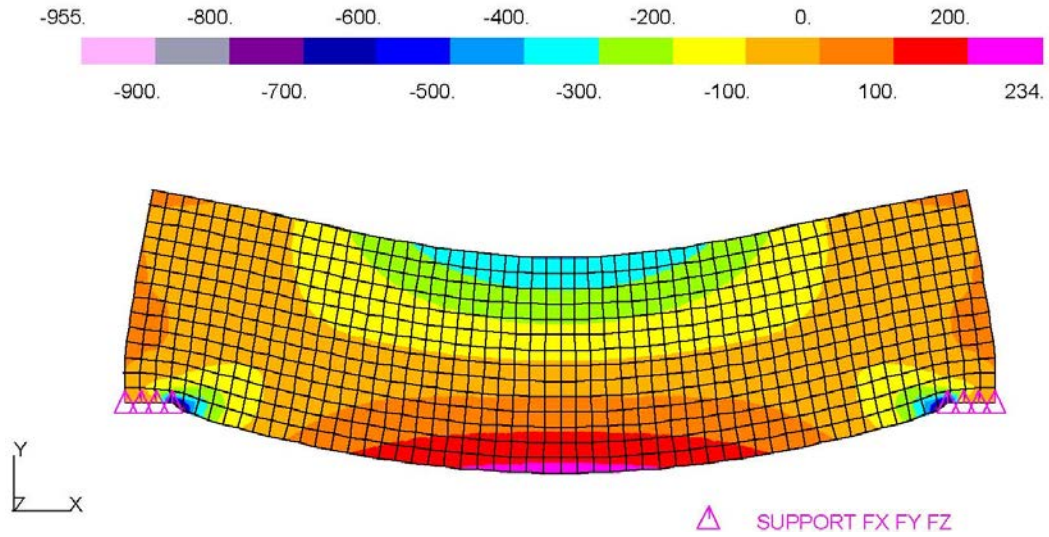


Figure A5-9: Stress contours for restraint of the translational degrees-of-freedom at the support corbel.

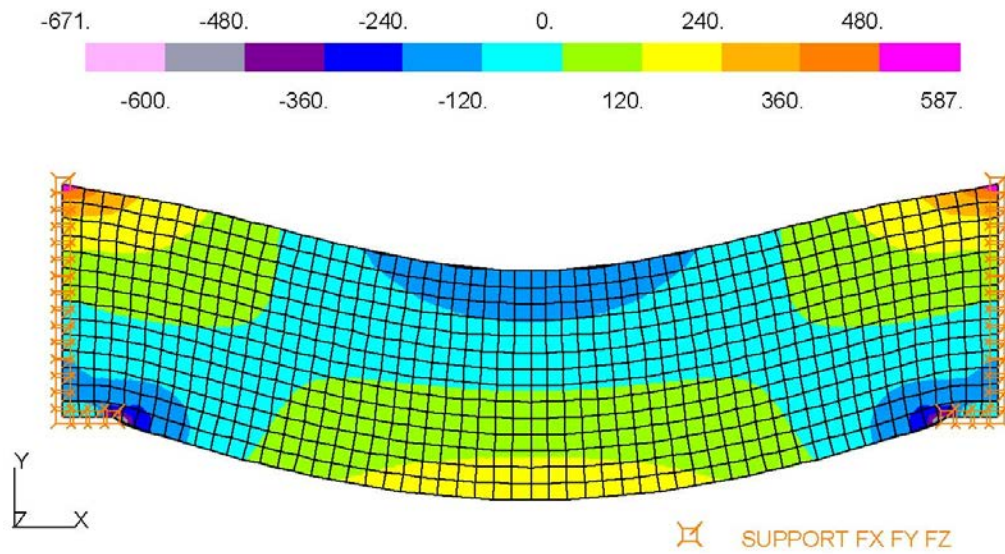


Figure A5-10: Stress contours for restraint of the translational degrees-of-freedom at the support corbel and along the vertical edge.

## Selecting Analytic Tools for Concrete Dams to Address Key Events Along Potential Failure Mode Paths

---

Table A5-2: Summary of model results

Support condition	Stress at center span (lb/in <sup>2</sup> )	
	Tensile	Compressive
Beam action—fixed (see figure A5-8)	688	693
Deep beam—pinned (see figure A5-9)	234	400
Deep beam—fixed (see figure A5-10)	240	240

If the analysis is being performed using numerical methods, the options for boundary conditions are typically limited to fixing or releasing the translational and the rotational degrees-of-freedom at the supports. In addition to merely restraining or releasing the translational or rotational degrees-of-freedom, the engineer may utilize spring constants for any or all degrees-of-freedom. The spring constants are determined based on the stiffness of the foundation material and may be linear or nonlinear. The friction angle between the structure and foundation material will have an impact on the analysis results. The engineer will need to evaluate the effects of various foundation conditions on the structure if accurate material properties are not available and determine if it is necessary to perform testing to determine the foundation properties.

## **Appendix B**

# **Loads and Loading Requirements**



## **Appendix B: Loads and Loading Requirements**

There are several types of loads to consider in the complete analysis of concrete dams. Usually, no single load acting alone will cause stability problems, but the combinations of loads under certain conditions can lead to instability of a concrete dam. Although there are several types of loads, each load will fall into one of two categories: follower forces capable of doing work and high-frequency dynamic forces, or forces relieved by slight motion. Only follower forces can cause a dam to fail; however, other forces can cause damage, making it easier for follower forces to cause failure. Follower forces continue to load the structure as movement occurs (such as during foundation block sliding), such as loading from reservoir, gravity, or seismic activity. Loads that do not continue to apply force to the dam as movements occur are from temperature, ice, or silt.

### **B.1 Gravity/Dead Load**

The dead load is the weight of the structure plus any appurtenant structures, such as gates, piers, and bridges. For computational purposes, the dead load is the cross-sectional area of the dam section being analyzed times the unit weight of the material. The unit weight of mass concrete is largely dependent on the specific gravity of the aggregates. Unit weights can range from 130 pounds per cubic feet ( $\text{lb}/\text{ft}^3$ ) to  $160 \text{ lb}/\text{ft}^3$ . A unit weight of  $150 \text{ lb}/\text{ft}^3$  is usually assumed in analyses. Mass in the foundation is usually not included in static analyses because the foundation has settled from self-weight long before the construction of the dam and filling of the reservoir. The dam and reservoir add additional weight that the foundation has not had to previously support, causing it to deflect further. The method of building the dam in stages and relatively small concrete placements compared to the size of the dam are considered when applying static weight to the dam. Including the stage construction process in the application of static weight provides a more realistic stress distribution in the dam. This eliminates the effect of the dam hanging from the upper abutments, causing high stress concentration. Preferably, mass in the foundation is included in dynamic analysis. This way, inertial effects and radiation damping effects are included in the dynamic response of the dam-reservoir-foundation system.

### **B.2 Water Loading Conditions Resulting from Reservoir Water Surface Elevation**

All water loading conditions resulting from reservoir water surface and tailwater elevations (figure B-1) are based on hydrologic information, which gives water elevations in terms of return periods.

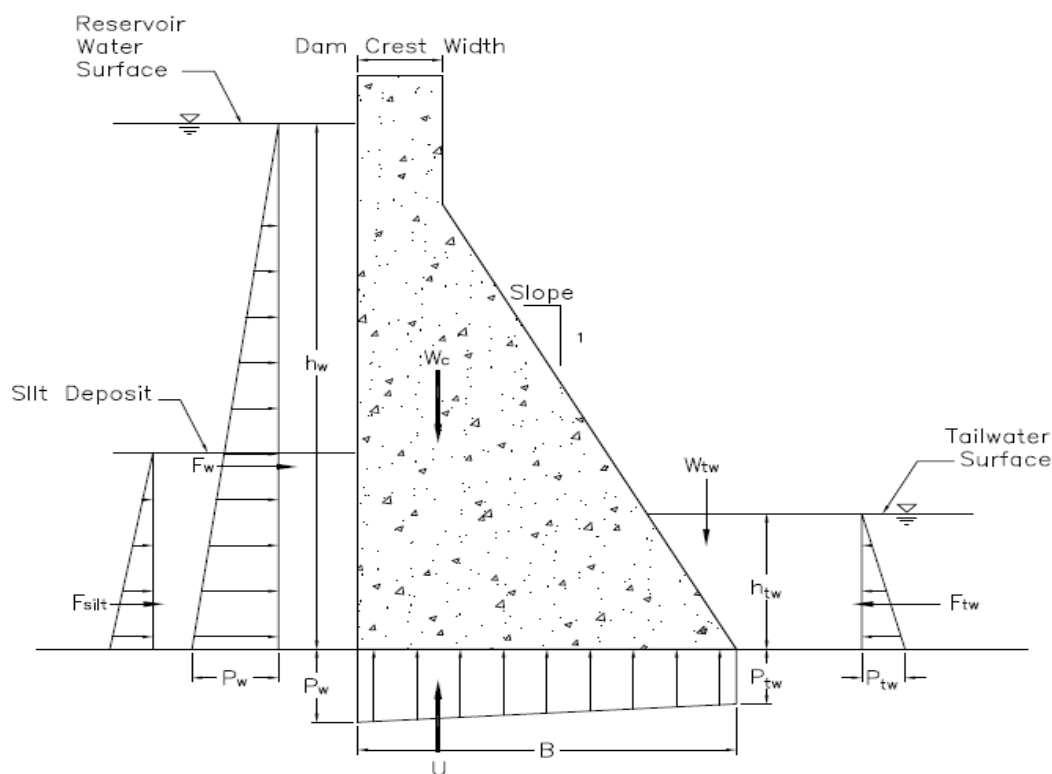


Figure B-1: Loads on typical gravity section—normal operating condition.

### B.2.1 Coincident Pool

Coincident pools represent the water elevations used in combination with seismic events.

### B.2.2 Normal Operation Pool

For hydropower dams, the pool will be fairly high for normal operation, while for some flood-control dams, the pool will be low for normal operation. For navigation projects, the maximum loading for normal operation might correspond to the normal water level, combined with the tailwater expected. Water loads defined by the normal operation loading condition are sometimes combined with other types of events.

### B.2.3 Nappe Forces and Tailwater

The forces acting on an overflow dam or spillway section are complicated by steady state hydrodynamic effects. Hydrodynamic forces result from water changing speed and direction as it flows over a spillway. At small discharges, nappe forces may be discounted in a stability analysis; however, when the discharge over an overflow spillway approaches the design discharge, nappe forces can become significant and should be taken into account in the analysis of dam stability. Some gravity dam guidance recommends ignoring the weight of the nappe on top of the structure and requiring that the tailwater be assumed to be 60 percent of its expected height, and some do not. This method does not sufficiently account for subatmospheric crest pressures and high bucket pressures, and in some cases, it can yield unconservative results. While this practice is still acceptable, it may be desirable to determine forces due to the nappe

and tailwater more rigorously. A procedure for computing the nappe and tailwater forces is presented in the Federal Energy Regulatory Commission *Engineering Guidelines* (2005).

### **B.3 Uplift Loads**

Uplift loads have significant impact on stability and should be consistent with the failure mode being considered. Measured uplift pressures may not be indicative of pressures occurring during failure. For instance, uplift pressures along a slide plane are very different if sliding has occurred. The joint might be dilated from riding up over aggregate, and the drain efficiency may be reduced or eliminated from interruption of the drain holes. Sliding stability, resultant location, and flotation are all aspects of a stability analysis where safety can be improved by reducing uplift pressures. Since uplift pressures are directly related to flow paths beneath the structure, uplift pressure distribution may be determined from a seepage analysis. Such an analysis must consider the types of foundation and backfill materials, their possible range of horizontal and vertical permeabilities, and the effectiveness of cutoffs and drains. Seepage analysis techniques to determine uplift pressures on structures may include flow nets, finite element methods, the line-of-creep method, and the method of fragments. Uplift pressures resulting from flow through fractures and jointed rock, however, are poorly understood and can only be accurately known by taking measurements at the point of interest. Joint asperities, changes in joint aperture, and the degree to which joints interconnect with tailwater influence uplift pressures and pressure distribution. Uplift pressures are site-specific and may vary at a given site due to changes in geology. Uplift pressures can be reduced through foundation drainage or by various cutoff measures such as grout curtains, cutoff walls, and impervious blankets. Uplift pressures should be based on relatively long-term water elevations. Short duration fluctuations, such as from waves or from vibrations due to high-velocity flows, may be safely assumed to have no effect on uplift pressures.

### **B.4 Silt**

Silt can accumulate upstream of dams. Not all dams will be susceptible to silt accumulation, and the structural engineer should consult with hydraulic engineers to determine if silt buildup was possible, and to what extent it might have accumulated over time. Measuring the silt level by hydrosurvey would be prudent.

For an approximation, horizontal silt pressure is assumed to be equivalent to that of a fluid weighing  $85 \text{ lb/ft}^3$ , and vertical silt pressure is determined as if silt were a soil having a density of  $120 \text{ lb/ft}^3$ . These values include the effects of water within the silt. If significant, the sediment depth for an existing dam can be based on hydrographic surveys.

Reservoir silt can reduce uplift under a dam, similar to an upstream apron, by increasing the seepage path or increasing the head loss through the silt layer. However, uplift reduction should be justified by instrumentation because potential liquefaction of the silt during a seismic event may negate uplift reduction. If liquefaction occurs, pore pressure in the silt will increase. This

condition of elevated pore pressure may persist for some time after the seismic event. For this reason, uplift reduction due to silt may not be relied upon when considering post-earthquake stability.

## **B.5 Thermal and Alkali/Aggregate Reactivity**

Volumetric changes caused by thermal expansion and contraction, or by alkali/aggregate reactivity, affect the cross-valley stresses in the dam. These stresses are important when three-dimensional behavior is being considered. Expansion will cause a straight gravity dam to wedge itself into the valley walls more tightly, increasing its stability. Contraction has the opposite effect. While these effects are acknowledged, the beneficial effect of expansion is difficult to quantify even with elaborate finite element models because it is contingent on the modulus of deformation of the abutments, which is highly variable. For this reason, the beneficial effects of expansion should not be relied upon in three-dimensional stability analyses. In the case of an arch dam, volumetric expansion causes upstream deflection of the arch and associated stresses. Volumetric contraction would have the opposite effect. The consequences of these stresses should be evaluated. If it appears that contraction will cause monolith joints to open and, thus, compromise force transfer from monolith to monolith, this effect should be considered.

## **B.6 Earthquake Loads**

Earthquake loads are used to represent the inertial effects attributable to the structure mass, the surrounding foundation, and the surrounding water (hydrodynamic pressures). Earthquake loadings should be selected after consideration of the accelerations that may be expected at each project site as determined by the geology of the site, proximity to major faults, and earthquake history of the region as indicated by available seismic records. Seismic zone maps can be used to establish the probability zone for projects that do not have detailed seismicity studies, but typically do not provide enough information for structures such as dams that can have large consequences associated with failure.

Site-specific seismic studies may be required for more critical structures. A set of seismic zone maps are available from the United States Geological Survey at:

<http://earthquake.usgs.gov>

Other widely accepted seismic zone maps can also be used as a starting point for determining seismic loading. General seismic hazard maps, such as that cited above, may not sufficiently account for local seismicity.

Several analytical methods are available to evaluate the dynamic response of structures during earthquakes: seismic coefficient, response spectrum, and time history. The current state-of-the-art method uses linear elastic and nonlinear finite element time history analysis procedures, which account for the dynamic interaction between the structure, foundation, soil, and water. The



seismic coefficient method fails to account for the true dynamic characteristics of the structure-water-foundation system, but it can give a preliminary indication for stiff structures.

The horizontal component of the dam inertial force is assumed to act at the structure's center of mass and that the structure is a rigid body. In actuality, almost all structures have some flexibility, and the use of the rigid body concept often underestimates the magnitude of the inertial force. The location of the horizontal inertial force is also related to the flexibility of the structure and usually acts at a location higher than the center of mass. However, because of the cyclic nature of earthquake loads, there is little probability of a rotational-stability related failure.

Backfill or silt material adjacent to a structure will induce inertial forces on the structure during an earthquake. The pseudo-static inertial force of the backfill or silt is added algebraically to the static lateral earth pressures in the seismic coefficient method. In a dynamic finite element analysis that incorporates reservoir interaction, the silt can be modeled as a saturated soil or more dense fluid.

Water that is above the ground surface and adjacent to or surrounding a structure will increase the inertial forces acting on the structure during an earthquake. The displaced structure moves through the surrounding water, thereby causing hydrodynamic forces to act on the structure. The water inside and surrounding the structure alters the dynamic characteristics of the structural system, increasing the periods of the fundamental modes of vibration and modifying the mode shapes. In seismic coefficient methods, the hydrodynamic effects are approximated by using the Westergaard method (equation B 1) (Westergaard, 1931). The hydrodynamic force can either increase or decrease the water force, depending on direction of seismic acceleration. Figure B-2 illustrates hydrodynamic pressures based on the Westergaard method.

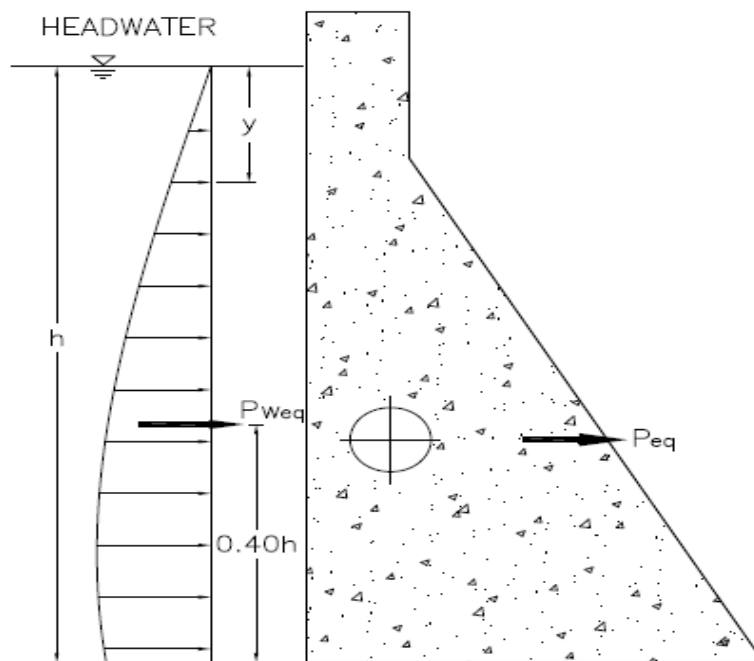


**Figure B-2: Hydrodynamic forces for freestanding water on a gravity dam.**

$$p_E = (7/8) \alpha_h \gamma_w h \quad \text{eq. B1}$$

where,

$p_E$  = hydrodynamic pressure at base of dam

$\alpha_h$  = horizontal seismic coefficient

$\gamma_w$  = unit weight of water

$h$  = water depth

The hydrodynamic pressure is added algebraically to the static water pressure to get the total water pressure on the structure. The pressure distribution is parabolic, and the line of action for the resulting force,  $P_{Weq}$ , is approximately 0.4  $h$  above the ground surface. The Westergaard method assumes the structure is rigid and the water is incompressible. In 1952, Zangar studied dynamic water pressures on sloping faces and provided adjustments to Westergaard's added mass. In the 1980s and 1990s, there was considerable work on formulating incompressible and compressible hydrodynamic approaches in finite element modeling. The incompressible formulation is more accurate than Westergaard's added mass because the reservoir topography and shape of the upstream face of the dam are modeled. Compressible material formulations have been observed to transmit pressure waves and damping mechanisms in the reservoir better than incompressible material formulations. Current-day finite element methods can model the reservoir with fluid elements. Analysts must use care to verify the dynamic behavior of the fluid elements and ensure static water pressures remain on the structure after the earthquake as the structure may displace.

Engineers using the seismic coefficient approach for stability analyses should be aware of the limitations and the simplifying assumptions made with respect to hydrodynamic pressures and their distribution on the structure.

When time history analysis is done, a suite of time earthquake records should be used. Peculiarities of one particular record may produce results that are different from the general behavior from all other time histories. The results should be used as an aggregate to predict potential behavior of the structure.

## **B.7 Ice Loads**

Ice pressure is created by thermal expansion of the ice and by wind drag (U.S. Army Corps of Engineers, 2002). Pressures caused by thermal expansion are dependent on the temperature rise of the ice, the thickness of the ice sheet, the coefficient of expansion, the elastic modulus, and the strength of the ice. Wind drag is dependent on the size and shape of the exposed area, the roughness of the surface, and the direction and velocity of the wind. Ice loads are usually transitory. Not all dams will be subject to ice pressure, and the engineer should decide whether an ice load is appropriate after considering all relevant factors. An example of the conditions conducive to the development of potentially high ice pressure would be a reservoir with hard rock reservoir walls that totally restrain the ice sheet. In addition, the site meteorological conditions would have to be such that an extremely rigid ice sheet develops. For the purpose of

the analysis of structures for which ice loading occurs, it is recommended that a pressure of 5,000 pounds per square foot (lb/ft<sup>2</sup>) be applied to the contact surface of the structure in contact with the ice, based on the expected ice thickness. The existence of a formal system for the prevention of ice formation, such as an air bubble system, may reduce or eliminate ice loading. Information showing the design and maintenance of such a system must be provided in support of this assumption. Ice pressure should be applied at the normal pool elevation. If the dam is topped with flashboards, the strength of the flashboards may limit the ice load.

## **B.8 Ice/Debris Impact**

Some rivers are subject to ice and debris flow. Current-borne ice sheets weighing several tons and/or debris can impact dams and cause local damage to piers, gates, or machinery. Several dams have experienced significant reservoir surcharges under moderate flood events due to debris or floating ice plugging spillway bays. When the ability of a spillway to pass floods is evaluated, the effect of ice and debris should be considered.

## **B.9 Wind Loads**

Wind loads are usually small compared to other forces acting on dams. A wind pressure of 50 lb/ft<sup>2</sup> has been applied to the exposed surfaces of dams to address stability, but it has usually been shown not to be a critical load. If it is critical, site-specific wind data are used.

## **References**

Federal Energy Regulatory Commission, *Engineering Guidelines for the Evaluation of Hydropower Projects*, Chapter 14, “Dam Safety Performance Monitoring Program,” 2005.

U.S. Army Corps of Engineers, *Ice Engineering*, 1110-2-1612, 2002.

Westergaard, H.M., “Water Pressures on Dams during Earthquakes,” Alfred R. Golze, ed., *American Society of Civil Engineers Transactions*, Paper No. 1835, November 1931 Proceedings.





**FEMA**

FEMA P-1016  
Catalog No. 14177-1